

University of the Witwatersrand

School of Electrical & Information Engineering, University of the
Witwatersrand, Private Bag 3, 2050, Johannesburg, South Africa

A Covariance Based Method To Describe Power Processing In Power Electronics Converters

Author:
Arlo EARDLEY
1108472

Supervisor:
Prof. Ivan HOFSAJER

May 2022



A Covariance Based Method To Describe Power Processing In Power Electronics Converters

Arlo Eardley 1108472

School of Electrical & Information Engineering, University of the Witwatersrand, Private Bag 3, 2050, Johannesburg, South Africa

Abstract: This paper explores the use of a new topology evaluation framework to describe the internal power processing of a power electronics converter. This method is called the matrix method and leverages off a covariance matrix to describe power processing patterns in a power electronics converter. Covariance measures how two signals interact with each other. The covariance between the power waveforms of the components in a converter describes how these components interact in terms of power. These are called “power interactions”. These power interactions between component powers provide insight into the power processing of a topology. The covariance matrix contains all combinations of component power pairs. This aims to describe all the power interactions components have in the entire converter. The covariance matrix is interpreted as describing the power processing inside a converter, where circulating power is occurring and which components are most involved in power processing. The covariance matrices of converters are able to be compared in a quantitative manner with the aim of providing a more justifiable reason for topology selection rather than personal bias. The matrix method is shown to be aligned with the principles of differential power theories. The matrix method is shown to be useful in comparing topologies, aiding in the topology selection process.

Key words: Topology Selection, DC-DC Converter, Power Processing, Covariance, Power Interactions

Contents

I	Definitions	5
I.I	Conversion effort	5
1	Introduction	6
2	The matrix method	8
2.1	Interpreting the covariance matrix	17
2.1.1	Interpreting variance	17
2.2	Properties of the covariance matrix of component powers	18
2.3	Reducing the covariance matrix	19
2.3.1	Using the reduction property to interpret results	21
2.4	Normalizing the matrix method	22
2.5	Zero-ripple approximations as a baseline comparison	23
2.5.1	Determining what a “good” topology looks like	25
2.6	Boost converter example using the matrix method	26
3	The matrix method and existing research	30
3.1	Linking the matrix method and differential power: Boost Converter	31
4	Case studies	34
4.1	Introduction	34
4.2	Interpretation of results	34
4.3	Step up converters	36
4.4	Step down converters	40
4.5	The modified boost converter	44
4.6	The boost vs quadratic boost : stepped duty cycle	48
4.7	The matrix method and ripple	51
4.8	The cascaded boost	52
4.9	The parallel interleaved boost	53
4.10	Summarized findings	55
5	Conclusion	56
6	Future work	56

7	Acknowledgements	56
A	Generalized proof of reduction technique	59
B	More reduction examples of the boost converter	61
B.1	Extended inductors	61
B.2	Extended inductors and capacitors	62
C	The matrix method and AC power theory	64
C.1	Introduction	64
C.2	Correlation and power factor	64
C.3	The dot product and covariance	65
C.4	The relationship between the matrix method and the power triangle	67
C.5	Power Factor Correction Circuit	70
C.6	Power Factor Correction Special Case with 45° Angle In The Load	73
D	A brief overview of differential power methods	77
D.1	Introduction	77
D.2	The fundamentals of differential power	77
D.3	Analysis of boost converter using differential power methods	79
D.4	Analysis of quadratic boost converter using differential power methods	82
D.5	Differential power methods application to multi-port systems	85
D.6	Extending differential power methods	86
E	More about differential power and the matrix method	88
E.1	Introduction	88
E.2	Linking the matrix method and differential power: Buck Converter	88
F	Case study unabridged results and test files	92
F.1	The boost vs quadratic boost : stepped duty cycle	92
F.1.1	Unabridged results	92
F.1.2	LTSpice Netlists	93
F.2	Step up converters	97
F.2.1	Unabridged results	97
F.2.2	LTSpice Netlists	98
F.3	Step down converters	102

F.3.1	Unabridged results	102
F.3.2	LTSpice Netlists	103
F.4	Matrix method and ripple	107
F.4.1	Unabridged results	107
F.4.2	LTSpice Netlists	107
F.5	Cascaded boost	109
F.5.1	Unabridged results	109
F.5.2	LTSpice Netlists	109
F.6	Interleaved boost converter	111
F.6.1	Unabridged results	111
F.6.2	LTSpice Netlists	111
F.7	Linearity of the matrix method	113
F.7.1	Unabridged results	113
F.7.2	LTSpice Netlists	113

I Definitions

1.1 Conversion effort

Conversion effort is defined as the “effort” required to convert power in a converter. It is used as a descriptive term for the difference between input and output voltage of a converter in this work. For example a converter has a low conversion effort if it were converting 10 V to 9 V as it does not have to manipulate a lot of power. A high conversion effort could describe a converter that is stepping 10 V down to 0.5 V where a lot of power has to be manipulated in order to achieve this. This is a relative term and is closely linked to the duty cycle of a converter but provides a more descriptive image of the “difficulty” a converter may face when performing conversion.

1 Introduction

Choosing the right circuit topology for an application is often a problem in power electronics. Engineers normally choose topologies using their experience or they leverage off popular topologies in recent literature. Building a new circuit topology for the first time and dealing with the pitfalls of the design can be risky when real world time constraints are considered. This difficulty in making a topology choice creates a design cycle where some particular aspect is shown to improve the performance of a converter. This aspect is over engineered and exhausted in literature until the next fashionable aspect gains popularity and starts the cycle again. This means that the popular topologies gain further popularity while overlooking unfamiliar or possibly better topologies. This process is beneficial to improving converters but it may be trying to out-engineer a fundamentally bad topology choice. This is because it is difficult to reach consensus on which metrics to use to compare converters since it is a multi-variable optimization problem.

The majority of topology design and proposal papers do not address the fundamental reason for choosing a particular topology to improve upon. It is implied by authors that it is a good topology for the application based on their experience. When researching topologies to choose for an application, the reader is bombarded with different options for the same application where each paper describes theirs as the best. This is confusing and makes one wonder why each approach to the same application in power electronics appears to require a brand new topology.

Although the problem of topology selection is well known it is easily observed in topology comparison papers that ultimately leave the reader with a list of suitable topologies for an application without a definite answer as to which is the best [1–9]. These papers represent typical comparative topology studies that focus on common metrics such as power ratings, EMI, component count, switch stress, efficiency, gain, complexity, control mechanism, modulation scheme and so on. All of these metrics are valid ways of comparing and analysing topologies for particular use cases, however, many of these metrics deal with effects introduced by appropriate component selection.

The primary function of a converter is to process power from input to output. These surface level metrics are not indicative of a viable power processing topology. Most of these metrics can be over engineered to squeeze the best performance out of a possibly inadequate topology. Typically, when designing a converter, popular or familiar topologies are considered. They are each optimized and compared to decide on a final topology. This is often done using a Pareto-front optimization for a desired operating point [10–13]. The problem with this approach is that it combines these metrics to find an optimal solution. However, since the topologies considered for optimizing can not be quantifiably justified, the solution could possibly be better when performed on a fundamentally better topology structure. There is a gap in this process of topology selection to identify the topologies that are worth optimizing using a suitable selection framework.

There is a need for a topology selection framework that is free of engineering personal bias. A topology selection framework that can evaluate topologies independently of any component choices, could leverage off the analysis of power processing in a converter. This is because the power processing of a converter is dependant on topology structure. There is a particular field of research called Partial Power Processing (PPP) that is focused on manipulating the power a converter has to process.

PPP is a technique that essentially configures a converter in a system in such a way as to process as little power as possible by eliminating unnecessary processing. PPP techniques come in a variety of flavours such that [14] define and review the different categories of PPP. [15] conducts an efficiency analysis of the benefits of applying PPP concepts and concludes PPP can increase converter efficiency. This is because less processed power creates less loss in the conversion process [16]. PPP is known for its increased efficiency and decreased component stress characteristics and has become popular, particularly with respect to PV systems [17–19].

Generally speaking PPP is mainly concerned with configuring complicated systems around the converter rather than the converter itself. A particular subset of PPP that can be applicable to the converter itself is differential power. Differential power methods are starting to address the problem with initial topology choice. This methods core principle is the idea that a converter can be configured to process a certain minimum amount of

power. This is known as “differential” power. It was first presented by Wilson [20] and subsequently proven by Wolaver [21] more than 50 years ago. Cobos et al have recently rediscovered this principle and used this idea successfully in their topology selection process [16, 22–24]. They also clearly define the terms used in PPP architectures and create a solid framework for analysing systems with respect to differential power. However, this technique only partially addresses the issue with topology selection because as it stands it is not able to aptly describe the inner power conversions of a topology, but rather explains more general system level power processing [25].

PPP is investigating how the structure of the topology influences power processing. Therefore to fundamentally compare two topologies a framework that describes how they internally process power can help make a topology choice. The power processing ability of a converter is important to analyse as it has been linked to volume and losses which impacts the overall performance of any converter [16]. This would be a framework free of personal bias to evaluate topologies. This framework would also be ignorant of component selection as it is based on the arrangement of the parts and not the parts themselves. The way the components interact with each other while processing power needs to be quantified and comparable.

A new method called the “matrix method” is to be explored in this work to start addressing the needs of this hypothetical framework. The matrix method aims to quantify the power interactions components have with each other to evaluate the power processing in a topology. Its purpose is to start providing insight into the power processes in a converter to make more informed decisions about topology structures. The matrix method takes an analytical approach to power electronics by using the covariance between a pair of component powers. The covariance is a metric used to describe how much two signals interact with each other. This describes the power interaction any two components have during power processing.

The covariance between each pair of component powers is calculated and placed in a covariance matrix hence the name “matrix method”. The covariance matrix is interpreted as describing all the power interactions taking place in a converter during steady state. By quantifying the power interactions, topologies could be compared based on their internal power processing ability. This method is shown in later sections to be potentially useful as a guideline when designing topologies.

Chapter 2 outlines the matrix method, its interpretation and the various mathematical properties of the method. Chapter 3 will then discuss how this method fits in with existing research on differential power as this method was inspired by the work of Cobos et al. Chapter 4 will apply the matrix method to a few common topologies and analyse the results of the method, with Chapter 5 concluding the dissertation.

2 The matrix method

The primary function of a converter is to process power between the input and output terminals. This processing is the result of the components in the converter exchanging power. This is qualitatively observed using regular current, voltage and power waveforms. In order to compare topologies it would be beneficial to quantify these power exchanges. The following scenario of a buck converter can be considered to investigate a method for quantifying power exchange. Consider a simple buck converter shown in *Figure 1* below:

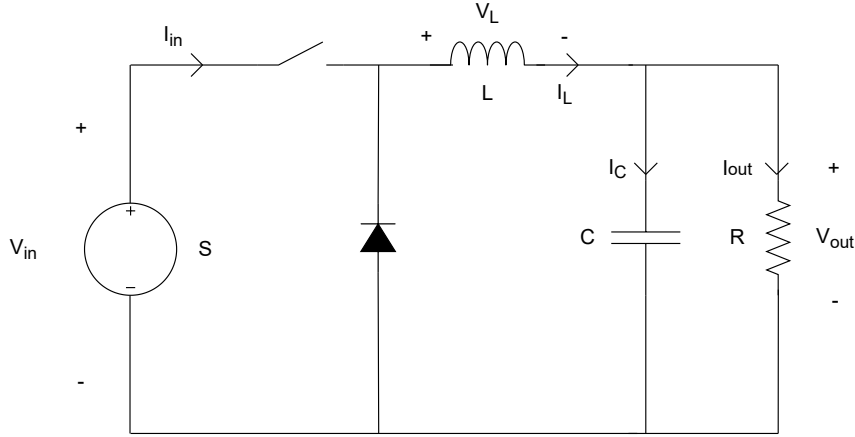


Figure 1: Buck converter

This buck converter is assumed to have a constant output voltage with the expected current and voltage waveforms shown in *Figure 2* below. The power waveforms at the bottom of *Figure 2* can be deduced using traditional power analysis from the product of the current and voltage waveforms above them using an absorbing power convention from *Figure 1*. This leads to the inversion of the source power waveform. An absorbing power convention is used to represent the power waveforms of each component in a standard power analysis and is merely used to calculate the powers of each component prior to using the matrix method.

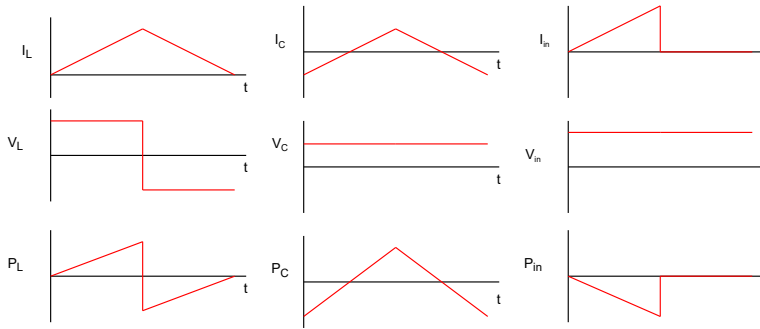


Figure 2: Buck converter current, voltage and power waveforms

Power relationships between the components in the converter can be observed from their power waveforms. As an example *Figure 3* illustrates a power relationship between the inductor and the source. The inductor stops absorbing power and starts to supply power when the source power goes to zero. This is easily observed but quantifying this relationship will allow for comparisons to be made between the power relationships of components in different topologies. As these components process power they are interacting with each other in terms of power. Covariance is used to describe the power interaction between components.

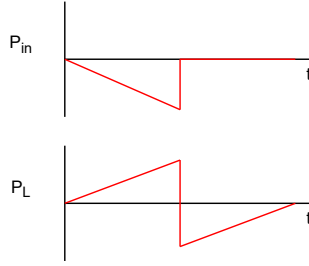


Figure 3: Buck converter source and inductor power waveform

Covariance is a method to quantitatively describe the relationship between any two signals as it is a statistical measure of how two signals or data sets interact with each other. When the covariance between two power waveforms is taken it describes the interaction between the signals from a power perspective and is termed a “power interaction”. These power interactions are an indication of power exchange since the components in a converter are only interacting in order to exchange power. In purely mathematical terms the covariance is described by equation 1 below:

$$COV(A, B) = \frac{1}{T} \int_0^T (A(t) - \overbrace{\bar{A}}^{\text{Average of A(t)}})(B(t) - \underbrace{\bar{B}}_{\text{Average of B(t)}})dt \quad (1)$$

Any electronic signal can be said to be comprised of a fluctuating AC portion superimposed on a DC average portion. To put Equation (1) into the context of electronics, the average or DC portion of each signal is deducted leaving the fluctuating or AC portions. The AC portions are then multiplied and an average is taken of the result. This means the covariance is measuring how the fluctuating portions of each signal interact with each other. Covariance is used because the power waveforms of most components in switch mode converters contain a fluctuating power. It is this fluctuating power in the components that is the heart of power processing in a converter. The work of differential power methods only considers the fluctuating powers in a topology to be the power that is processed by a converter [16].

To expand on this further a DC power transfer does not lead to power processing as it can not be altered by reactive components, it merely passes through. If DC power could be processed there would be no need for switching elements in converters. The elements of a converter that are performing power processing are the reactive components. In an ideal converter the input power and the output power of a converter are equal with no losses. The input power consists of a particular current and voltage and the output power consists of a different combination of current and voltage as a result of a step up/down conversion. The switching elements are used to convert the DC input power to a fluctuating power in order to take advantage of the reactive components ability to process power. Therefore the only type of power that can be processed and manipulated by the reactive components in a converter is a fluctuating power created by the switching elements.

As an example to illustrate the covariance of two power waveforms, the inductor and source power waveforms from the buck converter are shown in *Figure 4*. The source power has a peak of -50 W and an average of -12.5 W. The inductor power peaks at 25 W and troughs at -25 W with an average of 0 W.

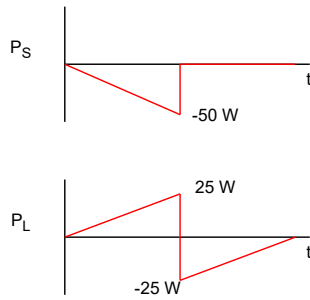


Figure 4: Buck converter source and inductor power waveforms

First the average DC values must be removed from each signal as per equation 1. By doing this each signal now has an average of 0 W and are referred to as being “zero mean”. Figure 5 below shows the source and inductor power waveforms with zero mean.

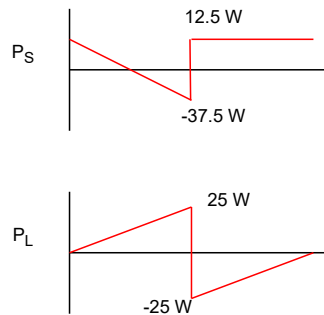


Figure 5: Buck converter source and inductor power waveforms with zero mean

Now the next step from equation 1 is to calculate the product of the waveforms in Figure 5. Figure 6 below shows the resulting product of the zero mean source and inductor waveforms in red. The blue line indicates the average value of this new red signal. This average value is the final covariance of the signals since it is the average of their zero mean product.

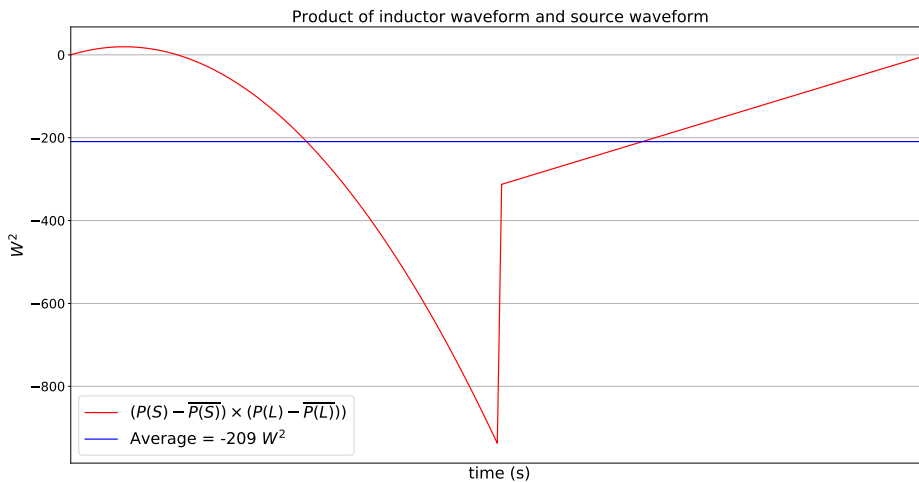


Figure 6: Product of zero mean inductor and source power waveforms

The covariance between the inductor and source power results in $-209 W^2$. The units of W^2 do not represent

a real world power quantity. Since the covariance is a measure of a relationship between two signals, the units of W^2 now describe the relationship between these two signals. These units are used to describe the power interaction between components. It should also be noted that covariance is commutative. Since it is the product of two powers and the order of multiplication does not matter the $COV(S,L)$ is the same as the $COV(L,S)$.

The covariance between the source and the inductor resulted in a negative value of $-209 W^2$. The inductor in the buck converter absorbs power from the source in one half cycle in order to release it in the next half cycle. There is an exchange of power occurring between these two components. This can also be observed in *Figure 4*. This relationship is quantitatively described by the interaction of $-209 W^2$.

A negative covariance means the signals move in opposite directions to each other on average. The smaller the negative value (the larger the absolute value) the more the signals oppose each other. As one is supplying power the other is absorbing power and thus oppose each other. In the context of component power waveforms a negative covariance is interpreted as the two components exchanging power. This is because a negative covariance only results from two signals having an inverse relationship. In power electronics when two signals have an inverse relationship, a power exchange can be observed qualitatively. Covariance describes this net exchange of power quantitatively with a negative value.

For the next example the covariance between the inductor and the capacitor will be calculated for the buck converter. The capacitor and inductor power waveforms are shown in *Figure 7*. The inductor power peaks at 25 W, troughs at -25 W with an average of 0 W. The capacitor power peaks at 5 W and troughs at -5 W with an average of 0 W.

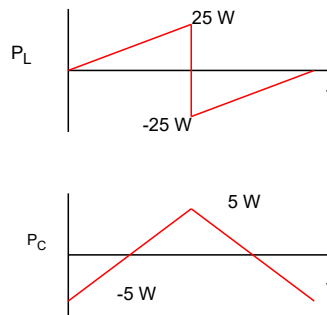


Figure 7: Buck converter capacitor and inductor power waveforms

First the average values must be removed from each signal as per equation 1. Since both of these signals are zero mean to begin with the next step from equation 1 is to calculate the product of the waveforms in *Figure 7*. *Figure 8* below shows the resulting product of the zero mean inductor and capacitor waveforms in red. The blue line indicates the average value of this new signal. This average value is the final covariance of the signals.

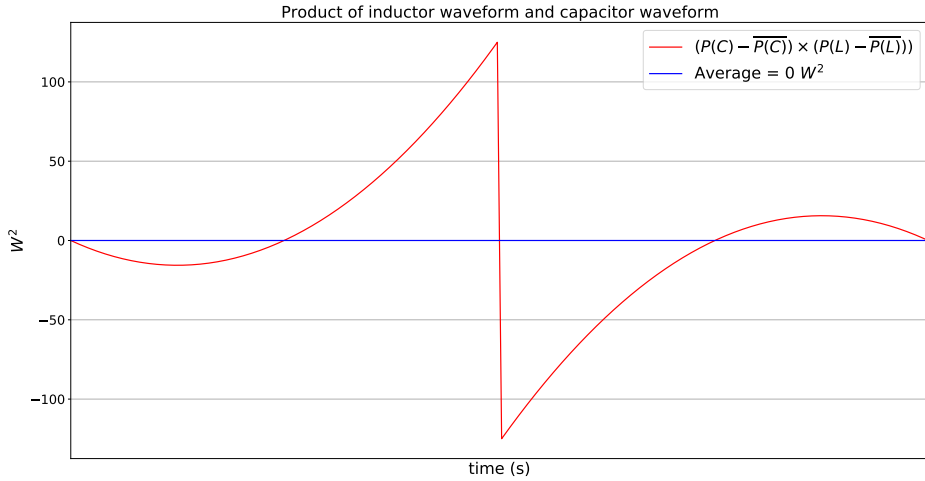


Figure 8: Product of zero mean inductor and capacitor power waveforms

The covariance between the capacitor and the inductor produced a zero result. This does not mean that there is absolutely no interaction between the signals, it means that at the end of a switching period there is no net exchange of power between the two components. Although there appears to be a lot of activity between these signals on an instantaneous basis, as an average over the switching period the result of their interaction is zero. A zero covariance only occurs when two signals have no linear relationship and neither signal is affected by their interaction. A zero covariance between two power waveforms is considered to describe no interaction between the signals since there is no net exchange of power contributing to power processing.

There may be DC interactions between the components where average power is transferred that is not described by the covariance. The covariance is only able to describe power exchange interactions and not DC power transfer. This is acceptable in the context of this work because the fluctuating powers are what is referred to as processed power. This is also the case in the work of Cobos where a direct power transfer is not regarded as processed power and only the fluctuating powers are considered processed [16].

So far a negative and a zero covariance have been discussed. The last result the covariance can take on is a positive result. In this buck converter example there are no two different component power signals that will result in a positive covariance to use as an example. This is not a general rule for all converter topologies but it is the case for the buck converter. To illustrate a positive covariance a hypothetical pair of signals has to be used since the buck waveforms will not produce one. Consider the hypothetical inductor power waveforms in Figure 9. Where L1 and L2 are two inductors in series in a hypothetical topology. L1 peaks at 15 W and troughs at -15 W with an average of 0 W. L2 peaks at 10 W, troughs at -10 W with an average of 0 W.

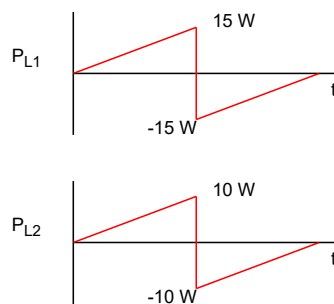


Figure 9: Hypothetical series inductors

First the average values must be removed from each signal as per equation 1. Since both of these signals are zero mean to begin with the next step from equation 1 is to calculate the product of the waveforms in *Figure 9*. *Figure 10* below shows the resulting product of the waveforms in red. The blue line indicates the average value of this new signal. This average value is the final covariance of the signals.

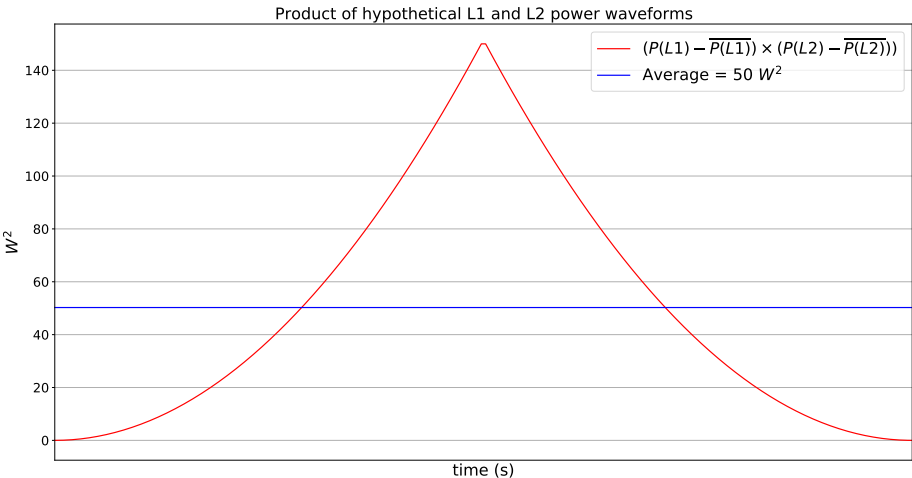


Figure 10: Hypothetical series inductors

The covariance between the hypothetical inductors L1 and L2 resulted in $50 W^2$. A positive covariance between two signals means the signals move in the same direction on average. They are moving together, charging and discharging at the same time on average, this is also observed in *Figure 9*. The larger the positive value the stronger the interaction between these signals. In the context of component power waveforms a positive covariance is interpreted as the two components achieving the same function. As one components power waveform increases so does the other. They may both be providing power to another component or they may both be receiving power from another component. Their interaction does not result in an exchange but rather describes a net ability of one or both components to contribute to a power exchange with other components.

Covariance is able to quantitatively describe the power interactions between two components. It would also be beneficial to be able to describe how the power waveform of one component fluctuates over one period. This will give insight into how much power is moving around inside one particular component. To illustrate this the single inductor from the buck converter example can be compared to itself using covariance. *Figure 11* shows the inductor waveform from this buck converter example. The inductor peaks at 25 W, troughs at -25 W with an average of 0 W. The inductor is represented twice in *Figure 11* to graphically illustrate the process of taking the covariance of the signal with itself.

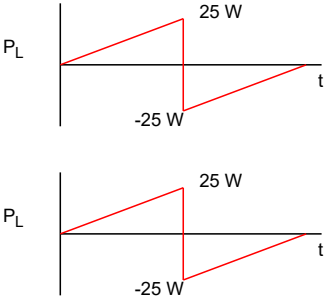


Figure 11: Buck converter inductor power waveform

First the average values must be removed from each signal as per equation 1. Since both of these signals are

zero mean to begin with the next step from equation 1 is to calculate the product of the waveforms in *Figure 11*. *Figure 12* shows the resulting product of the waveforms in red. The blue line indicates the average value of this new signal. This average value is the final covariance of the signals.

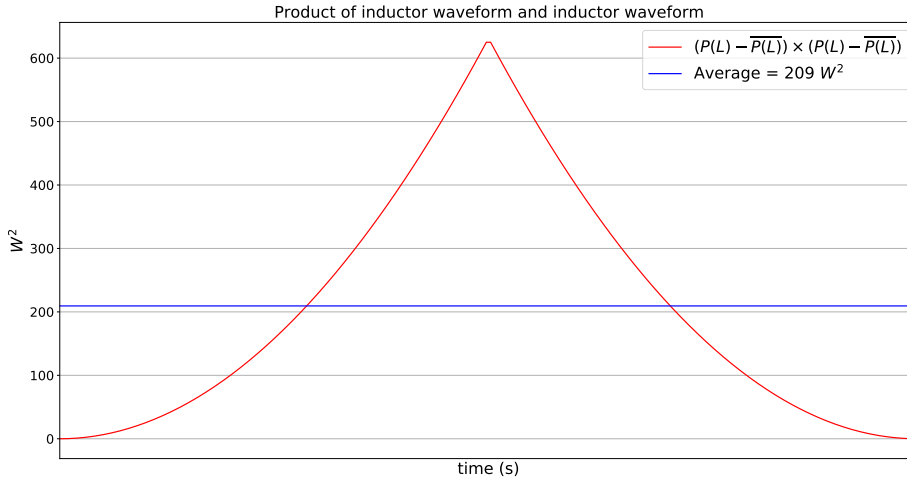


Figure 12: Product of zero mean inductor power waveforms with itself

The covariance of the inductor power waveform with itself results in a positive $209 W^2$. In general when the covariance between a signal and itself is calculated it is called variance. The variance of any changing signal will always be positive. Variance describes how the power waveform of a single component behaves. It describes how far from the mean DC value the signal fluctuates over a period. This quantifies the magnitude of the fluctuations in the component. This can be thought of as representing the “power activity” inside a component i.e a representation of how much effort it is exerting to process power. In mathematical terms this is described by equation 2 below:

$$COV(A, A) = \frac{1}{T} \int_0^T (A(t) - \overbrace{\widehat{A}}^{\text{Average of } A(t)})^2 = VAR(A)dt \quad (2)$$

In terms of electronics this is taking the average of the squared AC portion of the signal (with the DC portion removed).

Now the interactions between the power waveforms of components as well as the “power activity” of a single component can be quantified numerically. These power relationships can be compared to the power relationships of another converter topology. To do this it would be helpful to analyse the entire converter at once. A covariance matrix is used to display all the combinations of component power interactions in one place. This neatly packages all the power interactions inside a converter into a matrix that can be compared to the covariance matrix of another topology.

As an example to illustrate this, the covariance matrix for the buck converter in *Figure 13* will be created.

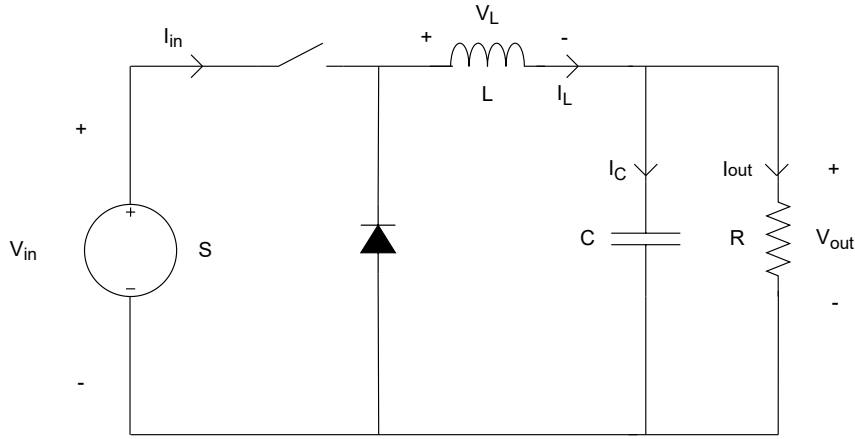


Figure 13: Buck converter

Using this circuit diagram the covariance matrix below contains every possible combination of covariance pairs from each components power waveforms.

	<i>S</i>	<i>L</i>	<i>C</i>	<i>R</i>
<i>S</i>	COV(<i>S,S</i>)	COV(<i>S,L</i>)	COV(<i>S,C</i>)	COV(<i>S,R</i>)
<i>L</i>	COV(<i>L,S</i>)	COV(<i>L,L</i>)	COV(<i>L,C</i>)	COV(<i>L,R</i>)
<i>C</i>	COV(<i>C,S</i>)	COV(<i>C,L</i>)	COV(<i>C,C</i>)	COV(<i>C,R</i>)
<i>R</i>	COV(<i>R,S</i>)	COV(<i>R,L</i>)	COV(<i>R,C</i>)	COV(<i>R,R</i>)

This matrix is symmetrical since the entries above the main diagonal are a mirror image of the entries below the main diagonal. This is because covariance is commutative as mentioned earlier. These mirrored entries are shown in matching colours. The main diagonal contains the variances of each component as it is the covariance of the component power waveform with itself. These entries are marked in orange. They describe the power activity inside a particular component. The off diagonal entries (entries not on the main diagonal) show the covariance power interaction between a particular pair of components.

As an example to illustrate the covariance matrix with numerical values consider the buck converter in *Figure 13* with a large enough capacitor and inductor to approach zero ripple with the following characteristics:

$$\begin{aligned}
 V_{in} &= 10 \text{ V} \\
 V_{out} &= 5 \text{ V} \\
 D &= 50 \% \\
 P_{out} &= 25 \text{ W}
 \end{aligned}$$

The following covariance matrix can be calculated using the same waveform approach that has been used in the previous examples. After the covariance is calculated it is placed in the matrix below.

$$\begin{matrix}
& & S & L & C & R \\
S & \left[\begin{array}{cccc}
625 & -625 & 0 & 0 \\
-625 & 625 & 0 & 0 \\
0 & 0 & 0 & 0 \\
0 & 0 & 0 & 0
\end{array} \right]
\end{matrix}$$

Now to understand what this matrix is depicting it can be thought of as a heat map of the power interactions between the components in a converter. The analogy of a heat map has been used in the same way a heat map shows hotspots and cool spots of some kind of measured activity, the covariance matrix also shows hotspots of power processing. The covariance matrix in *Figure 14* has its entries colour coded in the same way a heat map does to visually describe the interactions in the covariance matrix. Red depicts strong “power activity” and strong power interactions and blue depicts weak “power activity” and power interactions.



Figure 14: Buck converter covariance matrix depicted as a heat map

The main diagonal entries show the internal “power activity” of each component in the converter since these are the variances. This gives a sense how much strain the individual components are under during power processing. The more power fluctuating in a component results in a larger variance and the component is processing more power. The smaller the variance, the smaller the power fluctuations and the less power a particular component is processing. In the matrix above the source and the inductor both have large internal “power activity” and are internally processing more power than the capacitor or resistor.

The off diagonal entries show the power interactions between a pair of components. The magnitude of each entry represents the strength of the relationship between the two component power waveforms in question. Larger magnitude entries mean more power is being processed due to stronger interactions. Conversely smaller magnitudes of each entry imply less power processing with weaker power interactions. In the matrix above the source and inductor have large power interactions indicating a strong relationship between these two components. The source and the capacitor have very small interactions by comparison and therefore have weaker power interactions between them.

The spread of the entries (how the values are distributed across a row/column) also indicates how much power is “sloshing” around in the converter. To illustrate the spread of entries a hypothetical example is required to demonstrate this. Consider the hypothetical situation where the buck converter matrix shown in *Figure 14* looked like the matrix in *Figure 15* instead. Where the colour scheme depicts a sliding scale from strongest interactions (red) to weakest interactions (blue):

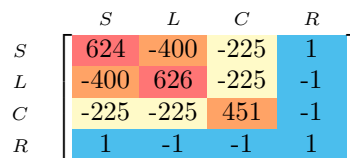


Figure 15: Hypothetical buck converter heat map

The interactions are now spread out across components suggesting that other components are sharing the responsibility of power processing in *Figure 15* as opposed to the strongly concentrated interactions shown in

Figure 14. Figure 15 describes more power “sloshing” around in the converter as the interactions are spread out across the rows and columns of the covariance matrix. Figure 14 does not have much power “sloshing” around since the interactions are concentrated between only two components in the covariance matrix.

This spread of interactions allows one to identify circulating power which may contribute to higher power processing. Many interactions between components that are large in magnitude suggest all the components in the converter are doing a great deal of processing which might be due to many current loops in a topology. Essentially this matrix is a numerical depiction of the spread of power in the converter, which components are doing the heavy lifting and where power may be circulating potentially causing ineffective power processing.

The covariance matrix can be used to evaluate how a converter topology responds to changes in design. For example changing the duty cycle or the conversion effort will change the power processing in the converter. The power interactions between the components will also change and paint a different power processing picture of the topology. This may be used to find a suitable range of operating characteristics for a particular topology.

2.1 Interpreting the covariance matrix

As touched on previously the key aspects to look for after computing the covariance matrix of a topology are the magnitude of the entries and the spread of the power interactions across rows and columns.

The magnitude of each entry represents the strength of the relationship between the two component power waveforms in question. As long as the covariance matrices being compared have the same output power the magnitude of the covariance values provide an indication of the effectiveness of the power processing of the converter. The magnitude of the entries does scale with the output power of the converter. It would therefore be naive to compare the magnitude of entries between converters that are producing different output power conversion.

The matrices may also be normalized to some power quantity common to all converters in the comparative study. For example input power or output power may be constant power quantities common to the converters in the study. Normalization is performed by dividing each entry in the matrix by the square of the normalizing variable. For example to normalize by output power the matrix would be divided by P_{out}^2 . The square must be used so that each entry in the matrix is unit-less and represents a ratio of the power processing each entry describes to the output power. This basically shows how much processing each element is performing relative to the output power.

2.1.1 Interpreting variance

The mathematical definition of variance may look familiar as it is essentially the same as the RMS formula without the final square root as shown below in Equation (3).

$$RMS = \sqrt{\frac{1}{T} \int_0^T (A(t))^2 dt} \quad (3)$$

The RMS of a power waveform is not something that engineers are typically familiar with, however, this does not mean that is not useful. [26] have made use of an RMS power definition and they have reported it as being a useful metric in their topology selection criterion. [27] define their non-active power formula using RMS power. These papers are difficult to dissect so lets look at a more fundamental interpretation of RMS power. RMS is calculated for a fluctuating voltage or current signal in order to sufficiently represent the fluctuating nature of the signal. The average and the peak values of a varying signal can be meaningless and may not sufficiently represent the signal. Therefore the RMS of a fluctuating power represents the effective magnitude of the signal.

RMS power was once considered in the development of the IEEE1459 standard for measuring power under non-sinusoidal conditions. Although RMS power is no longer part of the standard, F.Ghassemi recognized the RMS of instantaneous power had merit [28–30]. Willems then reviewed the work of F.Ghassemi and defined an oscillatory power and oscillatory power factor based on the RMS of a power waveform [31]. F.Ghassemi’s work was then discarded in [32] and [33] due to disagreement over some current and voltage definitions and as a result so was Willems work on oscillatory power.

However, the definitions of oscillatory power put forward by Willems were only discarded because they did not equate to reactive power in the particular use case of IEEE1459. RMS power is also unable to describe the oscillatory nature of power when the signal has a non-zero mean value. Since covariance/variance deduct the mean prior to integrating, the signal is always zero mean. Hence this issue with RMS power as a metric does not apply to the definition of fluctuating power represented in this dissertation using covariance.

The variance of a power waveform in this dissertation is interpreted as representing the magnitude of the fluctuating nature of the waveform from an electrical perspective. From a statistical perspective the variance describes how far from the average value the signal varies. This describes the magnitude of the power fluctuations in much the same way as Willems had defined the intended use of RMS power.

2.2 Properties of the covariance matrix of component powers

The covariance matrix of component powers is mathematically described as being a zero-sum line matrix. This is a particular subset of square matrices and have their own innate mathematical properties. The term “zero-sum line” refers to the property whereby the arithmetic sum of all entries in any row or column is zero. The fact that the covariance matrix of component powers is a zero-sum matrix is suspected to be due to power conservation. This can be observed in the buck converter covariance matrix below. Notice each row sums to zero as well as each column.

$$\begin{array}{c}
 S \\
 L \\
 C \\
 R
 \end{array}
 \begin{bmatrix}
 & S & L & C & R \\
 S & 625 & -625 & 0 & 0 \\
 L & -625 & 625 & 0 & 0 \\
 C & 0 & 0 & 0 & 0 \\
 R & 0 & 0 & 0 & 0
 \end{bmatrix}$$

The zero sum property only works out to exactly zero in the ideal case of a converter. In this research when results are sampled from a simulator such as LTSpice there is sampling and round-off error. This means when the matrices are calculated for non-ideal cases sampled from LTSpice the zero sum-line property of the matrix is not exactly zero. It approaches zero relative to the magnitude of the entries of the matrix.

Furthermore the zero sum-line property only approximates zero in these matrices because switching elements such as MOSFETs and diodes are excluded from the matrix as they only incur loss and are not interesting to analyse with regards to power processing. The absence of these elements from the matrices means there are elements missing from power conservation and therefore only approximate zero.

Zero-sum matrices also have the following properties:

1. All of the co-factors of an $n \times n$ zero sum line matrix are equal
2. An $n \times n$ zero sum line matrix is symmetric
3. An $n \times n$ zero sum line matrix has a 0 eigenvalue and an all 1 eigen vector of $1^{n \times 1}$

The properties pertaining to the eigen values and co-factors are not investigated in this research. It is mentioned here as a possibility for future work. The eigen values have been hypothesized to establish a component scaling law for the power interactions in a converter. In other words how the addition of a component influences the values in the matrix and hence the power interactions of a converter. The co-factor property is also not

investigated in this research but since any $n \times n$ zero sum matrix produces only one unique non-zero co-factor it may be a way of representing the entire matrix using a single value. This could lead to simple comparisons between converter matrices. These properties are not investigated further and are out of the scope of this research.

This zero-sum property of the covariance matrix also allows for the matrix dimensions to be reduced.

2.3 Reducing the covariance matrix

Up to this point the analysis of one converter has been shown using the matrix method. It would be useful in a topology comparison exercise to be able to compare the matrices each topology produces. The dimensions of the matrix are always equal to the number of components in the topology, excluding switching elements. When the number of components differs between topologies this can be difficult to compare matrices of differing dimensions. For example comparing a simple buck converter with a SEPIC (Single-Ended Primary-Inductor Converter) shown in *Figure 16* and *Figure 17*. The SEPIC has one more inductor and capacitor and therefore two extra rows and columns in its covariance matrix. To illustrate this the example to follow outlines how to reduce the dimensions of the SEPIC matrix to be able to compare with the buck covariance matrix.

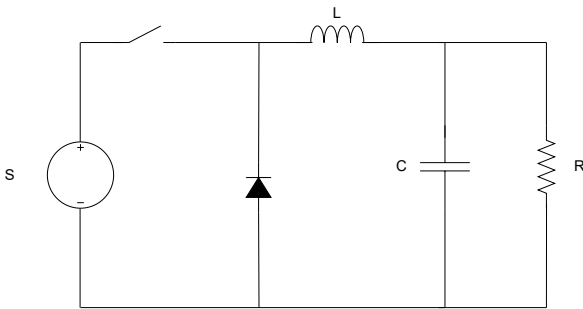


Figure 16: Buck converter

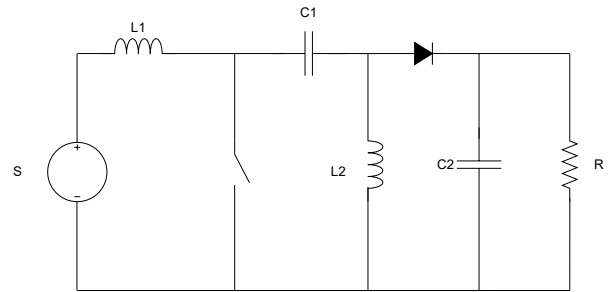


Figure 17: SEPIC converter

To create some covariance matrices to demonstrate reduction the following conditions under zero-ripple are used for the buck and the SEPIC:

$$\begin{aligned}
 V_{in} &= 10 \text{ V} \\
 V_{out} &= 5 \text{ V} \\
 D &= 50 \% \\
 P_{out} &= 25 \text{ W}
 \end{aligned}$$

$$\begin{matrix}
 S \\
 L \\
 C \\
 R
 \end{matrix}
 \begin{bmatrix}
 S & L & C & R \\
 \begin{matrix} 625 & -625 & 0 & 0 \\ -625 & 625 & 0 & 0 \\ 0 & 0 & 0 & 0 \\ 0 & 0 & 0 & 0 \end{matrix}
 \end{bmatrix}$$

Figure 18: Buck converter covariance matrix

$$\begin{matrix}
 S \\
 L1 \\
 L2 \\
 C1 \\
 C2 \\
 R
 \end{matrix}
 \begin{bmatrix}
 S & L1 & L2 & C1 & C2 & R \\
 \begin{matrix} 0 & 0 & 0 & 0 & 0 & 0 \\ 0 & 625 & 625 & -625 & -625 & 0 \\ 0 & 625 & 625 & -625 & -625 & 0 \\ 0 & -625 & -625 & 625 & 625 & 0 \\ 0 & -625 & -625 & 625 & 625 & 0 \\ 0 & 0 & 0 & 0 & 0 & 0 \end{matrix}
 \end{bmatrix}$$

Figure 19: SEPIC converter covariance matrix

These covariance matrices need to be comparable without worrying about the extra components complicating analysis. The SEPIC matrix can have its dimensions reduced to the same dimensions as the buck converter

matrix. The reduction of the SEPIC covariance matrix will create an effective representation of the original matrix while allowing for an easier comparison. It is possible using reduction to group the two inductors in the SEPIC matrix to represent an effective inductor. The two capacitors in the SEPIC matrix can also be grouped to represent an effective capacitor.

Reduction is achieved by replacing multiple rows and columns with a single effective row and column i.e the two inductor rows/columns are combined into a single effective inductor row/column and likewise for both capacitor rows/columns. This would result in a 4×4 covariance matrix with a single effective inductor to compare with the bucks single inductor and a single effective capacitor to compare with the bucks single capacitor. The reduction of the matrix always results in a square matrix to maintain the zero sum line property of the covariance matrix. This reduction can be thought of as a lumped effective representation of the entries being combined together. It is the same idea as creating a Thevenin equivalent but from a power interactions perspective.

Caution must be taken with reduction since information about the original interactions can be lost when creating the effective representation. This is also true when creating an equivalent Thevenin resistance, information about the original connections between the resistors is lost in the process. To continue the example, below is a colour coded illustration of the process of reducing the SEPIC matrix.

$$\begin{array}{c}
 S \\
 L1 \\
 L2 \\
 C1 \\
 C2 \\
 R
 \end{array}
 \begin{bmatrix}
 S & L1 & L2 & C1 & C2 & R \\
 0 & 0 & 0 & 0 & 0 & 0 \\
 0 & 625 & 625 & -625 & -625 & 0 \\
 0 & 625 & 625 & -625 & -625 & 0 \\
 0 & -625 & -625 & 625 & 625 & 0 \\
 0 & -625 & -625 & 625 & 625 & 0 \\
 0 & 0 & 0 & 0 & 0 & 0
 \end{bmatrix}$$

In the matrix above the two orange rows can be summed together with element wise addition and replaced with a single effective row that represents an effective inductor. The two blue rows can be summed together with element wise addition and be replaced by a single row that represents an effective capacitor row as seen below:

$$\begin{array}{c}
 S \\
 L_{effective} \\
 C_{effective} \\
 R
 \end{array}
 \begin{bmatrix}
 S & L1 & L2 & C1 & C2 & R \\
 0 & 0 & 0 & 0 & 0 & 0 \\
 0 & 1250 & 1250 & -1250 & -1250 & 0 \\
 0 & -1250 & -1250 & 1250 & 1250 & 0 \\
 0 & 0 & 0 & 0 & 0 & 0
 \end{bmatrix}$$

Now the columns of the matrix also need to be reduced in the same manner to result in a square matrix once again. In the matrix below the orange columns can be combined with element wise addition to represent an effective inductor column and the blue columns can be combined with element wise addition to represent an effective capacitor column.

$$\begin{array}{c}
 S \\
 L_{effective} \\
 C_{effective} \\
 R
 \end{array}
 \begin{bmatrix}
 S & L1 & L2 & C1 & C2 & R \\
 0 & 0 & 0 & 0 & 0 & 0 \\
 0 & 1250 & 1250 & -1250 & -1250 & 0 \\
 0 & -1250 & -1250 & 1250 & 1250 & 0 \\
 0 & 0 & 0 & 0 & 0 & 0
 \end{bmatrix}$$

This results in the final reduced covariance matrix for the SEPIC as seen below:

$$\begin{array}{c} S \\ L_{effective} \\ C_{effective} \\ R \end{array} \begin{array}{c} S \\ L_{effective} \\ C_{effective} \\ R \end{array} \begin{bmatrix} 0 & 0 & 0 & 0 \\ 0 & 1500 & -1500 & 0 \\ 0 & -1500 & 1500 & 0 \\ 0 & 0 & 0 & 0 \end{bmatrix}$$

Displaying the results side by side with the buck converter it is easier to compare the matrices along the same dimensions. Notice the zero sum property is still maintained and this new matrix for the SEPIC is an effective representation of the original matrix only with fewer dimensions allowing for easier comparisons.

$$\begin{array}{c} S \\ L \\ C \\ R \end{array} \begin{array}{c} S \\ L \\ C \\ R \end{array} \begin{bmatrix} 625 & -625 & 0 & 0 \\ -625 & 625 & 0 & 0 \\ 0 & 0 & 0 & 0 \\ 0 & 0 & 0 & 0 \end{bmatrix}$$

Figure 20: Buck converter Covariance matrix

$$\begin{array}{c} S \\ L_{effective} \\ C_{effective} \\ R \end{array} \begin{array}{c} S \\ L_{effective} \\ C_{effective} \\ R \end{array} \begin{bmatrix} 0 & 0 & 0 & 0 \\ 0 & 1500 & -1500 & 0 \\ 0 & -1500 & 1500 & 0 \\ 0 & 0 & 0 & 0 \end{bmatrix}$$

Figure 21: SEPIC converter Covariance matrix

It is now clear to see the buck converter has smaller interactions and component “power activity” than the SEPIC. The spread of power interactions in both converters is minimal and is concentrated between two components. The buck converter is the better choice at this operating point based on the magnitude of the power interactions in the converter. This conclusion is easier to observe after the reduction of the matrix.

2.3.1 Using the reduction property to interpret results

These effective representations created from reduction may be compared as long as components have the same positive/negative sign in their entries are being grouped i.e only grouping rows/columns with all positive entries and only grouping rows/columns with only negative entries. For example in a topology where an inductor and a capacitor both have the same positive or negative signs in each entry in their respective rows and columns they may be reduced. It is not advisable to reduce rows/columns that have opposite signs in their entries. [Figure 22](#) and [Figure 23](#) below show the difference this can make using the SEPIC covariance matrix.

$$\begin{array}{c} S \\ L_{effective} \\ C_{effective} \\ R \end{array} \begin{array}{c} S \\ L_{effective} \\ C_{effective} \\ R \end{array} \begin{bmatrix} 0 & 0 & 0 & 0 \\ 0 & 1500 & -1500 & 0 \\ 0 & -1500 & 1500 & 0 \\ 0 & 0 & 0 & 0 \end{bmatrix}$$

Figure 22: Reduced SEPIC Covariance matrix with effective inductor and capacitor

$$\begin{array}{c} S \\ L1,C1 \\ L2,C2 \\ R \end{array} \begin{array}{c} S \\ L1,C1 \\ L2,C2 \\ R \end{array} \begin{bmatrix} 0 & 0 & 0 & 0 \\ 0 & 0 & 0 & 0 \\ 0 & 0 & 0 & 0 \\ 0 & 0 & 0 & 0 \end{bmatrix}$$

Figure 23: Reduced SEPIC Covariance matrix with combined L1,C1 and combined L2,C2

The reduction of L1,C1 and L2,C2 reduces to an all zero matrix because the rows and columns being summed have opposite signs. This results in smaller entries in the matrix since information about the interactions is lost due to subtraction. The correct reduction is shown in [Figure 22](#) since entries of the same signs have been reduced to conserve the information about the power interactions.

The matrices of converters may often be able to be reduced into a simple 2×2 matrix where the entries are merely describing the total power processed by the entire converter. The equivalent SEPIC 2×2 matrix is shown below:

$$\begin{array}{l}
S, L_{effective} \\
R, C_{effective}
\end{array}
\begin{array}{l}
\begin{array}{l}
S, L_{effective} \\
R, C_{effective}
\end{array} \\
\begin{array}{l}
R, C_{effective} \\
S, L_{effective}
\end{array}
\end{array}
\begin{bmatrix}
1500 & -1500 \\
-1500 & 1500
\end{bmatrix}$$

It is now clear to see the total power interactions in the converter. This can be useful if the entries are spread across the matrix to create an effective total of the power processed for an entire converter. This simple matrix can be used to compare converters provided each topology is able to be reduced to such a state without “losing” information during the reduction process. In the case where a converter can not be reduced to a 2×2 , any dimension matrix can be created from the topologies in the comparison as long as they have the same dimensions to be able to compare the power interactions between the converters.

In general an $n \times n$ covariance matrix can be reduced to any $m \times m$ with the only condition that $m < n$. The reduced dimension m should be at least 2 since a 1×1 will yield a single entry of 0 due to the zero sum property of the matrix which is of no use to analyse.

Reduction is not always necessary and is completely up to the comparative problem at hand and the discretion of the engineer to decide if reduction is required to make the comparison easier. Where possible in this work matrices may be reduced to a 2×2 to make simple comparisons but in other cases it may be more interesting to make the matrices of each converter the same dimension in order to analyse the magnitude and spread of the entries across columns/rows. A generalized proof of the reduction property is provided in Appendix A.

2.4 Normalizing the matrix method

The covariance matrix can result in very large entries than can be distracting to analyse power processing patterns. The covariance matrix is able to scale proportionately with the output power of the converter as long as the conversion effort is the same. This property can be useful when comparing converters of different output power capabilities that have the same conversion effort. This property also allows the matrix to be normalized when analysing the results of the matrix. Normalizing will scale the numbers so they are smaller to deal with and easier to evaluate power processing patterns. The following example will demonstrate normalizing the covariance matrix. The results used in this example have been captured from LTSpice and the zero sum-line property will only approximate zero.

In this experiment a 100 W and a 350 W 3X step up boost converter are designed. They both have the same 30 % inductor current ripple and 10 % capacitor voltage ripple. They boost 50 V to 150 V. Figure 24 shows the boost converter topology with the covariance matrices for each case to follow:

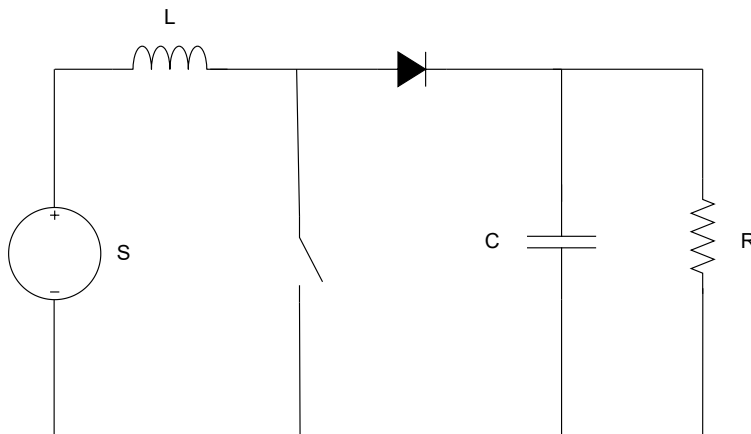


Figure 24: Boost converter

$$\begin{matrix} S & L & C & R \\ S & \begin{bmatrix} 0.01 & 10.07 & -10.01 & -0.01 \\ 10.07 & 20010.93 & -19876.81 & -29.62 \\ -10.01 & -19876.81 & 19743.59 & 29.42 \\ -0.01 & -29.62 & 29.42 & 0.04 \end{bmatrix} \\ L \\ C \\ R \end{matrix}$$

Figure 25: Boost converter 3X @ 100W step up.

$$\begin{matrix} S & L & C & R \\ S & \begin{bmatrix} 0.06 & 119.99 & -119.16 & -0.18 \\ 119.99 & 244433.41 & -242753.23 & -368.16 \\ -119.16 & -242753.23 & 241084.6 & 365.63 \\ -0.18 & -368.16 & 365.63 & 0.55 \end{bmatrix} \\ L \\ C \\ R \end{matrix}$$

Figure 26: Boost converter 3X @350 W step up

These matrices appear to represent different power processing in the same topology for the same conversion effort. This is because these matrices are currently being compared at different output powers. To make a valid comparison each matrix can be normalized to its respective output power. If each matrix is normalized to P_{out}^2 then each entry in the matrix is unit-less and represents a ratio of the power processing each entry describes to the output power of the converter. The matrices below have been normalized to P_{out}^2 :

$$\begin{matrix} S & L & C & R \\ S & \begin{bmatrix} 0 & 0 & 0 & 0 \\ 0 & 2.00 & -1.99 & 0 \\ 0 & -1.99 & 1.97 & 0 \\ 0 & 0 & 0 & 0 \end{bmatrix} \\ L \\ C \\ R \end{matrix}$$

Figure 27: Boost converter 3X @ 100W step up.

$$\begin{matrix} S & L & C & R \\ S & \begin{bmatrix} 0 & 0 & 0 & 0 \\ 0 & 2.00 & -1.98 & 0 \\ 0 & -1.98 & 1.97 & 0 \\ 0 & 0 & 0 & 0 \end{bmatrix} \\ L \\ C \\ R \end{matrix}$$

Figure 28: Boost converter 3X @350 W step up.

The normalized covariance matrices are the same now with the exception of slight rounding error. This is because each topology is still operating at the same 3X conversion effort. By normalizing each matrix to the square of the output power, the covariance matrix represents the power interactions independently of output power. The power processing patterns are now the same after normalizing because the topology and the conversion effort are unchanged. This is because the entries in the covariance matrix are closely related to the gain of the converter and as long as the converters are operating at the same conversion effort then the power at the terminals is essentially a scaling factor for the entries in the matrix. Therefore the topology still needs to process power relative to the conversion effort of the converter. These results show the covariance matrix scales linearly with the output power. This means that the covariance matrix is independent of output/input power and that the matrix can be normalized to a power quantity that is common to all converters in a comparative example.

2.5 Zero-ripple approximations as a baseline comparison

The matrix method relies on the covariance as a metric for comparing the power processing of converter topologies. The covariance only captures the varying portion of the power waveforms in each component. This means that any ripple in the current or voltage waveforms of a component or terminal characteristic will be reflected in the covariance matrix. This may not always paint a clear picture of how the topology fundamentally processes power. A zero ripple approximation of a topology may represent the smallest amount of power processing allowing topologies to truly be compared by their structure.

A zero ripple approximation is an equivalent circuit with a capacitor and inductor so large that there is no ripple on these components and are equivalent to a constant average value. This means the inductor can be replaced with a constant current source of the same value as the average value of the inductor. The capacitor can be replaced with a constant voltage source of the same value as the average value of the capacitor. The boost converter and its equivalent zero ripple approximation are shown symbolically in [Figure 29](#).

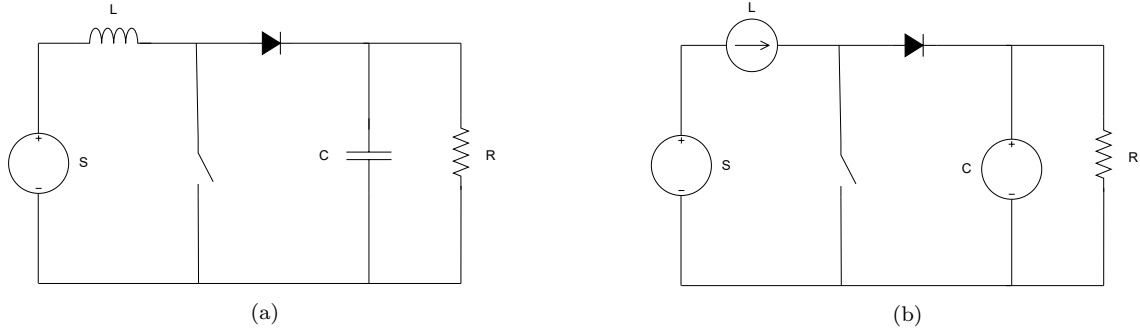


Figure 29: (a) represents a boost converter and (b) represents a zero ripple boost converter

To investigate this consider the boost converter and a quadratic boost converter using a zero ripple approximation. A quadratic boost converter is a type of boost converter that has its duty cycle increase quadratically. This means it can achieve higher boost ratios than a traditional boost converter since low duty cycles in the quadratic boost are exponentially greater than the boost ratios in a normal boost converter [34]. The quadratic boost converter is chosen to compare with the boost converter for its more complex topology structure with reportedly better ripple control at higher boost ratios. The circuit diagrams for each converter are shown below along with a table of operating conditions

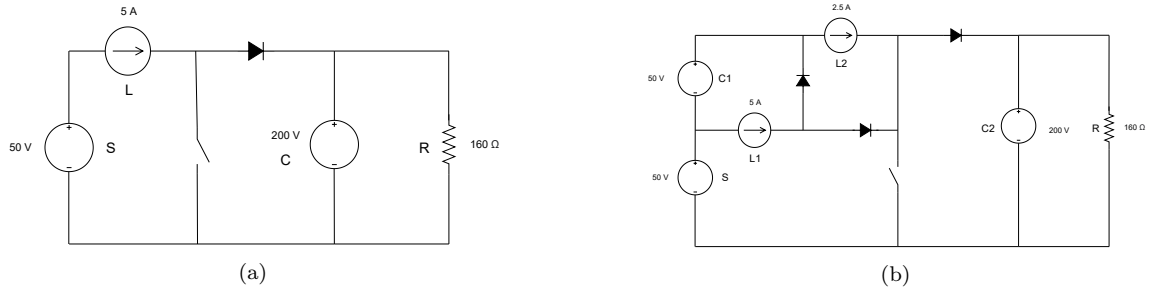


Figure 30: (a) represents a zero ripple boost approximation and (b) represents a zero ripple quadratic boost approximation

Table 1: Table of test conditions

Converter parameter	Value
V_{in}	50 V
V_{out}	200 V
P_{out}	250 W
f_s	100 kHz
Δi_L	0 %
Δv_c	0 %

First the zero ripple approximation of each converter is simulated and their covariance matrices are calculated, normalized and shown below.

$$\begin{array}{c}
S \\
L \\
C \\
R
\end{array}
\begin{array}{c}
S \\
L \\
C \\
R
\end{array}
\begin{array}{c}
C \\
R
\end{array}
\begin{array}{c}
R \\
R
\end{array}
\begin{array}{c}
R \\
R \\
R \\
R
\end{array}
\left[\begin{array}{cccc}
0 & 0 & 0 & 0 \\
0 & 3.01 & -3.00 & 0 \\
0 & -3.00 & 2.98 & 0 \\
0 & 0 & 0 & 0
\end{array} \right]$$

Figure 31: Boost converter zero ripple

$$\begin{array}{c}
S \\
L1,L2 \\
C1,C2 \\
R
\end{array}
\begin{array}{c}
S \\
L1,L2 \\
C1,C2 \\
R
\end{array}
\begin{array}{c}
L1,L2 \\
C1,C2 \\
R
\end{array}
\begin{array}{c}
R \\
R \\
R \\
R
\end{array}
\begin{array}{c}
R \\
R \\
R \\
R
\end{array}
\left[\begin{array}{cccc}
0.25 & -1.00 & 0.75 & 0 \\
-1.00 & 3.99 & -2.99 & 0 \\
0.75 & -2.99 & 2.24 & 0 \\
0 & 0 & 0 & 0
\end{array} \right]$$

Figure 32: Quadratic boost converter ripple

These covariance matrices describe what power interactions are a minimum requirement to achieve the conversion effort. Since there is no ripple in this simulation the fluctuations of the powers are as minimal as they could be. This means that when ripple is added into the system the fluctuations will be larger. Some converters produce better ripple than others at the same conversion effort. For example the boost converter is well known for struggling with ripple at high conversion effort. For comparison the matrices below are the same two converters simulated with an inductor current ripple of 30% and capacitor voltage ripple of 10%:

$$\begin{array}{c}
S \\
L \\
C \\
R
\end{array}
\begin{array}{c}
S \\
L \\
C \\
R
\end{array}
\begin{array}{c}
C \\
R
\end{array}
\begin{array}{c}
R \\
R
\end{array}
\begin{array}{c}
R \\
R \\
R \\
R
\end{array}
\left[\begin{array}{cccc}
0 & 0 & 0 & 0 \\
0 & 3.05 & -3.04 & 0 \\
0 & -3.04 & 3.02 & 0 \\
0 & 0 & 0 & 0
\end{array} \right]$$

Figure 33: Boost converter with ripple

$$\begin{array}{c}
S \\
L1,L2 \\
C1,C2 \\
R
\end{array}
\begin{array}{c}
S \\
L1,L2 \\
C1,C2 \\
R
\end{array}
\begin{array}{c}
L1,L2 \\
C1,C2 \\
R
\end{array}
\begin{array}{c}
R \\
R \\
R \\
R
\end{array}
\begin{array}{c}
R \\
R \\
R \\
R
\end{array}
\left[\begin{array}{cccc}
0.27 & -1.05 & 0.78 & 0 \\
-1.05 & 4.13 & -3.06 & -0.02 \\
0.78 & -3.06 & 2.27 & 0.01 \\
0 & -0.02 & 0.01 & 0
\end{array} \right]$$

Figure 34: Quadratic boost converter with ripple

Note that even though there is a 30% current ripple on the boost converter source current due to the inductor, the source still contains a zero entry in the covariance matrix because the ripple is small enough that it approaches zero after normalizing the matrix. The source does contain non-zero entries prior to normalizing as seen in the extended results in Appendix F.4.

Now these matrices are a representation of what the power interactions would look like when realized in a physical system with ripple. The impact of ripple is small but not negligible. Especially in the case of the quadratic boost. This suggests the quadratic boost requires more power interactions to cope with the ripple in the system at this operating point. This is seen in the magnitudes of the entries in the quadratic boost covariance matrix. This means that a zero ripple approximation of a topology could be the most ideal case for how the topology structure influences power processing, since ripple may be incurred as a result of topology structure. This means topologies can be compared with each other based fundamentally on their structure using a zero ripple approximation as it negates the the “correct” sizing of reactive filtering volume in the converter.

The zero ripple approximation can be used in initial topology selection to evaluate which topology structures are better suited for power processing before component selection and even sizing of reactive volume. The caveat is that the zero-ripple approximation may give great results but a converter may struggle with ripple at the particular operating points which would yield unfavourable results when reactive volume is calculated.

2.5.1 Determining what a “good” topology looks like

The previous subsections have outlined the matrix method and covered all its intended uses and properties. This method has been developed as a comparative tool to help in the topology selection process. In order to compare topologies a sense of a “winner” is needed to make a final decision. In this example a boost and a quadratic boost converter will be examined to decide on a winning topology for a particular application. The same covariance matrices used earlier in this subsection will be compared with each other. These are the examples conducted with inductor current ripple of 30% and capacitor voltage ripple of 10%. They are displayed below again for convenience

$$\begin{array}{c}
S \\
L \\
C \\
R
\end{array}
\begin{array}{c}
S \\
L \\
C \\
R
\end{array}
\begin{array}{c}
L \\
C \\
R
\end{array}
\begin{array}{c}
C \\
R
\end{array}
\begin{array}{c}
R \\
\end{array}
\begin{array}{c}
0 \\
0 \\
0 \\
0
\end{array}
\begin{array}{c}
0 \\
3.05 \\
-3.04 \\
0
\end{array}
\begin{array}{c}
-3.04 \\
3.02 \\
0 \\
0
\end{array}
\begin{array}{c}
0 \\
0 \\
0 \\
0
\end{array}
\end{array}$$

Figure 35: Boost converter with ripple

$$\begin{array}{c}
S \\
L1,L2 \\
C1,C2 \\
R
\end{array}
\begin{array}{c}
S \\
L1,L2 \\
C1,C2 \\
R
\end{array}
\begin{array}{c}
L1,L2 \\
C1,C2 \\
R
\end{array}
\begin{array}{c}
C1,C2 \\
R
\end{array}
\begin{array}{c}
R \\
\end{array}
\begin{array}{c}
0.27 \\
-1.05 \\
0.78 \\
0
\end{array}
\begin{array}{c}
-1.05 \\
4.13 \\
-3.06 \\
-0.02
\end{array}
\begin{array}{c}
0.78 \\
-3.06 \\
2.27 \\
0.01
\end{array}
\begin{array}{c}
0 \\
-0.02 \\
0.01 \\
0
\end{array}
\begin{array}{c}
0 \\
-0.02 \\
0.01 \\
0
\end{array}
\end{array}$$

Figure 36: Quadratic boost converter with ripple

It is clear to see that the boost converter has all of its interactions concentrated between only two components, where the quadratic boost converter has interactions spread across the entries of the matrix. This means the boost converter has very localized power interactions suggesting fewer current loops that may cause unnecessary power processing. This was outlined as one of the key aspects to look for in the results in Section 2. This difference suggests the quadratic boost has many current loops where power is fluctuating between all of the components which is why most of the entries are non-zero. It shows that the source has a larger fluctuating power than the boost converter as the source entries are non-zero. The inductors and capacitors in the quadratic boost are exchanging the bulk of the power in the converter with large power interactions between them. By comparison the source entries of the boost converter are smaller than the quadratic boost which means it is much less susceptible to input current fluctuations as it has a filter inductor at the input. This suggests the boost converter is better than the quadratic boost for input fluctuations if input fluctuations are a concern for a particular application.

The other key aspect to look for is the magnitude of the entries in the matrix. The boost converter has smaller entries than the quadratic boost especially when it comes to the entry for the inductors. This suggests the quadratic boost has large power fluctuations inside the inductors. This suggests more power processing is occurring in the quadratic boost converter than in the boost converter. This can also be seen using the fully reduced 2×2 matrices for each converter as shown below.

$$\begin{array}{c}
S,L \\
C,R
\end{array}
\begin{array}{c}
S,L \\
C,R
\end{array}
\begin{array}{c}
C,R \\
\end{array}
\begin{array}{c}
C,R \\
\end{array}
\begin{array}{c}
3.05 \\
-3.04 \\
-3.04 \\
3.02
\end{array}
\begin{array}{c}
-3.04 \\
3.02 \\
\end{array}
\end{array}$$

Figure 37: Boost converter with ripple

$$\begin{array}{c}
S,C1,C2,R \\
L1,L2
\end{array}
\begin{array}{c}
S,C1,C2,R \\
L1,L2
\end{array}
\begin{array}{c}
L1,L2 \\
\end{array}
\begin{array}{c}
L1,L2 \\
\end{array}
\begin{array}{c}
4.12 \\
-4.12 \\
-4.12 \\
4.13
\end{array}
\begin{array}{c}
-4.12 \\
4.13 \\
\end{array}
\end{array}$$

Figure 38: Quadratic boost converter with ripple

Now it is clear to see that when reduced to a 2×2 the boost converter appears to process less power than the quadratic boost converter at this operating point because the magnitude of the power interactions are smaller than the quadratic boost converter. This smaller matrix describes all the power processed in this converter as an effective total.

In a comparative study between converters using the matrix method, the best option in terms of power processing will be the matrix with the smallest entries (on the whole). This implies the least amount of processed power. The spread of the entries across the rows/columns should be as small as possible as this implies the converter has little circulating power possibly leading to unnecessary power processing. In this comparison the boost converter is the better topology to choose at this operating point with the included ripple due to the low spread of power processing across the converter as well as smaller entries on the whole.

2.6 Boost converter example using the matrix method

This example will run through a complete numerical example of applying the matrix method to a converter as well as using reduction and normalization in the end to combine all these concepts. Two topologies are examined in this example. A regular boost converter and a boost converter with four output capacitors in parallel to illustrate the use of reduction. The extended parallel capacitors sum to the same effective capacitance as the capacitor in the traditional boost converter topology. From an electrical point of view these are the exact same converter. This of course makes no difference to the performance of the converter with no parasitic effects, but

it will increase the dimensions of the boost converter covariance matrix for the extended capacitor case. This example is simulated in LTSpice with ideal components and will be subject to round off and sampling error. The zero sum-line property approximates zero.

Below is a table of converter specifications for the boost example analysis to follow:

Table 2: Boost converter example specifications

Specification	Value
V_{in}	50 V
V_{out}	200 V
P_{out}	500 W
R	80 Ω
Δ_{i_L}	30%
Δ_{v_C}	1%

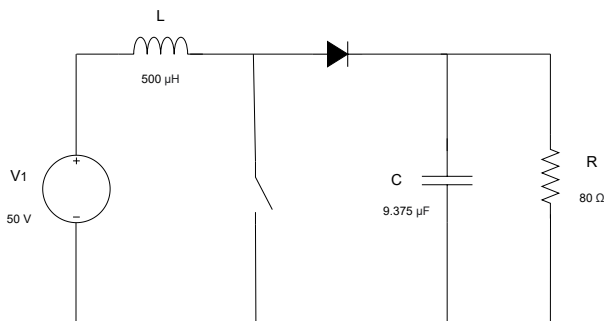


Figure 39: Boost converter

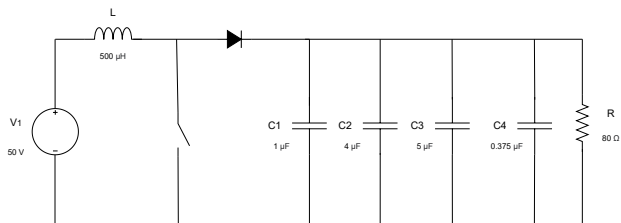


Figure 40: Boost converter with extended parallel capacitors

Each converter is simulated in LTSpice and the current and voltage waveforms are recorded over a switching interval. The current and voltage waveforms can be multiplied together to achieve the power waveform of each component. Using these power waveforms the covariance matrix for each boost converter is calculated and shown below:

$$\begin{matrix} & V1 & L & C & R \\
V1 & \left[\begin{array}{cccc} 0.01 & 69.38 & -69.08 & 0.0 \\ 69.38 & 766180.47 & -762848.57 & -21.29 \\ -69.08 & -762848.57 & 759531.17 & 21.19 \\ 0.0 & -21.29 & 21.19 & 0.0 \end{array} \right] \\
L & & & & \\
C & & & & \\
R & & & &
\end{matrix}$$

Figure 41: Boost converter

$$\begin{matrix} & V1 & L & C1 & C2 & C3 & C4 & R \\
V1 & \left[\begin{array}{ccccccccc} 0.01 & 67.87 & -6.51 & -26.05 & -32.57 & -2.44 & -0.0 \\ 67.87 & 766205.11 & -73530.03 & -294120.12 & -367650.15 & -27573.76 & -18.86 \\ -6.51 & -73530.03 & 7056.42 & 28225.68 & 35282.1 & 2646.16 & 1.81 \\ -26.05 & -294120.12 & 28225.68 & 112902.72 & 141128.4 & 10584.63 & 7.24 \\ -32.57 & -367650.15 & 35282.1 & 141128.4 & 176410.5 & 13230.79 & 9.05 \\ -2.44 & -27573.76 & 2646.16 & 10584.63 & 13230.79 & 992.31 & 0.68 \\ -0.0 & -18.86 & 1.81 & 7.24 & 9.05 & 0.68 & 0.0 \end{array} \right] \\
L & & & & & & & \\
C1 & & & & & & & \\
C2 & & & & & & & \\
C3 & & & & & & & \\
C4 & & & & & & & \\
R & & & & & & &
\end{matrix}$$

Figure 42: Boost converter with extended capacitors

In order to compare these matrices the extended capacitors can be reduced to an equivalent capacitor so the dimensions of each converters covariance matrix are the same. Rows 3,4,5,6 are summed together using regular element wise addition to create an effective row. Rows 3,4,5,6 are then replaced with this new single row. Then columns 3,4,5,6 are summed together using element wise addition to create an effective column. The columns 3,4,5,6 are then replaced with this new column. This yields the following reduced 4×4 matrix.

$$\begin{matrix} & V1 & L & C & R \\
V1 & \left[\begin{array}{cccc} 0.01 & 69.38 & -69.08 & 0.0 \\ 69.38 & 766180.47 & -762848.57 & -21.29 \\ -69.08 & -762848.57 & 759531.17 & 21.19 \\ 0.0 & -21.29 & 21.19 & 0.0 \end{array} \right] \\
L & & & & \\
C & & & & \\
R & & & &
\end{matrix}$$

Figure 43: Boost converter

$$\begin{matrix} & V1 & L & C_{effective} & R \\
V1 & \left[\begin{array}{cccc} 0.01 & 67.87 & -67.57 & 0 \\ 67.87 & 766205.11 & -762874.06 & -18.86 \\ -67.57 & -762874.06 & 759557.47 & 18.78 \\ 0 & -18.86 & 18.78 & 0 \end{array} \right] \\
L & & & & \\
C_{effective} & & & & \\
R & & & &
\end{matrix}$$

Figure 44: Boost converter with extended capacitors reduced

Now each matrix can be normalized the output power of $(500W)^2$. This results in the covariance matrices below.

$$\begin{array}{c}
V1 \\
L \\
C \\
R
\end{array}
\begin{bmatrix}
V1 & L & C & R \\
0 & 0 & 0 & 0 \\
0 & 3.06 & -3.05 & 0 \\
0 & -3.05 & 3.03 & 0 \\
0 & 0 & 0 & 0
\end{bmatrix}$$

Figure 45: Normalized boost converter

$$\begin{array}{c}
V1 \\
L \\
C_{effective} \\
R
\end{array}
\begin{bmatrix}
V1 & L & C_{effective} & R \\
0 & 0 & 0 & 0 \\
0 & 3.06 & -3.05 & 0 \\
0 & -3.05 & 3.03 & 0 \\
0 & 0 & 0 & 0
\end{bmatrix}$$

Figure 46: Reduced and normalized Boost converter with extended capacitors

Now it is clear to see that these matrices represent the exact same converter from an electrical and power processing perspective. Since the extended capacitors are electrically the same as a single capacitor of the equivalent value, the covariance matrix reduces to same power processing picture as the non-extended boost converter. Reduction has made it easy to compare the covariance matrices of each converter. Normalizing the matrices removes the large distracting numbers to focus on where the important power interactions are occurring. Two more examples on the reduction property used in this boost converter are available in Appendix B.

3 The matrix method and existing research

The matrix method has been inspired by the recent work on differential power methods by Cobos et al. The matrix method has possible links to differential power methods that will be explored in this chapter.

The ideas of differential power processing have been around for quite some time. Originating with Wilson's paper on *Basic Considerations for DC to DC Conversion Networks* in 1966 which was subsequently proven by Wolaver in *Fundamental Study of DC to DC Conversion Systems* in 1969 [20, 21]. Simply put the idea is that not all power that enters a converter has to be processed and some portion of the power may be able to be passed directly from source to load without being processed. This is achieved via a direct line of current between source and load in a switching state where DC power can be transferred straight through the reactive components.

The output power of the converter therefore consists of some portion of power that had to be processed and some portion that has been passed through directly to the load. Converter systems can be configured to process a certain minimum amount of power. Each topology has a fundamental limit of power that is required to be processed and cannot be avoided. This is a result of the structure of the topology. This power is known as "Differential Power". In practice the actual power processed by a topology is more than the fundamental limit as a result of non-ideal operating conditions. The goal of this method is to design topologies in such a way that their processed power approaches this fundamental limit.

Cobos et al. have recently rediscovered these principles and have put this idea to work in recent literature. Their extension on these methods divides the power processed by a converter into three categories. Differential power as the fundamental lower limit that a topology must process in order to fulfil its conversion. Direct power as the portion of the power that may be transferred from source to load without contributing to the converter's losses. This power is not processed, does not require storage in reactive components and is transferred directly from source to load. Direct power requires a direct line of current between source and load during a switching state. The direct line of current is merely a circuit connection between source and load that allows a loop current to join both circuit elements. Some topologies have a direct line of current such as the boost converter in the off state. Other topologies such as the buck-boost converter are not able to achieve direct power as there is no direct loop current between source and load in either switching state. This means the buck-boost converter must process all of its power since there is no direct line of current.

Finally, Indirect power is the third category and is defined as the actual power that is processed by the converter in a system that is not operating at the fundamental limit of differential power. This means indirect power is greater than or equal to differential power when the topology is not in a completely ideal scenario. Direct and indirect power transfer in a boost converter are shown in *Figure 47* below. The blue arrow shows the direct power transferred from source to load that skips the reactive components. The orange arrow shows indirect power that is processed by the reactive components before appearing at the load. The blue dotted line shows the direct line of current between source and load in the off state of the boost converter that allows for direct power to be transferred. Differential power is not depicted in the figure as differential power is the theoretical lower limit of indirect power, it is a baseline of what has to be processed where indirect power is what is actually processed in a real system.

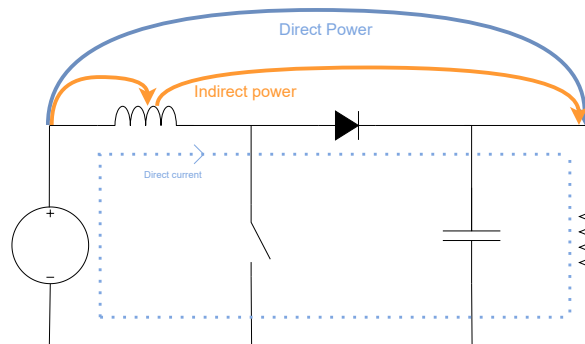


Figure 47: Direct and indirect power transfer in a boost converter

An in-depth outline of how these principles can be applied to converters is described in Appendix D. It is possible to identify these differential power definitions in both the buck and boost converter using an analytical approach to the matrix method. The boost converter will be used in the example to follow to demonstrate this link while the buck converter is analysed in Appendix E

3.1 Linking the matrix method and differential power: Boost Converter

This experiment will characterize a boost converter as a zero ripple approximation to allow for a simple mathematical analysis of the power waveforms in the converter. The mathematical expressions for the power quantities in each component will be linked to concepts from differential power methods such as direct, indirect and differential power.

Using the zero ripple approximation Figure 48 below shows the simplification of a Boost converter and its respective on and off state forms:

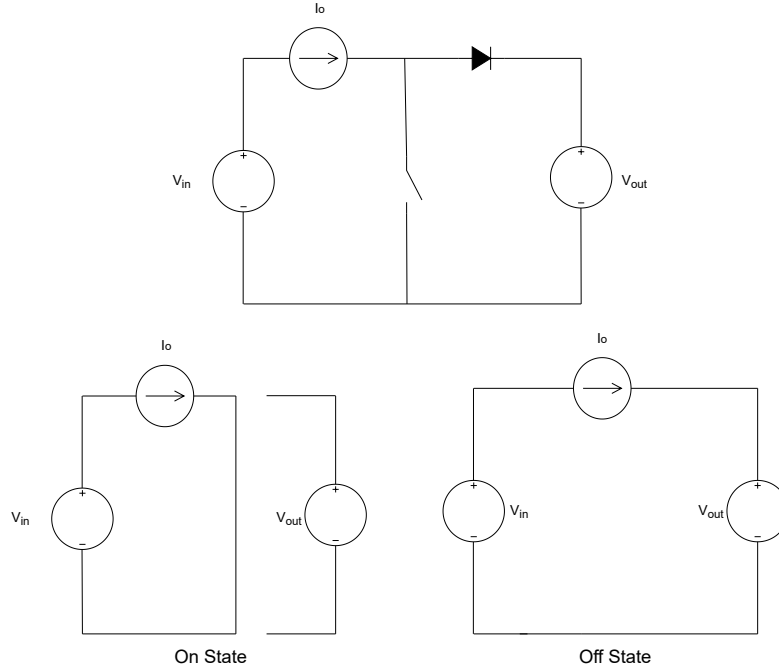


Figure 48: Diagram of the simplification of a Boost converter using the zero ripple approximation

In the proceeding analysis ‘S’ denotes the input source, ‘L’ denotes the load source and the current source in the middle is to be denoted by ‘X’. The on and off times refer to the duty cycle causing switching states. The input and output voltage of a Boost converter are related by the following equation:

$$V_{out} = \frac{V_{in}}{1 - D}$$

Now the power waveforms per state can be tabulated as follows:

Table 3: Table of on and off state powers

State	P_S	P_X	P_L
On State	$-V_{in} \frac{I_o}{1-D}$	$V_{in} \frac{I_o}{1-D}$	$-V_{out} I_o$
Off State	$-V_{in} \frac{I_o}{1-D}$	$(V_{in} - V_{out}) \frac{I_o}{1-D}$	$V_{out} (\frac{I_o}{1-D} - I_o)$

Analytically the covariance matrix can be derived as follows. For more about how this is derived the buck converter example is shown in full detail in Appendix E:

$$\begin{matrix} S \\ X \\ L \end{matrix} \begin{bmatrix} S & X & L \\ 0 & 0 & 0 \\ 0 & \frac{-D(I_{out}V_{in})^2}{(D-1)^3} & \frac{D(I_{out}V_{in})^2}{(D-1)^3} \\ 0 & \frac{D(I_{out}V_{in})^2}{(D-1)^3} & \frac{-D(I_{out}V_{in})^2}{(D-1)^3} \end{bmatrix}$$

Cobos et al. define the boost converter as the most basic step up cell with the following differential power definitions.

$$P_{diff} = (G - 1)V_{in}I_o$$

$$P_{dir} = V_{in}I_o$$

$$G = \max\left(\frac{I_{out}}{I_{in}}, \frac{V_{out}}{V_{in}}\right)$$

P_{diff} is differential power, P_{dir} is direct power and G is the gain of the converter.

The matrix above can be manipulated to align with cobos' definitions of power. Making the substitutions for $V_{out} = \frac{V_{in}}{(1-D)}$, $I_o = (1 - D)I_{in}$ and $D = 1 - \frac{1}{G}$ gives the following matrix

$$\begin{matrix} S \\ X \\ L \end{matrix} \begin{bmatrix} S & X & L \\ 0 & 0 & 0 \\ 0 & G^2(I_oV_{in})^2(G-1) & -G^2(I_oV_{in})^2(G-1) \\ 0 & -G^2(I_oV_{in})^2(G-1) & G^2(I_oV_{in})^2(G-1) \end{bmatrix}$$

Substituting in for P_{diff} and P_{dir} the following covariance matrix is achieved:

$$\begin{matrix} S \\ X \\ L \end{matrix} \begin{bmatrix} S & X & L \\ 0 & 0 & 0 \\ 0 & G^2P_{dir}P_{diff} & -G^2P_{dir}P_{diff} \\ 0 & -G^2P_{dir}P_{diff} & G^2P_{dir}P_{diff} \end{bmatrix}$$

This suggests the entries of the matrix method may be able to be described in terms of differential power definitions. To further this example consider the zero-ripple boost converter from earlier with the following covariance matrix:

$$\begin{matrix} V1 \\ L \\ C \\ R \end{matrix} \begin{bmatrix} V1 & L & C & R \\ 0 & 0 & 0 & 0 \\ 0 & 3.01 & -3.00 & 0 \\ 0 & -3.00 & 2.98 & 0 \\ 0 & 0 & 0 & 0 \end{bmatrix}$$

The relevant operating characteristics for this converter are as follows:

Table 4: Table of test conditions

Converter parameter	Value
V_{in}	50 V
V_{out}	200 V
P_{out}	250 W
f_s	100 kHz
Δi_L	0 %
Δv_c	0 %

Using the definitions for P_{diff} , P_{dir} and G stated earlier they can be calculated for the operating conditions of the boost as:

$$\begin{aligned}
 G &= 4 \\
 P_{diff} &= 187.5 \text{ W} \\
 P_{dir} &= 62.5 \text{ W}
 \end{aligned}$$

Substituting these differential power values into the manipulated symbolic covariance matrix gives the following covariance matrix:

$$\begin{array}{c}
 S \\
 X \\
 L
 \end{array}
 \begin{bmatrix}
 S & X & L \\
 0 & 0 & 0 \\
 0 & 187500 & -187500 \\
 0 & -187500 & 187500
 \end{bmatrix}$$

Now normalizing the matrix by P_{out}^2 to achieve the same matrix as before:

$$\begin{array}{c}
 S \\
 X \\
 L
 \end{array}
 \begin{bmatrix}
 S & X & L \\
 0 & 0 & 0 \\
 0 & 3 & -3 \\
 0 & -3 & 3
 \end{bmatrix}$$

In the simple cases where differential power has clearly defined equations for P_{diff} and P_{dir} such as in the step down and step up converter cells it is easy to link these concepts to the matrix method. In more complicated converters where differential power methods do not eloquently describe the converters operation the analysis gets incredibly complex. The matrix method has not been investigated for links to differential power methods for any other converter cells other than the basic step up and step down and this may not be a generalized case. However, this example shows the potential link between the two theories and suggests the matrix method could be a superset of differential power since the matrix method can describe the differential powers.

4 Case studies

4.1 Introduction

This chapter will analyse a few scenarios of the application of the matrix method that make an interesting case for the method. This method was created from mainly analysing the boost step up converter so other converters will also be used to extend the analysis to other topologies.

The first case study analyses various step up converters and how their topology structures differ in terms of power interactions. The boost and buck-boost were chosen for their simplicity and then some more complex converter topologies were chosen to contrast their performance on the assumption that more complex topologies will yield different covariance matrix results. The quadratic boost is a popular alternative to a boost converter for achieving higher boost ratios. Therefore two different kinds of quadratic boost converter are considered.

Following this, the application of the matrix method to step down converters is investigated. Once again the aim is to create the contrast in power processing between simple and complex topologies. The buck is chosen as the simplest step down converter. The SEPIC and CUK are also chosen as moderately complex topologies and finally a quadratic buck converter is chosen to provide significantly more complexity.

After these case studies investigate the differences in topology structure and the covariance matrix, a further example is investigated to determine the impact on power processing by slightly modifying a boost converter topology. This scenario is used to understand how subtle topology changes can influence the covariance matrix of a converter. The boost converter is chosen for simplicity.

After topology structure and the covariance matrix are analysed, the impact of duty cycle and the covariance matrix is investigated. The boost and a quadratic boost converter are tested here to combine both the contrast between simple and complex topologies as well as how changes in conversion effort influence the covariance matrix. Each converter is made to work harder by increasing the output voltage as a result of increasing the duty cycle. This creates an interesting scenario to investigate how a boost converter, known for bad performance at high duty ratios, compares to a converter that was designed specifically for high boost ratios. The use of step up converters in this study is inspired by high boost ratio converter research in the application to PV.

A prevalent issue with high boost ratio converters is the seemingly unavoidable ripple at high duty cycles. The impact of current and voltage ripple on the covariance matrix is investigated using a three stage approach of zero, moderate and high ripple conditions.

Finally the results of the previous case studies with the boost converter suggest overall good performance. Therefore two case studies are conducted to investigate potential improvements to the boost converter and their influence over the covariance matrix. First the comparison between a cascaded system and a single converter are investigated and finally the impact of interleaved inductors is studied as this is a popular design improvement in boost converters.

4.2 Interpretation of results

This chapter will outline multiple case studies and apply the matrix method to various scenarios of power converters. The covariance matrix of each converter scenario will be analysed and interpreted. In most cases the case-studies are comparative examples between converters. Interpreting the covariance matrix of each converter will be comparative in nature between the multiple covariance matrices in each case study. The key aspects to look for are the magnitude of the entries and the spread of the power interactions across rows and columns. The magnitude of the entries in each case study are comparable as each converter is simulated with the same output power. Where possible matrices will be reduced to a 2x2 to easily compare different converter topologies with multiple elements. All of the entries in the matrices are to be normalized to the square of the output power to scale the numbers in the matrices and make power interaction patterns easier to identify. Normalizing the matrix in this way also allows each entry to represent its role in producing one unit of output power. The

normalized matrices therefore show how much power is processed as a ratio of the output power of the converter.

The full unabridged results for each case study are available in Appendix F. Unless otherwise specified all case studies are captured using LTSpice waveform data. They will be vulnerable to the round off and sampling error and therefore there is some error margin in each matrix when conforming to the zero-sum property of the covariance matrix.

4.3 Step up converters

This case study analyses how different step up converter topologies process power to achieve the same conversion ratio. The boost, inverting buck-boost and two different types of quadratic boost converter are compared with each other with regards to power processing. Quadratic boost converter A appears in [34] and quadratic boost converter B appears in [35]. These two converters are presented as transformer-less high duty ratio boost converters that achieve better boost ratios than the normal boost converter. This is because the duty cycle increases quadratically which allows for higher boost ratios at a lower duty cycle which allows them to surpass the boost ratios of the normal boost converter with lower output ripple.

This case study highlights how processed power is affected by topology structure. Each converter will be configured to run at a 4X and a 10X step up ratio to show the differences between each converter as the conversion effort increases. Each of these experiments are simulated using LTSpice under ideal conditions without parasitic effects. The circuit diagrams for each converter are shown in *Figure 49* to *Figure 52*. The test conditions for each converter are shown in *Table 5*.

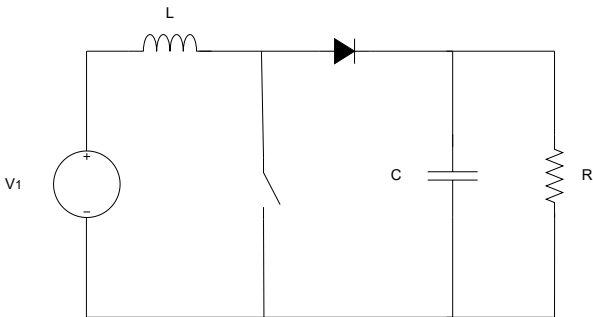


Figure 49: Boost converter

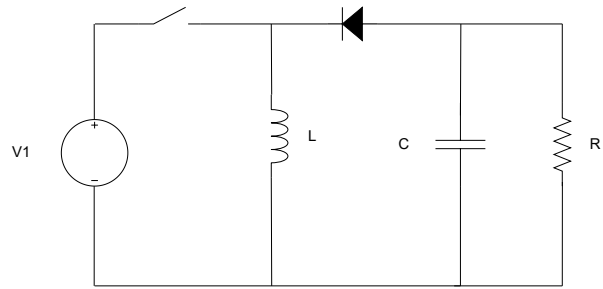


Figure 50: Buck-boost converter

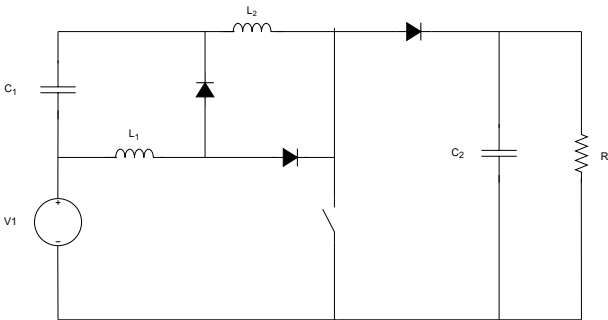


Figure 51: Quadratic boost converter A

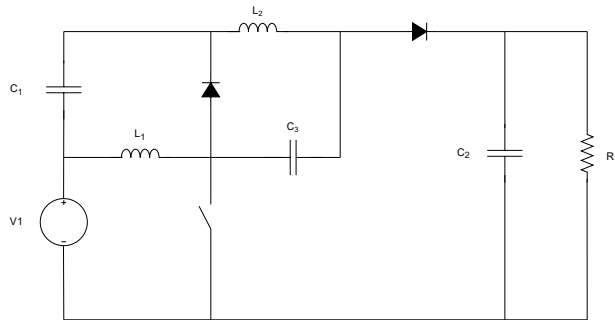


Figure 52: Quadratic boost converter B

Table 5: Table of test conditions

Converter parameter	Value
V_{in}	50 V
P_{out}	250 W
f_s	100 kHz
Δi_L	30 %
Δv_c	10 %

For the 4X step up ratio (50 V to 200 V) case the covariance matrix for each converter is shown below:

$$\begin{matrix} & V_{1,L} & C,R \\ V_{1,L} & \begin{bmatrix} 3.09 & -3.08 \\ -3.08 & 3.07 \end{bmatrix} \end{matrix}$$

Figure 53: Boost converter 4X step up.

$$\begin{matrix} & V_{1,C,R} & L \\ V_{1,C,R} & \begin{bmatrix} 6.46 & -6.48 \\ -6.48 & 6.51 \end{bmatrix} \\ L & \end{matrix}$$

Figure 54: Buck-boost converter 4X step up

$$\begin{matrix} & V_{1,C1,C2,R} & L_{1,L2} \\ V_{1,C1,C2,R} & \begin{bmatrix} 4.29 & -4.30 \\ -4.30 & 4.30 \end{bmatrix} \\ L_{1,L2} & \end{matrix}$$

Figure 55: Quadratic boost converter A 4X step up

$$\begin{matrix} & V_{1,C2,C3,R} & L_{1,L2,C1} \\ V_{1,C2,C3,R} & \begin{bmatrix} 3.97 & -3.99 \\ -3.99 & 4.01 \end{bmatrix} \\ L_{1,L2,C1} & \end{matrix}$$

Figure 56: Quadratic boost converter B 4X step up.

These results show that the converter at this step up ratio that processes the least amount of power is the boost converter as it has the smallest entries in its covariance matrix. The buck-boost converter is then the converter that processes the most amount of power with quadratic converters A and B sitting in the middle. At this particular operating point it seems like the boost converter is the best choice based on the smallest numbers in the matrix. The worst converter to choose would be the buck-boost converter.

Now consider the 10X step up conversion ratio case. Below are the covariance matrices for each converter in the 10X step up conversion ratio scenario:

$$\begin{matrix} & V_{1,L} & C,R \\ V_{1,L} & \begin{bmatrix} 9.42 & -9.41 \\ -9.41 & 9.39 \end{bmatrix} \\ C,R & \end{matrix}$$

Figure 57: Boost converter 10X step up

$$\begin{matrix} & V_{1,C,R} & L \\ V_{1,C,R} & \begin{bmatrix} 11.87 & -11.89 \\ -11.89 & 11.91 \end{bmatrix} \\ L & \end{matrix}$$

Figure 58: Buck-boost converter 10X step up

$$\begin{matrix} & V_{1,C1,C2,R} & L_{1,L2} \\ V_{1,C1,C2,R} & \begin{bmatrix} 8.14 & -8.14 \\ -8.14 & 8.14 \end{bmatrix} \\ L_{1,L2} & \end{matrix}$$

Figure 59: Quadratic boost converter A 10X step up

$$\begin{matrix} & V_{1,C2,C3,R} & L_{1,L2,C1} \\ V_{1,C2,C3,R} & \begin{bmatrix} 11.36 & -11.39 \\ -11.39 & 11.41 \end{bmatrix} \\ L_{1,L2,C1} & \end{matrix}$$

Figure 60: Quadratic boost converter B 10X step up

These matrices suggest that at this higher operating point the boost converter is having to work harder and process more power. The size of the entries in the covariance matrix now show that quadratic boost converter A is the best choice with both the buck-boost and the quadratic boost converter B being the worst to choose.

These 2×2 matrices have shown the overall power interactions in each converter. Now consider the interactions between the components in the converters. In order to view these interactions the original covariance matrices are reduced to 4×4 matrices.

$$\begin{array}{c} V1 \\ L \\ C \\ R \end{array} \begin{bmatrix} V1 & L & C & R \\ 0 & 0 & 0 & 0 \\ 0 & 3.05 & -3.04 & 0 \\ 0 & -3.04 & 3.02 & 0 \\ 0 & 0 & 0 & 0 \end{bmatrix}$$

Figure 61: Boost converter 4X step up

$$\begin{array}{c} V1 \\ L \\ C \\ R \end{array} \begin{bmatrix} V1 & L & C & R \\ 0.25 & -1.25 & 1.00 & 0 \\ -1.25 & 6.33 & -5.05 & 0 \\ 1.00 & -5.05 & 4.03 & 0 \\ 0 & 0 & 0 & 0 \end{bmatrix}$$

Figure 62: Buck-boost converter 4X step up

$$\begin{array}{c} V1 \\ L1,L2 \\ C1,C2 \\ R \end{array} \begin{bmatrix} V1 & L1,L2 & C1,C2 & R \\ 0.27 & -1.05 & 0.78 & 0 \\ -1.05 & 4.13 & -3.06 & -0.02 \\ 0.78 & -3.06 & 2.27 & 0.01 \\ 0 & -0.02 & 0.01 & 0 \end{bmatrix}$$

Figure 63: Quadratic boost converter A 4X step up

$$\begin{array}{c} V1 \\ L1,L2,C3 \\ C1,C2 \\ R \end{array} \begin{bmatrix} V1 & L1,L2,C3 & C1,C2 & R \\ 0.09 & -0.62 & 0.52 & 0.01 \\ -0.62 & 4.10 & -3.40 & -0.06 \\ 0.52 & -3.40 & 2.82 & 0.05 \\ 0.01 & -0.06 & 0.05 & 0 \end{bmatrix}$$

Figure 64: Quadratic boost converter B 4X

The entries in these matrices have been normalized to P_{out}^2 . Each entry then describes how much power is being processed per unit of output power. The boost converter has the lowest amount of processing and the least amount of spread across its components. This implies that there is little power being circulated and potentially wasted during its conversion. The quadratic boost converters have lower processing than the buck-boost but higher processing than the boost converter. They also have their interactions spread out across the converter. This implies all the components are interacting to achieve conversion with greater potential for wasted processing.

The buck-boost converter has the highest amount of processing occurring as well as a much larger spread in the entries since there are large magnitude in each entry across the source row. The source entries in the first row and column of the buck-boost converter matrix show the source is acting like more of a reactive component than in the quadratic converters with larger entries.

Now consider the 4×4 matrices for the 10X case:

$$\begin{array}{c} V1 \\ L \\ C \\ R \end{array} \begin{bmatrix} V1 & L & C & R \\ 0 & 0 & 0 & 0 \\ 0 & 9.69 & -9.67 & 0 \\ 0 & -9.67 & 9.66 & 0 \\ 0 & 0 & 0 & 0 \end{bmatrix}$$

Figure 65: Boost converter 10X step up

$$\begin{array}{c} V1 \\ L \\ C \\ R \end{array} \begin{bmatrix} V1 & L & C & R \\ 0.10 & -1.10 & 1.00 & 0 \\ -1.10 & 12.12 & -10.99 & 0 \\ 1.00 & -10.99 & 9.97 & 0 \\ 0 & 0 & 0 & 0 \end{bmatrix}$$

Figure 66: Buck-boost converter 10X step up

$$\begin{array}{c}
V1 \\
L1,L2 \\
C1,C2 \\
R
\end{array}
\begin{bmatrix}
V1 & L1,L2 & C1,C2 & R \\
0.20 & -1.25 & 1.05 & 0 \\
-1.25 & 7.91 & -6.64 & -0.02 \\
1.05 & -6.64 & 5.57 & 0.02 \\
0 & -0.02 & 0.02 & 0
\end{bmatrix}
\qquad
\begin{array}{c}
V1 \\
L1,L2,C3 \\
C1,C2 \\
R
\end{array}
\begin{bmatrix}
V1 & L1,L2,C3 & C1,C2 & R \\
0.04 & -0.71 & 0.66 & 0 \\
-0.71 & 11.28 & -10.47 & -0.08 \\
0.66 & -10.47 & 9.71 & 0.07 \\
0 & -0.08 & 0.07 & 0
\end{bmatrix}$$

Figure 67: Quadratic boost converter A 10X step up Figure 68: Quadratic boost converter B 10X step up

At this operating point although the spread of the power interactions in the boost converter is still the least, it has higher entries than quadratic boost converter A. Now even if the quadratic converter A has spread its power interactions across all of its components it is still not having to process as much power as the boost converter is. This makes it the winner at this operating point. Although the topology could be circulating power and wasting it, its still more effective than the boost. This could be due to the boost converter struggling with ripple at larger conversion ratios where the quadratic converter is able to handle this ripple better. Ripple has already been shown in this work to impact the magnitude of the power processing entries.

In terms of the spread of entries quadratic converter A has as large a spread of entries as the buck-boost, but the power interactions between the reactive components in quadratic converter A is lower than than any of the other converters. It might even be possible to improve these circulating powers in quadratic boost converter A.

This experiment has shown that more complex topology structures are able to outperform the simpler topologies at certain operating points. It is not necessarily true that a simpler topology structure will yield lower power processing across the board. Although the topology structure plays a role in power processing it is not a defining characteristic of better power processing. The boost converter appears to be the best converter for low operating points while quadratic boost converter A is the best choice for high conversion efforts. This is probably because the quadratic boost converter A had been designed to combat larger ripples at high boost ratios allowing it to outperform the standard boost converter.

4.4 Step down converters

This case study will analyse the impact of topology structure on power processing using step down converters. Four step down converters namely the buck, SEPIC, cuk and a quadratic buck converter will be simulated using LTSpice to analyse their covariance matrices. The quadratic buck converter appeared in [36] and is a specialized type of buck converter that has a quadratic relationship with duty cycle. This allows it to have very low duty ratios for larger step down tasks in contrast to the normal buck converter. All four converters are configured to step down the same input voltage to a specific output voltage at a 4X and 10X reduction with the same output power. This will investigate the impact on power processing as the conversion effort increases. Each of these converters are simulated under ideal conditions without parasitic effects. The circuit diagrams for each converter are shown in Figure 69 to Figure 72. The test conditions for each converter are shown in Table 6.

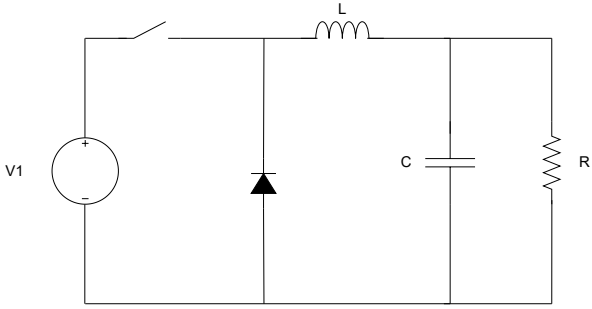


Figure 69: Buck converter

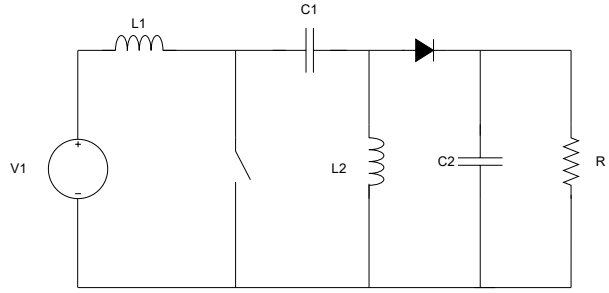


Figure 70: SEPIC converter

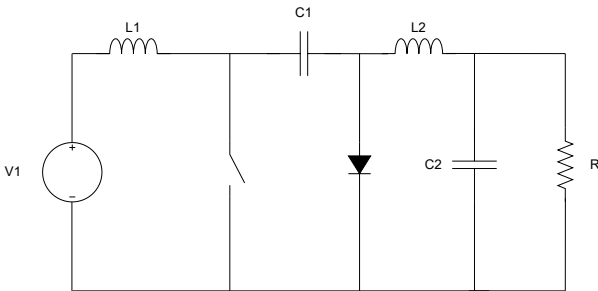


Figure 71: Cuk converter

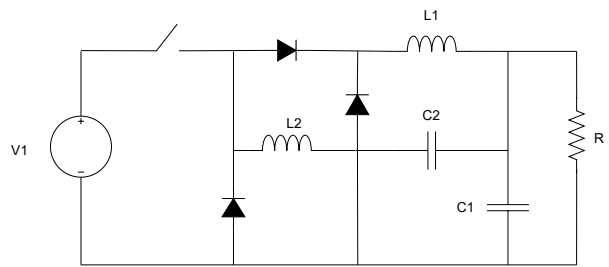


Figure 72: Quadratic buck converter

Table 6: Table of test conditions

Converter parameter	Value
V_{in}	500 V
P_{out}	250 W
f_s	100 kHz
Δi_L	30 %
Δv_c	10 %

The covariance matrices for the 4X step down (500 V to 125 V) conversion are shown below:

$$\begin{array}{c} V_{1,R} \\ L,C \end{array} \begin{array}{cc} V_{1,R} & L,C \\ \left[\begin{array}{cc} 3.18 & -3.19 \\ -3.19 & 3.19 \end{array} \right] \end{array}$$

Figure 73: Buck converter 4X step down

$$\begin{array}{c} V_{1,L1,L2} \\ C_{1,C2,R} \end{array} \begin{array}{cc} V_{1,L1,L2} & C_{1,C2,R} \\ \left[\begin{array}{cc} 6.22 & -6.21 \\ -6.21 & 6.20 \end{array} \right] \end{array}$$

Figure 74: SEPIC 4X step down

$$\begin{array}{c} V_{1,L1,L2,C2} \\ C_{1,R} \end{array} \begin{array}{cc} V_{1,L1,L2,C2} & C_{1,R} \\ \left[\begin{array}{cc} 6.46 & -6.45 \\ -6.45 & 6.44 \end{array} \right] \end{array}$$

Figure 75: Cuk converter 4X step down

$$\begin{array}{c} V_{1,C2,R} \\ L_{1,L2,C1} \end{array} \begin{array}{cc} V_{1,C2,R} & L_{1,L2,C1} \\ \left[\begin{array}{cc} 6.93 & -6.93 \\ -6.93 & 6.94 \end{array} \right] \end{array}$$

Figure 76: Quadratic buck converter 4X step down

These matrices suggest the buck converter is the best topology choice as it has the lowest entries in the covariance matrices which suggest it has the lowest power processing at this operating point. The SEPIC and the Cuk are very similar in structure and is most likely why their matrices are almost identical too. Although the quadratic buck converter is not far behind the SEPIC and CUK it is performing the worst with the largest entries in the matrix and therefore the most power processing.

The covariance matrices for the 10X step down conversion (500V to 50 V) are shown below:

$$\begin{array}{c} V_{1,R} \\ L,C \end{array} \begin{array}{cc} V_{1,R} & L,C \\ \left[\begin{array}{cc} 9.20 & -9.22 \\ -9.22 & 9.24 \end{array} \right] \end{array}$$

Figure 77: Buck converter 10X step down

$$\begin{array}{c} V_{1,L1,L2} \\ C_{1,C2,R} \end{array} \begin{array}{cc} V_{1,L1,L2} & C_{1,C2,R} \\ \left[\begin{array}{cc} 11.93 & -11.92 \\ -11.92 & 11.91 \end{array} \right] \end{array}$$

Figure 78: SEPIC 10X step down.

$$\begin{array}{c} V_{1,L1,L2,C2} \\ C_{1,R} \end{array} \begin{array}{cc} V_{1,L1,L2,C2} & C_{1,R} \\ \left[\begin{array}{cc} 12.05 & -12.03 \\ -12.03 & 12.02 \end{array} \right] \end{array}$$

Figure 79: Cuk converter 10X step down

$$\begin{array}{c} V_{1,C2,R} \\ L_{1,L2,C1} \end{array} \begin{array}{cc} V_{1,C2,R} & L_{1,L2,C1} \\ \left[\begin{array}{cc} 19.03 & -19.03 \\ -19.03 & 19.03 \end{array} \right] \end{array}$$

Figure 80: Quadratic buck converter 10X step down

At this operating point the buck converter is still the better topology in terms of its lower power processing. However, the gap between the buck, SEPIC and Cuk is much smaller at this higher operating point. Suggesting that although the buck is still better, the buck has had the largest change in processed power between these three converters between the 4X and 10X cases. The SEPIC and Cuk are still very close together but the SEPIC seems to be handling this operating point better than the Cuk. The quadratic buck is still the worst topology with the highest amount of power processing, this is most likely due to the specialized nature of the topology. [36] described the topology as being ideal for low conversion effort tasks, since the 10X reduction is a large conversion effort it makes intuitive sense that this specialized topology would fair worse than the other topologies considered here.

These 2×2 matrices have shown the overall power interactions in each converter. Now consider the interactions between the components in the converters. In order to view these interactions the original covariance matrices are reduced to 4×4 matrices.

$$\begin{array}{c} V1 \\ L \\ C \\ R \end{array} \begin{bmatrix} V1 & L & C & R \\ 2.98 & -3.03 & -0.04 & 0.09 \\ -3.03 & 3.08 & 0.04 & -0.09 \\ -0.04 & 0.04 & 0.00 & 0.00 \\ 0.09 & -0.09 & 0.00 & 0.00 \end{bmatrix}$$

Figure 81: Buck converter 4X step down

$$\begin{array}{c} V1 \\ L1,L2 \\ C1,C2 \\ R \end{array} \begin{bmatrix} V1 & L1,L2 & C1,C2 & R \\ 0.00 & 0.03 & -0.03 & 0.00 \\ 0.03 & 6.17 & -6.14 & -0.04 \\ -0.03 & -6.14 & 6.12 & 0.04 \\ 0.00 & -0.04 & 0.04 & 0.00 \end{bmatrix}$$

Figure 82: SEPIC converter 4X step down.

$$\begin{array}{c} V1 \\ L1,L2,C2 \\ C1 \\ R \end{array} \begin{bmatrix} V1 & L1,L2,C2 & C1 & R \\ 0.00 & 0.02 & -0.02 & 0.00 \\ 0.02 & 6.48 & -6.36 & -0.12 \\ -0.02 & -6.36 & 6.25 & 0.12 \\ 0.00 & -0.12 & 0.12 & 0.00 \end{bmatrix}$$

Figure 83: Cuk converter 4X step down.

$$\begin{array}{c} V1 \\ L1,L2,C1 \\ C2 \\ R \end{array} \begin{bmatrix} V1 & L1,L2,C1 & C2 & R \\ 6.04 & -6.47 & 0.39 & 0.04 \\ -6.47 & 6.94 & -0.42 & -0.04 \\ 0.39 & -0.42 & 0.03 & 0.00 \\ 0.04 & -0.04 & 0.00 & 0.00 \end{bmatrix}$$

Figure 84: Quadratic buck converter 4X.

At this operating point there is very little spread across all components in the buck, SEPIC and cuk. This suggests these three topologies have little circulating power between their components that is potentially wasted power processing. The entries in the reactive components of the buck are much smaller than those of the SEPIC and CUK making it the better topology in terms of power processing. The quadratic buck also has a low spread between all the reactive components and the source with the majority of the power interactions concentrated between the V1,L1,L2 and C1. At this operating point the CUK, SEPIC and quadratic buck are very similar with the buck being the best choice.

And for the 10X case:

$$\begin{array}{c} V1 \\ L \\ C \\ R \end{array} \begin{bmatrix} V1 & L & C & R \\ 8.91 & -8.99 & -0.05 & 0.11 \\ -8.99 & 9.06 & 0.05 & -0.11 \\ -0.05 & 0.05 & 0.00 & 0.00 \\ 0.11 & -0.11 & 0.00 & 0.00 \end{bmatrix}$$

Figure 85: Buck converter 10X step down.

$$\begin{array}{c} V1 \\ L1,L2 \\ C1,C2 \\ R \end{array} \begin{bmatrix} V1 & L1,L2 & C1,C2 & R \\ 0.00 & 0.07 & -0.07 & 0.00 \\ 0.07 & 11.78 & -11.78 & -0.07 \\ -0.07 & -11.78 & 11.77 & 0.07 \\ 0.00 & -0.07 & 0.07 & 0.00 \end{bmatrix}$$

Figure 86: SEPIC converter 10X step down.

$$\begin{array}{c} V1 \\ L1,L2,C2 \\ C1 \\ R \end{array} \begin{bmatrix} V1 & L1,L2,C2 & C1 & R \\ 0.00 & 0.06 & -0.06 & 0.00 \\ 0.06 & 12.23 & -12.15 & -0.11 \\ -0.06 & -12.15 & 12.08 & 0.11 \\ 0.00 & -0.11 & 0.11 & 0.00 \end{bmatrix}$$

Figure 87: Cuk converter 10X step down

$$\begin{array}{c} V1 \\ L1,L2,C1 \\ C2 \\ R \end{array} \begin{bmatrix} V1 & L1,L2,C1 & C2 & R \\ 17.96 & -18.49 & 0.46 & 0.07 \\ -18.49 & 19.03 & -0.47 & -0.07 \\ 0.46 & -0.47 & 0.01 & 0.00 \\ 0.07 & -0.07 & 0.00 & 0.00 \end{bmatrix}$$

Figure 88: Quadratic buck converter 10X step down.

At this operating point all the converters still have very little spread and therefore little circulating power. The entries in the reactive components are just larger in the SEPIC and Cuk compared to the buck. Suggesting the buck is still the better topology at this operating point. At this operating point although the quadratic buck still maintains a low spread of power interactions the magnitude of the entries is significantly greater than the other topologies considered. This is because the converter is being pushed past its intended use case at a

large conversion effort. This confirms that the quadratic buck converter is better at low conversion effort as the literature stated.

This suggests that topologies such as the SEPIC and Cuk that are more complex than the buck do not necessarily create circulating power as seen by the spread of the entries. The most complex topology here is the quadratic buck which appears to suffer at high conversion efforts. The more complex a topology structure gets, it appears to cause more power processing. This is not a generalized trend as the results from the step up converters case study confirmed this. Topology structure does influence the power processing of a topology but it not the defining factor. Although the topology structure is important, conversion effort appears to be equally as important. A careful balance between these two factors is required for effective power processing. The buck converter is not as prone to struggling with ripple as the boost converter is known for at larger conversion effort and may be the reason the simplest topology has out performed the others in this particular step down case.

4.5 The modified boost converter

This case study demonstrates how small changes to a topology structure can alter the way a converter processes power. It will consider what will be called the “modified boost converter”. This is essentially a boost converter with a second voltage source connected between the input voltage source and the output node. This case study is conducted using purely analytical methods in a mathematically ideal scenario with zero ripple. The analysis technique uses zero ripple for this case study because it is the easiest method to model the converters when calculating the component powers analytically. This also removes ripple from the scenario and will give a true reflection of how a topologies power processing is altered by structural changes.

Consider a conventional boost converter. It is possible to redraw the boost converter with a voltage source between the input and output as shown in *Figure 89* below:

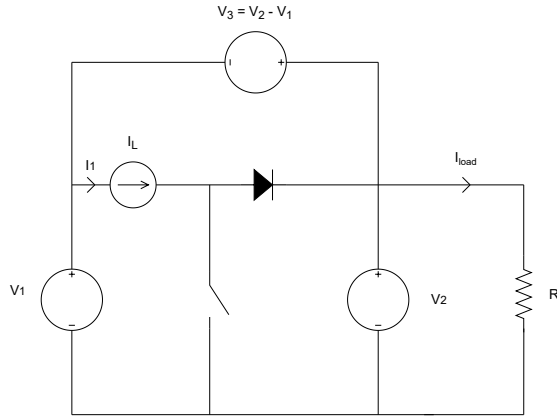


Figure 89: Diagram of the modified boost converter

As this is a loop any one of the sources can be removed and the circuit is unchanged since $V3 = V2 - V1$. By removing $V2$ the boost circuit is redrawn below. The load resistor is now across $V1$ and $V3$. This can be done in a practical circuit by replacing $V2$ and $V3$ with large size capacitors.

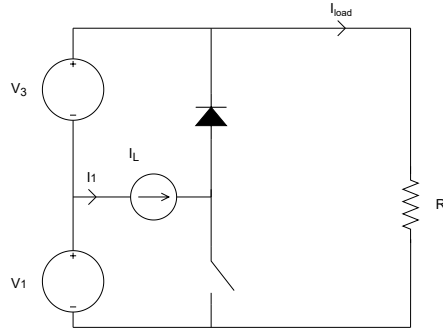


Figure 90: Simplified diagram of the modified boost converter

The impact of this change can be observed using a zero ripple experiment. First an analysis of the conventional boost converter is required under zero ripple conditions following an absorbing power convention. The analytical representation of the conventional boost converter is shown below:

$$\frac{V_2}{V_1} = \frac{1}{1 - D} = \frac{I_1}{I_{Load}}$$

Table 7: Table of on and off state powers for boost converter

State	P_{V1}	P_L	P_{V2}	P_R
On State	$-V_1 I_1$	$V_1 I_1$	$-V_2 I_{Load}$	$V_2 I_{Load}$
Off State	$-V_1 I_1$	$(V_1 - V_2) I_1$	$V_2 (I_1 - I_{Load})$	$V_2 I_{Load}$

Using these relationships for the on/off state powers the following covariance matrix for the boost converter can be calculated mathematically:

$$\begin{matrix} & V1 & L & V2 & R \\ \begin{matrix} V1 \\ L \\ V2 \\ R \end{matrix} & \left[\begin{array}{cccc} 0 & 0 & 0 & 0 \\ 0 & -\frac{D(I_{Load})^2 V_1^2}{(D-1)^3} & \frac{D(I_{Load})^2 V_1^2}{(D-1)^3} & 0 \\ 0 & \frac{D(I_{Load})^2 V_1^2}{(D-1)^3} & -\frac{D(I_{Load})^2 V_1^2}{(D-1)^3} & 0 \\ 0 & 0 & 0 & 0 \end{array} \right] \end{matrix}$$

This shows that there is no varying power in V1 or R since their covariance is zero. The interactions are only between L and V2. Now the same analysis for the modified boost converter is conducted using the same absorbing power convention. The analytical representation of the “modified boost” converter is shown below:

$$V_{out} = V_1 + V_3$$

Table 8: Table of on and off state powers for modified boost converter

State	P_{V1}	P_L	P_{V2}	P_R
On State	$\frac{-I_{Load} V_1 (D-2)}{D-1}$	$\frac{-I_{Load} V_1}{D-1}$	$\frac{D I_{Load} V_1}{D-1}$	$\frac{-I_{Load} V_1}{D-1}$
Off State	$-V_1 I_{Load}$	$\frac{-D I_{Load} V_1}{(D-1)^2}$	$\frac{D^2 I_{Load} V_1}{(D-1)^2}$	$\frac{-I_{Load} V_1}{D-1}$

Using these relationships for the on/off state powers the following covariance matrix for the ”modified boost” converter can be calculated mathematically:

$$\begin{matrix} & V1 & L & V3 & R \\ \begin{matrix} V1 \\ L \\ V3 \\ R \end{matrix} & \left[\begin{array}{cccc} \frac{-D I_{Load}^2 V_1^2}{D-1} & \frac{-D I_{Load}^2 V_1^2}{(D-1)^2} & \frac{D^2 I_{Load}^2 V_1^2}{(D-1)^2} & 0 \\ \frac{-D I_{Load}^2 V_1^2}{(D-1)^2} & \frac{-D I_{Load}^2 V_1^2}{(D-1)^3} & \frac{D^2 I_{Load}^2 V_1^2}{(D-1)^3} & 0 \\ \frac{D^2 I_{Load}^2 V_1^2}{(D-1)^2} & \frac{D^2 I_{Load}^2 V_1^2}{(D-1)^3} & -\frac{D^3 I_{Load}^2 V_1^2}{(D-1)^3} & 0 \\ 0 & 0 & 0 & 0 \end{array} \right] \end{matrix}$$

Now it is clear that V1 is involved in the power processing since it has a varying entry in the covariance matrix. To compare these covariance matrices it is easier with defined numerical values for each converter. Let $V_{in} = 50V$, $V_{out} = 200V$ with an output power of 10 W. Substituting these values in produces the following covariance matrices:

$$\begin{array}{c}
V1 \\
L \\
V2 \\
R
\end{array}
\begin{bmatrix}
V1 & L & V2 & R \\
0 & 0 & 0 & 0 \\
0 & 300 & -300 & 0 \\
0 & -300 & 300 & 0 \\
0 & 0 & 0 & 0
\end{bmatrix}$$

Figure 91: Boost converter zero ripple covariance matrix

$$\begin{array}{c}
V1 \\
L \\
V3 \\
R
\end{array}
\begin{bmatrix}
V1 & L & V3 & R \\
18.75 & -75 & 56.25 & 0 \\
-75 & 300 & -225 & 0 \\
56.25 & -225 & 168.75 & 0 \\
0 & 0 & 0 & 0
\end{bmatrix}$$

Figure 92: Modified Boost converter zero ripple covariance matrix

The conventional boost converter only has power interactions between L and V2 where the power activity in the modified boost converter is spread across both voltage sources and L. In the modified boost converter the sources V1 and V3 appear to share the processing responsibility. In contrast the boost converter V2 has sole responsibility for this same power processing task.

An interesting observation to compare these two converters is the sum of the square roots of the diagonal. The idea behind this is that each entry along the main diagonal represents the power activity inside a component. By taking the square root of each power activity the result has units of watts. By summing these square roots of each entry along the main diagonal the result represents a power processing representation for the converter. The caveat to this is that this can only be used when both converters have the same wave shape. Technically the main diagonal entries represent the product of some form factor and the power processed in the component. It is therefore naive to use this to compare converters which may not have the same wave shape. However, since these converters are zero ripple it can be applied in this scenario. The other case studies do not always consider converters under zero ripple, since in practise converters are not zero ripple and it would be more helpful to use the matrix method to analyse real world scenarios. This means this observation of the sum of the square roots of the diagonal can not always be applied to real converter scenarios but it can be interesting to analyse in the ideal case.

A discussion of this property has purposefully been left out in Chapter 2 to prevent this being used in any and all scenarios. Since this case study is a suitable example of its correct application it is only used here but may be useful given some further investigation into generalizing the technique.

This possible representation of power processing is calculated by the square rooting each main diagonal entry and summing them:

For the conventional boost: $17.3 + 17.3 = 34.6W$
For the modified boost: $4.33 + 17.32 + 12.99 = 34.6W$

This appears to suggest that both of these converters may be processing the same amount of power just in different ways seeing as the total power activity in each component is identical in each converter. This is just an observation and may not be true in all cases. The reduced 2×2 matrices below show that both converters appear to have the same cumulative power processing.

$$\begin{array}{c}
V1,L \\
V2,R
\end{array}
\begin{bmatrix}
V1,L & V2,R \\
300 & -300 \\
-300 & 300
\end{bmatrix}$$

Figure 93: Boost converter zero ripple covariance matrix

$$\begin{array}{c}
V1,V3 \\
L,R
\end{array}
\begin{bmatrix}
V1,V3 & L,R \\
300 & -300 \\
-300 & 300
\end{bmatrix}$$

Figure 94: Modified Boost converter zero ripple covariance matrix

The results of this case study indicate that the power processing properties of a converter may not be unique to a topology. Both of these converters appear to process the same amount of power as evident from their

covariance matrices. The structure of the topology dictates which components take responsibility for the power processing and in this case does not alter the power processing. It merely split the responsibility of power processing between multiple components. A simple converters ability to process power may be the same as a more complex combination of components. Even though the power processing may be shared among many elements in a converter thus resulting in lower component powers, they may still have the same cumulative impact on the total power processing of a converter.

This observation may only be easy identified when the matrix is reduced to combine the effects of the elements that are sharing the processing responsibility. This is why the matrices in the previous case studies have been reduced to 2×2 matrices as it would negate this phenomenon between simple and more complex topology structures. A case by case basis is required to compare topology structures with one another since a simpler topology may be doing the same job as a more complex converter.

4.6 The boost vs quadratic boost : stepped duty cycle

This case study analyses the differences in topology structure to obtain the same input/ output characteristics using two different converters. Comparing a simple boost converter with a more complex quadratic boost converter A, shown in *Figure 95*, provides insight into how topology structure influences power processing as the conversion effort varies. Quadratic boost converter A has been chosen as it was shown to out perform the boost converter in the 10X case in 4.3. This makes for an interesting investigation to observe at which point quadratic boost converter A starts to outperform the normal boost converter. The duty cycle of each converter will be stepped from a 10% step up to a 90% step up ratio. The experimental conditions for each converter are outlined in *Table 9*.

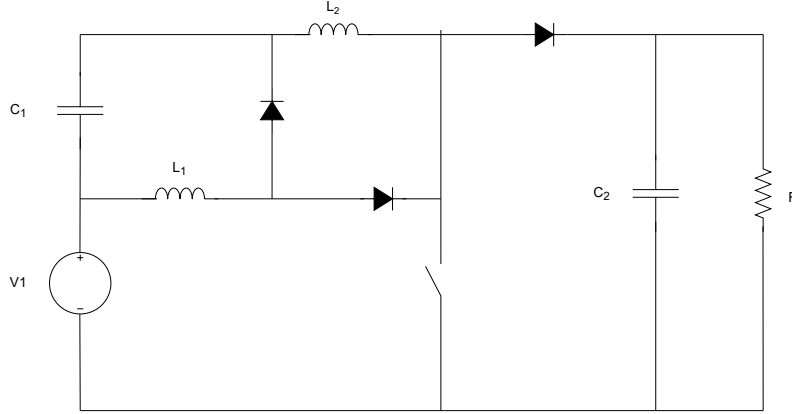


Figure 95: Quadratic boost converter A

Table 9: Table of test conditions for stepped duty cycle test on the boost and the quadratic boost

V_{out}	R_{load}	Boost D	Quadratic boost D
55.55 V	12.34 Ω	10%	5.127%
71.42 V	20.4 Ω	30%	16.329%
100 V	40 Ω	30%	29.289%
166.66 V	111.1 Ω	70%	45.227%
500 V	1000 Ω	90%	69.8%

Both converters are configured to boost an input voltage of 50 V to the output voltages and the required duty cycles as outlined in the table above. At all operating points both converters have a switching frequency of 100 kHz, output power of 250 W, inductor current ripple ratio of 30% and an output voltage ripple ratio of 10%. These converters are simulated using ideal circuit components without parasitic effects. The covariance matrices for this experiment are reduced to 2×2 and normalized to output power for the sake of brevity. The unabridged matrices are available in *Appendix F* for further review. The covariance matrices for each run of the simulation are listed below:

$$V1,L \begin{bmatrix} V1,L & CR \\ 0.109 & -0.107 \\ CR & -0.107 & 0.105 \end{bmatrix}$$

$$V1,C1,C2,R \begin{bmatrix} V1,C1,C2,R & L1,L2 \\ 0.187 & -0.188 \\ L1,L2 & -0.188 & 0.188 \end{bmatrix}$$

Figure 96: Boost converter @ 10% duty cycle.

Figure 97: Quadratic boost converter @ 5.127% duty cycle.

$$\begin{array}{c} V_{1,L} \\ CR \end{array} \begin{bmatrix} V_{1,L} & CR \\ 0.423 & -0.418 \\ -0.418 & 0.413 \end{bmatrix}$$

Figure 98: Boost converter @ 30% duty cycle.

$$\begin{array}{c} V_{1,C1,C2,R} \\ L_{1,L2} \end{array} \begin{bmatrix} V_{1,C1,C2,R} & L_{1,L2} \\ 0.707 & -0.710 \\ -0.710 & 0.714 \end{bmatrix}$$

Figure 99: Quadratic boost converter @ 16.329% duty cycle.

$$\begin{array}{c} V_{1,L} \\ CR \end{array} \begin{bmatrix} V_{1,L} & CR \\ 1.001 & -0.992 \\ -0.992 & 0.984 \end{bmatrix}$$

Figure 100: Boost converter @ 50% duty cycle.

$$\begin{array}{c} V_{1,C1,C2,R} \\ L_{1,L2} \end{array} \begin{bmatrix} V_{1,C1,C2,R} & L_{1,L2} \\ 1.997 & -2.004 \\ -2.004 & 2.011 \end{bmatrix}$$

Figure 101: Quadratic boost converter @ 29.289% duty cycle.

$$\begin{array}{c} V_{1,L} \\ CR \end{array} \begin{bmatrix} V_{1,L} & CR \\ 2.385 & -2.373 \\ -2.373 & 2.360 \end{bmatrix}$$

Figure 102: Boost converter @ 70% duty cycle.

$$\begin{array}{c} V_{1,C1,C2,R} \\ L_{1,L2} \end{array} \begin{bmatrix} V_{1,C1,C2,R} & L_{1,L2} \\ 3.142 & -3.145 \\ -3.145 & 3.148 \end{bmatrix}$$

Figure 103: Quadratic boost converter @ 45.227% duty cycle.

$$\begin{array}{c} V_{1,L} \\ CR \end{array} \begin{bmatrix} V_{1,L} & CR \\ 9.912 & -9.894 \\ -9.894 & 9.876 \end{bmatrix}$$

Figure 104: Boost converter @ 90% duty cycle.

$$\begin{array}{c} V_{1,C1,C2,R} \\ L_{1,L2} \end{array} \begin{bmatrix} V_{1,C1,C2,R} & L_{1,L2} \\ 8.14 & -8.14 \\ -8.14 & 8.14 \end{bmatrix}$$

Figure 105: Quadratic boost converter @ 69.8% duty cycle.

This experiment shows the general trend for the entries in the matrices to increase for both converters. This means that power processing increases as the conversion effort increases. This makes intuitive sense as it requires more effort to convert 50 V to 500 V than it would to convert 50 V to 55 V. This means that power processed and conversion effort have a positive relationship between them. As conversion effort increases so does the power processing. The interesting result here is how the boost converter seems to dominate at lower conversion efforts but it is surpassed by the quadratic converter as soon as the boost starts to struggle with ripple at larger boost ratios.

The graph below summarizes the results of this power processing experiment. The graph depicts the trend between output voltage and power processed as a function of increasing duty cycle. The processed power being the normalized entries in the covariance matrices outlined above.

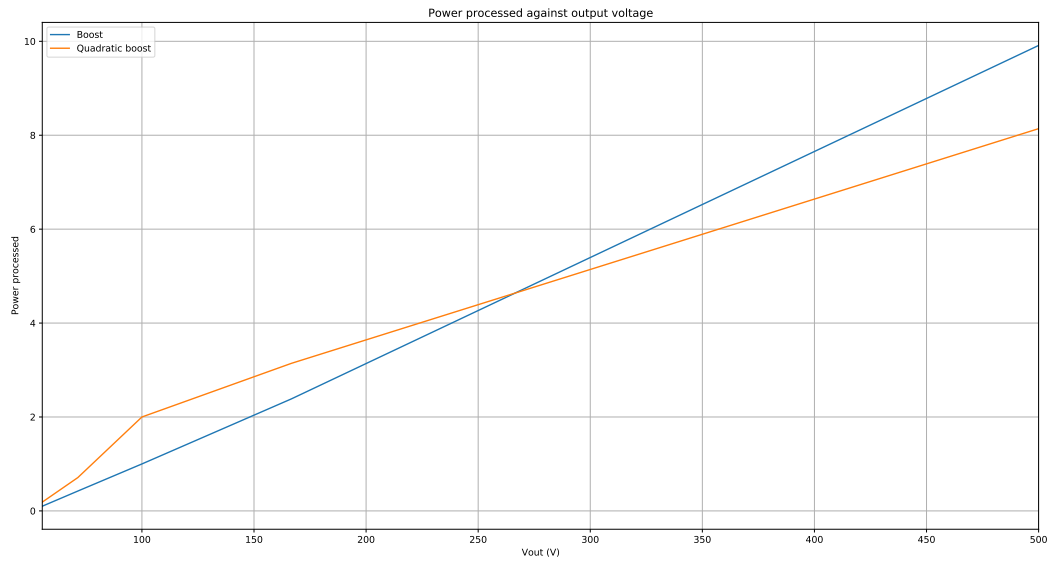


Figure 106: Graph of total processed power by all elements against output voltage for the stepped duty cycle simulations

Although both of these converters are performing the same conversion efforts at each operating point, there is a clear distinction where the boost converter can not keep up with the increased power processing and starts to exceed the quadratic boost converters power processing. The boost converter has also almost reached its practical limit at 90% where the quadratic boost converter is only at approximately 70% and would outperform the boost converter for boost ratios higher than this. This suggests that at higher boost ratios the quadratic boost converter is the better choice as its design intended.

4.7 The matrix method and ripple

This case study will address the impact of current and voltage ripple in reactive components on the covariance matrix of component powers. Inductors experience current ripple and capacitors experience voltage ripple. Since the power of the component is a direct result of the voltage and current in a component, any ripple in either signal will cause ripple in the power waveform. This will then have an impact on the matrix method, since the matrix method contains variances along the main diagonal. The variance is the variability from the mean which has a positive relationship with to the current or voltage ripple in a component. As the ripple increases so does the variance.

To investigate this a boost converter operating with a 4X step up conversion ratio is designed to be tested in three different scenarios. One with a zero ripple approximation, one with a 30% current ripple and 10% voltage ripple and the last case has pushed both the current and voltage ripple to the border between CCM and DCM operation. The matrices below show the results of this experiment.

$$\begin{array}{c}
 V1 \\
 L \\
 C \\
 R
 \end{array}
 \begin{bmatrix}
 V1 & L & C & R \\
 0 & 0 & 0 & 0 \\
 0 & 3.01 & -3.00 & 0 \\
 0 & -3.00 & 2.98 & 0 \\
 0 & 0 & 0 & 0
 \end{bmatrix}
 \qquad
 \begin{array}{c}
 V1 \\
 L1 \\
 C1 \\
 R
 \end{array}
 \begin{bmatrix}
 V1 & L1 & C1 & R \\
 0 & 0 & 0 & 0 \\
 0 & 3.11 & -3.10 & 0 \\
 0 & -3.10 & 3.09 & 0 \\
 0 & 0 & 0 & 0
 \end{bmatrix}$$

Figure 107: Boost converter zero ripple 4X step up Figure 108: Boost converter defined ripple 4X step up

$$\begin{array}{c}
 V1 \\
 L \\
 C \\
 R
 \end{array}
 \begin{bmatrix}
 V1 & L & C & R \\
 0.30 & 0 & -0.29 & 0 \\
 0 & 3.93 & -3.92 & 0 \\
 -0.29 & -3.92 & 2.65 & 0 \\
 0 & 0 & 0 & 0
 \end{bmatrix}$$

Figure 109: Boost converter on border of DCM 4X step up.

The zero-ripple approximation of the boost converter out-performs the other experiments but not by much in the case of normal ripple. Suggesting that without the ripple in the reactive components that power processing is able to be lower in order to achieve the input-output characteristics of the converter. A small amount of ripple induced on the inductor with 30% current ripple is the normal ripple case. It is only slightly worse off than the desired ripple case but is still fairly close to an ideal performance. The border between DCM and CCM with as large a current ripple as possible increases the overall power processed by the converter. Although it is not significantly greater than the controlled ripple case, it is still hampered by the current ripple when processing power.

This result appears to suggest that the zero-ripple approximation is an ideal approximation of the power processing requirements of a topology at a particular conversion effort. Ripple has a direct impact on the power processing ability of a converter. This is interesting since volume of reactive components has been shown to be linked to losses in a converter, converters that intrinsically produce large ripples that need to be controlled with large components[22]. This means that either way a converter prone to creating large ripple will suffer with processing power since the measures taken to curb that ripple merely increases losses and decreases the power processing ability of the converter.

4.8 The cascaded boost

This case study investigates the impact on power processing of cascading two boost converters each with a 2X step up to achieve an overall 4X step up against a single boost converter with a 4X step up ratio. The circuit diagrams for each converter in this experiment are shown in Figure 110a and Figure 110b. This case study is conducted in LTSpice and the converters are simulated without parasitic effects. Table 10 outlines the test conditions for this case study.

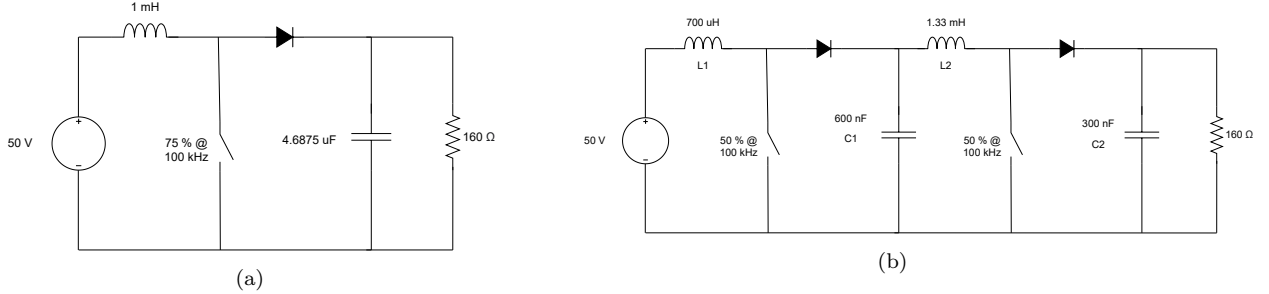


Figure 110: (a) represents a 4X step up boost converter and (b) represents a 4X step up cascaded boost converter

Table 10: Table of test conditions

Converter parameter	Value
V_{in}	50 V
V_{out}	200 V
P_{out}	250 W
f_s	100 kHz
Δi_L	30 %
Δv_c	10 %

Below are the covariance matrices for these two converters:

$$\begin{matrix} & V_{1,L} & C,R \\ V_{1,L} & \begin{bmatrix} 3.07 & -3.05 \end{bmatrix} \\ C,R & \begin{bmatrix} -3.05 & 3.04 \end{bmatrix} \end{matrix}$$

$$\begin{matrix} & V_{1,L1,L2} & C1,C2,R \\ V_{1,L1,L2} & \begin{bmatrix} 4.26 & -4.23 \end{bmatrix} \\ C1,C2,R & \begin{bmatrix} -4.23 & 4.20 \end{bmatrix} \end{matrix}$$

Figure 111: Boost converter 4X step up

Figure 112: Cascaded boost converter 4X step up

Even though both of these converters are performing the same function and have the same step up ratio the cascaded topology processes more power. This makes intuitive sense since the second leg of the cascaded topology must process some power again that has already been processed by the first stage. This implies that cascading smaller effort converters together to get the equivalent power output hampers power processing and results in a topology that is less capable of processing power effectively even if the original topology was good to start with. Therefore cascading converters to achieve the same conversion effort as a single converter does not give an improvement in power processing ability, it degrades the topologies power processing.

4.9 The parallel interleaved boost

The parallel interleaved boost converter is regarded as a more efficient and reliable topology when compared to the boost converter as it boasts lower current ripple. This improvement on a boost converter is an interesting case to analyse since the previous sections have shown that the boost converter is better at power processing than the other topologies considered at low conversion efforts. To make a fair comparison the interleaved boost converter is designed with the same operating specifications as the boost converter with both a 4X and a 10X conversion case. *Figure 113a* and *Figure 113b* show the interleaved boost converter circuits simulated in this case study in LTSpice without parasitic effects. Table 11 outlines the test conditions for this case study.

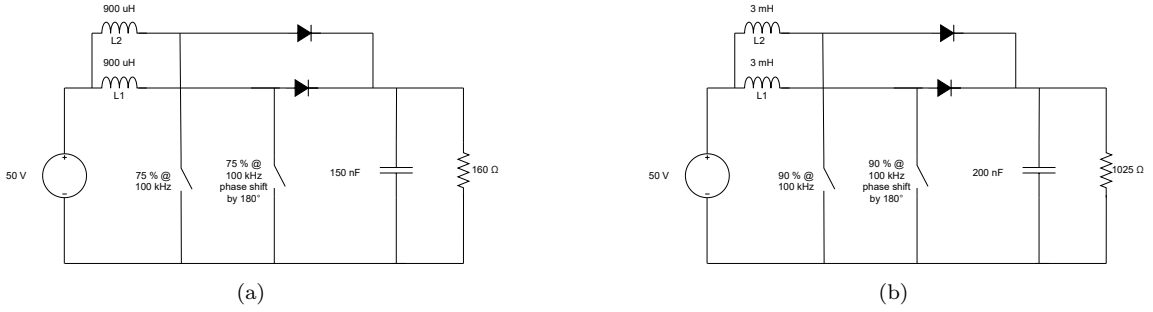


Figure 113: (a) represents a 4X step up interleaved boost converter and (b) represents a 10X step up interleaved boost converter

Table 11: Table of test conditions

Converter parameter	Value
V_{in}	50 V
V_{out} 4X	200 V
V_{out} 10X	500 V
P_{out}	250 W
f_s	100 kHz
Δi_L	30 %
Δv_c	10 %

Under these conditions the covariance matrices for these converters are shown below:

$$\begin{array}{c}
V1 \\
L1 \\
L2 \\
C \\
R
\end{array}
\begin{bmatrix}
V1 & L1 & L2 & C & R \\
0 & 0 & 0 & 0 & 0 \\
0 & 0.77 & -0.25 & -0.51 & 0 \\
0 & -0.25 & 0.77 & -0.51 & 0 \\
0 & -0.51 & -0.51 & 1.01 & 0 \\
0 & 0 & 0 & 0 & 0
\end{bmatrix}$$

Figure 114: Interleaved boost converter 4X step up.

$$\begin{array}{c}
V1 \\
L1 \\
L2 \\
C \\
R
\end{array}
\begin{bmatrix}
V1 & L1 & L2 & C & R \\
0 & 0 & 0 & 0 & 0 \\
0 & 2.36 & -0.26 & -2.10 & 0 \\
0 & -0.26 & 2.36 & -2.10 & 0 \\
0 & -2.10 & -2.10 & 4.20 & 0 \\
0 & 0 & 0 & 0 & 0
\end{bmatrix}$$

Figure 115: Interleaved boost converter 10X step up.

For comparison here are the boost converters matrices again:

$$\begin{array}{c}
V1 \\
L \\
C \\
R
\end{array}
\begin{bmatrix}
V1 & L & C & R \\
0 & 0 & 0 & 0 \\
0 & 3.05 & -3.04 & 0 \\
0 & -3.04 & 3.02 & 0 \\
0 & 0 & 0 & 0
\end{bmatrix}$$

Figure 116: Boost converter 4X step up

$$\begin{array}{c}
V1 \\
L \\
C \\
R
\end{array}
\begin{bmatrix}
V1 & L & C & R \\
0 & 0 & 0 & 0 \\
0 & 9.69 & -9.67 & 0 \\
0 & -9.67 & 9.66 & 0 \\
0 & 0 & 0 & 0
\end{bmatrix}$$

Figure 117: Boost converter 10X step up

It is clear to see that the power processing ability of the interleaved boost converter is significantly better than the boost in both cases. The entries in the covariance matrix are on the whole much smaller than that of the boost converter. This may be due to the lower current ripple this converter is known for. As demonstrated in the zero ripple approximation, a lower ripple will result in a smaller covariance since the deviation from the mean is not as great with lower ripple. Even though both of these converters were run with the same current and voltage ripple, the phase shift in the inductor currents creates a much lower output current ripple. There is also a smaller current in each inductor which lowers the power in the component and therefore lowers its entries in the covariance matrix. All of these factors will lead to smaller covariance entries and thus improved power processing.

The parallel interleaved boost is also the only case study considered in this work that cannot be reduced to a 2×2 without “losing” information. This is most likely due to the phase shift in the inductor currents that results in a negative power interaction between the inductors. This negative power interaction between them prevents the matrix from being reduced to a 2×2 .

The interleaved boost converter also outperforms the quadratic boost converter A from the step up converters case study (4.3) at almost a quarter of the power processing. Interleaved inductors appear to be one way to improve the power processing ability of a converter. Therefore interleaved inductors appear to be better than the simple boost cell from a power processing perspective.

4.10 Summarized findings

The covariance matrix has shown to be an interesting technique to apply to power electronic converters. It is easy to compute and can be easily compared due to its normalization and reduction properties. These case studies have found that the topology structure and conversion effort have an impact on the power processing patterns the covariance matrix describes. With the exception of high boost ratios, the boost converter appears to be a well performing topology in the ideal case when compared to other converters and in the specific operating points investigated. At high boost ratios the interleaved boost converter is the best converter followed by quadratic boost converter A. The best improvement to make to a boost converter to improve its power processing activity is to reduce the ripple as much as possible and to interleave the inductors. Both of these modifications yielded better results in comparison to the normal boost converter. The worst thing to do for a system is to cascade smaller effort converters together. Both the results pertaining to ripple and cascading are consistent with traditional engineering intuition.

Subtle changes in the structure of a topology can cause the power processing activity to spread out to other components in the converter as seen in the modified boost converter example where the source starts to take on a reactive supply responsibility.

5 Conclusion

The matrix method has exposed some interesting things about power interactions in converters. It has the potential to enable engineers to quantify the power interactions between the components in a converter. This provides more insight into how power electronics topologies fundamentally process power. A better understanding of power processing will lead to improvements in topologies. The covariance matrix has been explored to describe all the power interactions between components in one place allowing engineers to visualize the power processing patterns in a topology. This means the covariance matrix could be consulted during the design process to compare the power interactions of converters prior to choosing a topology. This could allow for topology design research to validate initial topology choices using an unbiased covariance matrix as opposed to personal experience. This could reinforce the topology selection decision and allow unfamiliar topologies to be evaluated to investigate their potential. A zero ripple approximation of a converter has been shown to be the best case scenario in the evaluation of power processing. This may be an effective way to broaden the horizons for designers unsure of how a topology may perform compared to what they already know to work. Removing this unknown could improve the field of topology research and design. The reduction property of the matrix method makes this comparative analysis between converters easier by creating effective representations of converters that are comparable. The matrix method has shown consistency with engineering intuition as it has quantitatively confirmed the feeling that cascading topologies hinders power processing and that interleaved inductors improve the power processing of the boost converter. The covariance matrix has also been explored in relation to differential power methods, an already established theory.

6 Future work

In future work the magnetic effects and the covariance matrix need to be analysed for the use of coupled inductors and transformers. This is required to include the analysis of popular topologies such as the flyback converter. Although this work has concentrated on DC-DC power converters, the matrix method is intended to be applicable to all converters. Further study is required to apply the matrix method to converters that operate with AC conversion. The co-factor property of the covariance matrix could be investigated if it can produce a scaling law for converters. In other words how adding a component to the topology changes the power interactions which could help predict the power relationships of converter that may be generated using algorithms. The use of the matrix method in describing traditional AC power theory and existing power theories could be investigated as it could be useful in some scenarios as the mathematics in the covariance matrix is easier to calculate than complex vector mathematics that is currently being used to describe similar things. The matrix method also required a detailed interpretation of the numbers as this work has interpreted the patterns they create.

7 Acknowledgements

The authors would like to extend a special thanks to Jacques Naude for providing the initial idea to extend Kirchhoff's circuit laws using a statistical analysis. This idea snowballed into all the research that came out of this dissertation.

REFERENCES

- [1] M. Forouzesh, Y. P. Siwakoti, S. A. Gorji, F. Blaabjerg, and B. Lehman, "Step-Up DC–DC Converters: A Comprehensive Review of Voltage-Boosting Techniques, Topologies, and Applications," vol. 32, no. 12, pp. 9143–9178.
- [2] W. Josias de Paula, D. d. S. Oliveira Júnior, D. d. C. Pereira, and F. L. Tofoli, "Survey on non-isolated high-voltage step-up dc–dc topologies based on the boost converter," vol. 8, no. 10, pp. 2044–2057. [Online]. Available: <https://digital-library.theiet.org/content/journals/10.1049/iet-pel.2014.0605>
- [3] K. Tytelmaier, O. Husev, O. Veligorskyi, and R. Yershov, "A review of non-isolated bidirectional dc-dc converters for energy storage systems," in *2016 II International Young Scientists Forum on Applied Physics and Engineering (YSF)*. IEEE, pp. 22–28. [Online]. Available: <http://ieeexplore.ieee.org/document/7753752/>
- [4] S. Khosrogorji, H. Torkaman, and F. Karimi, "A short review on multi-input DC/DC converters topologies," in *The 6th Power Electronics, Drive Systems & Technologies Conference (PEDSTC2015)*. IEEE, pp. 650–654. [Online]. Available: <http://ieeexplore.ieee.org/document/7093351/>
- [5] M. A. Chewale, R. A. Wanjari, V. B. Savakhande, and P. R. Sonawane, "A Review on Isolated and Non-isolated DC-DC Converter for PV Application," in *2018 International Conference on Control, Power, Communication and Computing Technologies (ICCPCT)*. IEEE, pp. 399–404. [Online]. Available: <https://ieeexplore.ieee.org/document/8574312/>
- [6] Z. S. Du, P. Channegowda, P. Kshirsagar, and S. Dwari, "High Density High Power DC-DC Converter Architectures for Future Electric Transportation Applications," in *2019 IEEE Energy Conversion Congress and Exposition (ECCE)*. IEEE, pp. 5862–5869. [Online]. Available: <https://ieeexplore.ieee.org/document/8913313/>
- [7] J. D. Paez, D. Frey, J. Maneiro, S. Bacha, and P. Dworakowski, "Overview of DC–DC Converters Dedicated to HVdc Grids," vol. 34, no. 1, pp. 119–128. [Online]. Available: <https://ieeexplore.ieee.org/document/8379435/>
- [8] S. Patil, S. Vemuru, V. Devabhaktuni, and K. Al-Olimat, "Comparison of multilevel DC-DC converter topologies," in *IEEE International Conference on Electro-Information Technology, EIT 2013*. IEEE, pp. 1–5. [Online]. Available: <http://ieeexplore.ieee.org/document/6632681/>
- [9] K. George and S. Ang, "Topology survey for GaN-based high voltage step-down single-input multi-output DC-DC converter systems," in *2016 IEEE 4th Workshop on Wide Bandgap Power Devices and Applications (WiPDA)*. IEEE, pp. 340–343. [Online]. Available: <http://ieeexplore.ieee.org/document/7799964/>
- [10] L. Torok, N. Christensen, S. Munk-Nielsen, and S. Beczkowski, "Optimization of isolated DC-DC converter topologies for fuel cell applications," in *2019 21st European Conference on Power Electronics and Applications (EPE '19 ECCE Europe)*. IEEE, pp. P.1–P.7. [Online]. Available: <https://ieeexplore.ieee.org/document/8915427/>
- [11] Y. Kashihara and J.-i. Itoh, "Performance evaluation among four types of five-level topologies using Pareto front curves," in *2013 IEEE Energy Conversion Congress and Exposition*. IEEE, pp. 1296–1303. [Online]. Available: <http://ieeexplore.ieee.org/document/6646854/>
- [12] M. Mirjafari, S. Harb, and R. S. Balog, "Multiobjective Optimization and Topology Selection for a Module-Integrated Inverter," vol. 30, no. 8, pp. 4219–4231. [Online]. Available: <http://ieeexplore.ieee.org/document/6891355/>
- [13] T. Diekhans, R. B. GmbH, T. Diekhans, and R. W. D. Doncker, "A Pareto-Based Comparison of Power Electronic Topologies for Inductive Power Transfer," p. 9.
- [14] J. Anzola, I. Aizpuru, A. A. Romero, A. A. Loiti, R. Lopez-Erauskin, J. S. Artal-Sevil, and C. Bernal, "Review of Architectures Based on Partial Power Processing for DC-DC Applications," *IEEE Access*, vol. 8, pp. 103 405–103 418, 2020.
- [15] J. Zhao, K. Yeates, and Y. Han, "Analysis of high efficiency DC/DC converter processing partial input/output power," in *2013 IEEE 14th Workshop on Control and Modeling for Power Electronics (COMPEL)*. IEEE, pp. 1–8. [Online]. Available: <http://ieeexplore.ieee.org/document/6626440/>
- [16] J. A. Cobos, H. Cristobal, D. Serrano, R. Ramos, J. A. Oliver, and P. Alou, "Differential power as a metric to optimize power converters and architectures," in *2017 IEEE Energy Conversion Congress and Exposition (ECCE)*. IEEE, pp. 2168–2175. [Online]. Available: <http://ieeexplore.ieee.org/document/8096427/>
- [17] M. S. Agamy, M. Harfman-Todorovic, A. Elasser, Song Chi, R. L. Steigerwald, J. A. Sabate, A. J. McCann, Li Zhang, and F. J. Mueller, "An Efficient Partial Power Processing DC/DC Converter for Distributed PV Architectures," vol. 29, no. 2, pp. 674–686. [Online]. Available: <http://ieeexplore.ieee.org/document/6490064/>
- [18] J. R. Rakoski Zientarski, J. R. Pinheiro, M. L. da Silva Martins, and H. L. Hey, "Understanding the partial power processing concept: A case-study of buck-boost dc/dc series regulator," in *2015 IEEE 13th Brazilian Power Electronics Conference and 1st Southern Power Electronics Conference (COBEP/SPEC)*.

Fortaleza: IEEE, Nov. 2015, pp. 1–6.

- [19] V. M. Iyer, S. Guler, G. Gohil, and S. Bhattacharya, “Extreme fast charging station architecture for electric vehicles with partial power processing,” in *2018 IEEE Applied Power Electronics Conference and Exposition (APEC)*. San Antonio, TX, USA: IEEE, Mar. 2018, pp. 659–665.
- [20] E. Moore and T. Wilson, “Basic considerations for DC to DC conversion networks,” vol. 2, no. 3, pp. 620–624. [Online]. Available: <http://ieeexplore.ieee.org/document/1065901/>
- [21] D. Wolaver, “Fundamental Study of DC to DC conversion systems.” [Online]. Available: <https://dspace.mit.edu/bitstream/handle/1721.1/13632/24233372-MIT.pdf?sequence=2&isAllowed=y>
- [22] C. Li, Y. E. Bouvier, A. Berrios, P. Alou, J. A. Oliver, and J. A. Cobos, “Revisiting ”Partial Power Architectures” from the ”Differential Power” Perspective,” in *2019 20th Workshop on Control and Modeling for Power Electronics (COMPEL)*. IEEE, pp. 1–8. [Online]. Available: <https://ieeexplore.ieee.org/document/8769667/>
- [23] C. Li and J. A. Cobos, “Differential Power Processing Architectures Accounting for the Differential Power of the Converters,” in *2019 IEEE Conference on Power Electronics and Renewable Energy (CPERE)*. IEEE, pp. 88–93. [Online]. Available: <https://ieeexplore.ieee.org/document/8980018/>
- [24] C. Li, P. Enjeti, and J. A. Cobos, “Analysis and Comparison of Indirect Power in DC-AC or AC-DC Topologies by Quasi-static DC-DC Modeling,” in *2019 IEEE Conference on Power Electronics and Renewable Energy (CPERE)*. IEEE, pp. 76–81. [Online]. Available: <https://ieeexplore.ieee.org/document/8980059/>
- [25] C. Li and J. A. Cobos, “Classification of Differential Power Processing Architectures Based on VA Area Modeling,” pp. 1–1. [Online]. Available: <https://ieeexplore.ieee.org/document/9468632/>
- [26] Z. Xiao, Z. He, H. Wang, A. Luo, Z. Shuai, and J. M. Guerrero, “General High-Frequency-Link Analysis and Application of Dual Active Bridge Converters,” vol. 35, no. 8, pp. 8673–8688. [Online]. Available: <https://ieeexplore.ieee.org/document/8950398/>
- [27] N. G. F. Santos, H. L. Hey, J. R. R. Zientarski, and M. L. d. S. Martins, “Piecewise Fryze power theory analysis applied to PWM DC–DC converters,” vol. 13, no. 10, pp. 2029–2038. [Online]. Available: <https://onlinelibrary.wiley.com/doi/10.1049/iet-pel.2019.1053>
- [28] F. Ghassemi, “Verification of the new concept in AC power theory using energy conversion medium,” in *Ninth International Conference on Harmonics and Quality of Power. Proceedings (Cat. No.00EX441)*, vol. 1. IEEE, pp. 155–161. [Online]. Available: <http://ieeexplore.ieee.org/document/897016/>
- [29] —, “New concept in AC power theory,” vol. 147, no. 6, p. 417. [Online]. Available: <https://digital-library.theiet.org/content/journals/10.1049/ip-gtd.20000783>
- [30] —, “What is wrong with electric power theory and how it should be modified,” in *Ninth International Conference on Metering and Tariffs for Energy Supply*, vol. 1999. IEE, pp. 109–114. [Online]. Available: https://digital-library.theiet.org/content/conferences/10.1049/cp_19990116
- [31] J. Willems, “Reflections on Apparent Power and Power Factor in Nonsinusoidal and Polyphase Situations,” vol. 19, no. 2, pp. 835–840. [Online]. Available: <http://ieeexplore.ieee.org/document/1278447/>
- [32] S.-J. Jeon, “Considerations on a Reactive Power Concept in a Multiline System,” vol. 21, no. 2, pp. 551–559. [Online]. Available: <http://ieeexplore.ieee.org/document/1610662/>
- [33] S. Orts-Grau, N. Munoz-Galeano, J. C. Alfonso-Gil, F. J. Gimeno-Sales, and S. Segui-Chilet, “Discussion on Useless Active and Reactive Powers Contained in the IEEE Standard 1459,” vol. 26, no. 2, pp. 640–649. [Online]. Available: <https://ieeexplore.ieee.org/document/5688289/>
- [34] Y. Ye and K. W. Eric Cheng, “Quadratic boost converter with low buffer capacitor stress,” vol. 7, no. 5, pp. 1162–1170. [Online]. Available: <https://onlinelibrary.wiley.com/doi/10.1049/iet-pel.2013.0205>
- [35] L. Qin, L. Zhou, W. Hassan, J. L. Soon, M. Tian, and J. Shen, “A Family of Transformer-Less Single-Switch Dual-Inductor High Voltage Gain Boost Converters With Reduced Voltage and Current Stresses,” vol. 36, no. 5, pp. 5674–5685. [Online]. Available: <https://ieeexplore.ieee.org/document/9233969/>
- [36] S. Lica, M. Gurbina, D. Draghici, D. Iancu, and D. Lascu, “A new quadratic buck converter,” in *2014 11th International Symposium on Electronics and Telecommunications (ISETC)*. IEEE, pp. 1–4. [Online]. Available: <http://ieeexplore.ieee.org/document/7010741/>

Appendix

A Generalized proof of reduction technique

The following analysis provides a more generalized proof of the mathematics involved in reducing the covariance matrix.

$$\begin{bmatrix} a & b & c & d \\ e & f & g & h \\ i & j & k & l \\ m & n & o & p \end{bmatrix}$$

This matrix has the following properties in the rows:

$$\begin{aligned} a + b + c + d &= 0 \\ e + f + g + h &= 0 \\ i + j + k + l &= 0 \\ m + n + o + p &= 0 \end{aligned}$$

And in the columns:

$$\begin{aligned} a + e + i + m &= 0 \\ b + f + j + n &= 0 \\ c + g + k + o &= 0 \\ d + h + l + p &= 0 \end{aligned}$$

Since this is a zero sum line matrix any co-factor can be calculated as they are all the same. The first co-factor of the minor matrix $M_{1,1}$ is :

$$f(kp - lo) - g(jp - ln) + h(jo - kn)$$

Now let us reduce the orange rows 2 and 3 and columns 2 and 3 to form an equivalent 3×3 matrix:

$$\begin{bmatrix} a & b+c & d \\ e+i & f+g+j+k & h+l \\ m & n+o & p \end{bmatrix}$$

The resulting matrix above has been reduced by combining columns 2 and 3 as well as rows 2 and 3 to combine the effect of these entries together into an equivalent representation of the entries in these rows and columns. Both the rows and columns must be reduced to maintain the square symmetrical and zero sum properties of the original matrix. The zero sum relationships for the new equivalent row 2 and column 2 are unchanged. They still sum to zero as before.

This reduced matrix now gives the following co-factor using the minor matrix $M_{1,1}$:

$$(f + g + j + k)(p) - (h + l)(n + o)$$

Now the co-factors of this new reduced matrix have significantly changed during reduction, meaning the fundamental properties of the matrix have changed in terms of mathematical matrix properties since the co-factors are no longer equivalent:

$$(f + g + j + k)(p) - (h + l)(n + o) = f(kp - lo) - g(jp - ln) + h(jo - kn)$$

As a visual representative tool this can show the effective combined effect of a group of components but it alters the mathematical properties of the matrix. This is because traditional row reduction or column reduction using matrix reduction techniques actually multiply the affected row or column by a constant which preserves the mathematical properties of the matrix. It is equivalent to left multiplying the matrix by a constant matrix. This is also because the rows and columns are not removed during the reduction which leaves the matrix intact mathematically.

Any number of rows and columns may be combined to create an effective row and column representation. The only caveat with reduction is summing entries that are of opposite signs. This will create smaller entries in the effective sum and may "hide" the original effect of the components that were lumped together. It is advised that when reducing, the rows and columns that are chosen to be reduced have the same sign so as not to lose information about the effect the original components had and create an accurate representation of their power interactions.

B More reduction examples of the boost converter

These two examples will use the same boost converter as mentioned in 2.6 of the main dissertation. The first example has its inductors extended and the second example has both the extended inductors and capacitors to show how a large matrix can be reduced to describe the same original boost converter. The original boost converter covariance matrix is shown below for reference:

$$\begin{matrix} & V1 & L & C & R \\ V1 & \left[\begin{array}{cccc} 0.01 & 69.38 & -69.08 & 0.0 \\ 69.38 & 766180.47 & -762848.57 & -21.29 \\ -69.08 & -762848.57 & 759531.17 & 21.19 \\ 0.0 & -21.29 & 21.19 & 0.0 \end{array} \right] \\ L & & & & \\ C & & & & \\ R & & & & \end{matrix}$$

B.1 Extended inductors

The same boost converter can have its inductors extended into four series inductors that still achieve the required $500\mu H$.

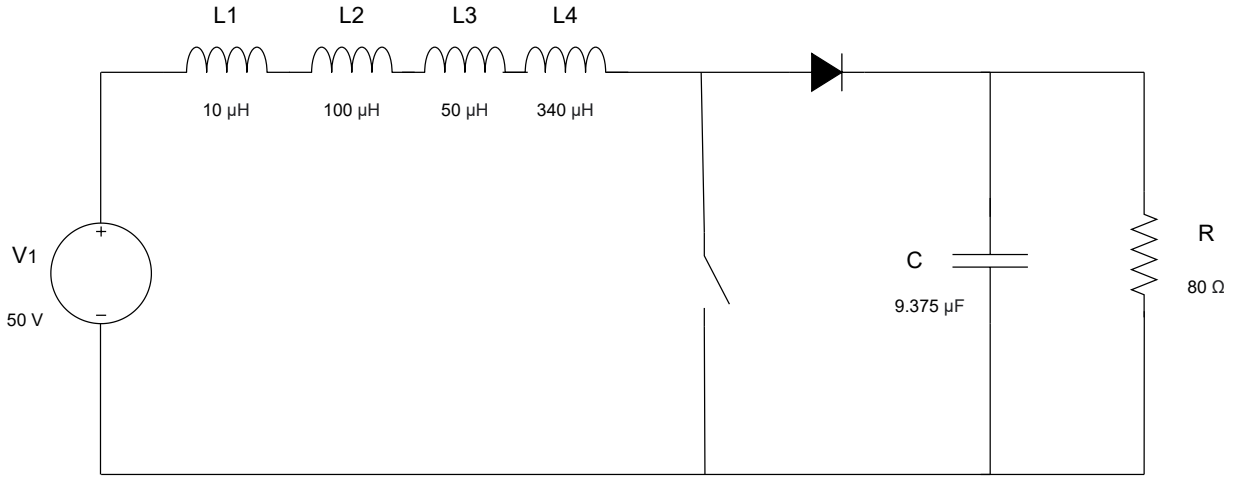


Figure 118: Traditional Boost converter with extended series inductors

The covariance matrix for this circuit is as follows:

$$\begin{matrix} & V1 & L1 & L2 & L3 & L4 & C & R \\ V1 & \left[\begin{array}{cccccc} 0.01 & 1.38 & 13.84 & 6.92 & 47.05 & -68.89 & -0.0 \\ 1.38 & 305.73 & 3057.3 & 1528.65 & 10394.82 & -15219.97 & -0.42 \\ 13.84 & 3057.3 & 30573.03 & 15286.51 & 103948.32 & -152200.0 & -4.25 \\ 6.92 & 1528.65 & 15286.51 & 7643.26 & 51974.15 & -76099.98 & -2.12 \\ 47.05 & 10394.82 & 103948.32 & 51974.15 & 353424.35 & -517480.06 & -14.44 \\ -68.89 & -15219.97 & -152200.0 & -76099.98 & -517480.06 & 757688.63 & 21.14 \\ -0.0 & -0.42 & -4.25 & -2.12 & -14.44 & 21.14 & 0.0 \end{array} \right] \\ L1 & & & & & & & \\ L2 & & & & & & & \\ L3 & & & & & & & \\ L4 & & & & & & & \\ C & & & & & & & \\ R & & & & & & & \end{matrix}$$

Once again reducing the effect of the inductors power processing into a single effective inductor yields the following covariance matrix.

$$\begin{matrix} V1 \\ L_{effective} \\ C \\ R \end{matrix} \begin{bmatrix} V1 & L_{effective} & C & R \\ 0.01 & 69.19 & -68.89 & 0 \\ 69.19 & 764325.87 & -761000.01 & -21.23 \\ -68.89 & -761000.01 & 757688.63 & 21.14 \\ 0 & -21.23 & 21.14 & 0 \end{bmatrix}$$

The same result is achieved when combining the inductors. With the slight variation in rounding and measurement error this reduced matrix represents the same power interactions relationship as the original boost converter circuit.

B.2 Extended inductors and capacitors

The same boost converter can have its inductors and capacitors extended as shown below:

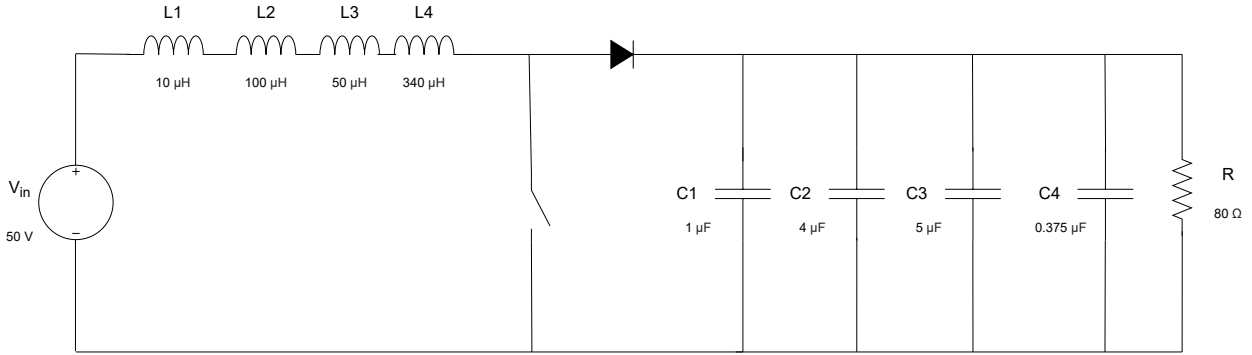


Figure 119: Traditional Boost converter with extended series inductors and extended parallel capacitors

The covariance matrix for this circuit is as follows:

$$\begin{matrix} V1 \\ L1 \\ L2 \\ L3 \\ L4 \\ C1 \\ C2 \\ C3 \\ C4 \\ R \end{matrix} \begin{bmatrix} V1 & L1 & L2 & L3 & L4 & C1 & C2 & C3 & C4 & R \\ 0.01 & 1.35 & 13.54 & 6.77 & 46.02 & -6.49 & -25.98 & -32.47 & -2.44 & -0.0 \\ 1.35 & 305.74 & 3057.4 & 1528.7 & 10395.15 & -1467.03 & -5868.14 & -7335.17 & -550.14 & -0.38 \\ 13.54 & 3057.4 & 30574.01 & 15287.0 & 103951.66 & -14670.37 & -58681.47 & -73351.84 & -5501.39 & -3.76 \\ 6.77 & 1528.7 & 15287.0 & 7643.5 & 51975.82 & -7335.18 & -29340.73 & -36675.92 & -2750.69 & -1.88 \\ 46.02 & 10395.15 & 103951.66 & 51975.82 & 353435.7 & -49879.26 & -199517.04 & -249396.3 & -18704.72 & -12.8 \\ -6.49 & -1467.03 & -14670.37 & -7335.18 & -49879.26 & 7039.3 & 28157.21 & 35196.51 & 2639.74 & 1.81 \\ -25.98 & -5868.14 & -58681.47 & -29340.73 & -199517.04 & 28157.21 & 112628.83 & 140786.04 & 10558.95 & 7.22 \\ -32.47 & -7335.17 & -73351.84 & -36675.92 & -249396.3 & 35196.51 & 140786.04 & 175982.55 & 13198.69 & 9.03 \\ -2.44 & -550.14 & -5501.39 & -2750.69 & -18704.72 & 2639.74 & 10558.95 & 13198.69 & 989.9 & 0.68 \\ -0.0 & -0.38 & -3.76 & -1.88 & -12.8 & 1.81 & 7.22 & 9.03 & 0.68 & 0.0 \end{bmatrix}$$

Once again combining the inductors into an effective inductor and the capacitor into an effective capacitor this yields the following covariance matrix:

$$\begin{matrix} V1 \\ L_{effective} \\ C_{effective} \\ R \end{matrix} \begin{bmatrix} V1 & L_{effective} & C_{effective} & R \\ 0.01 & 67.68 & -67.38 & 0 \\ 67.68 & 764350.41 & -761025.39 & -18.82 \\ -67.38 & -761025.39 & 757714.86 & 18.74 \\ 0 & -18.82 & 18.74 & 0 \end{bmatrix}$$

The result is still the same equivalent representation of the boost converter from a power processing perspective

of the reactive components. The ability to reduce the matrices allows for easier to read matrices that can represent large systems without bombarding the reader with too much information. This makes it easier to draw comparisons and pick out patterns in the power interactions of the converter components.

C The matrix method and AC power theory

C.1 Introduction

This chapter aims to establish a link between the matrix method and traditional power factor theories. It would be useful for the matrix to be able to describe real, reactive and apparent power in other sinusoidal applications other than power electronics. This chapter aims to establish some foundation in traditional power theories. Many of the findings in this chapter have not been generalized or expanded to their full extent. This ground work in the link to AC power theories is left in this research for enrichment on the origins of the matrix method and a possible foundation in AC power applications.

C.2 Correlation and power factor

One of the originating discoveries that lead to the creation of the matrix method was the idea that a correlation and a power factor are some what analogous terms. A correlation is not a part of the matrix method but correlation and covariance are related terms in data processing. A correlation is defined as a connection between two data sets and describes the degree to which these two data sets are related in a linear fashion. Its statistical meaning is the same as the everyday English meaning of “cause and effect”. Consider the following mathematical proof describing the link between a correlation and a traditional power factor.

If power factor is defined as follows:

$$\cos(\phi) = \frac{|P|}{|S|} \quad (4)$$

Where:

$$\begin{aligned} P &= \text{real power [W]} \\ S &= \text{apparent power [VA]} \end{aligned}$$

Let v be the input voltage such that:

$$v = \tilde{v} + V$$

Where:

$$\begin{aligned} \tilde{v} &= \text{AC component [V]} \\ V &= \text{DC component [V]} \end{aligned}$$

Let i be the input current such that:

$$i = \tilde{i} + I$$

Where:

$$\begin{aligned} \tilde{i} &= \text{AC component [A]} \\ I &= \text{DC component [A]} \end{aligned}$$

Then the apparent power at the source is:

$$S = v_{RMS} \times i_{RMS} \quad (5)$$

Then the average input power can be represented as:

$$\begin{aligned}
v &= \tilde{v}\sin(\omega_0 t) + V \\
i &= \tilde{i}\sin(\omega_0 t + \phi) + I \\
\langle vi \rangle &= \tilde{v}\tilde{i} \langle \sin(\omega_0 t)[\sin(\omega_0 t)\cos(\phi) + \cos(\omega_0 t)\sin(\phi)] \rangle \\
\langle vi \rangle &= \tilde{v}\tilde{i} \langle \sin^2(\omega_0 t) \rangle \cos(\phi) + \tilde{v}\tilde{i} \langle \sin(\omega_0 t)\cos(\omega_0 t) \rangle \sin(\phi) \\
\langle vi \rangle &= \tilde{v}\tilde{i} \langle \frac{1}{2}(1 - \cos(2\omega_0 t)) \rangle + \tilde{v}\tilde{i}\sin(\phi) \\
\langle vi \rangle &= \frac{\tilde{v}\tilde{i}}{2}\cos(\phi) \langle 1 \rangle - \frac{\tilde{v}\tilde{i}}{2}\cos(\phi) \langle \cos(2\omega_0 t) \rangle \\
\langle vi \rangle &= \frac{\tilde{v}\tilde{i}}{2}\cos(\phi) \\
\langle vi \rangle &= \cos(\phi) \frac{\tilde{v}}{\sqrt{2}} \frac{\tilde{i}}{\sqrt{2}} \\
\langle vi \rangle &= l_{vi}\sigma_v\sigma_i
\end{aligned}$$

Where l_{vi} is the correlation between the current and the voltage:

$$\begin{aligned}
l_{vi} &= \frac{\langle vi \rangle}{\sigma_v\sigma_i} \\
l_{vi} &= \frac{P}{S}
\end{aligned}$$

Therefore the correlation between current and voltage is a kind of power factor. Since the matrix method utilizes covariance it is important to understand how a correlation and a covariance are related from a statistical perspective. The correlation and the covariance are related by the following equation:

$$l_{xy} = \frac{COV(x, y)}{\sigma_x \cdot \sigma_y} \quad (6)$$

Where σ_x and σ_y are the standard deviation of the signals x and y. This means by extension the covariance is related to a power factor by the following relationship:

$$COV(x, y) = \frac{P}{S} \sigma_x \cdot \sigma_y \quad (7)$$

The standard deviations of these signals is equivalent to the RMS value of each signal. Therefore the covariance of two signals is equivalent to the power factor between them divided by the product of each signals RMS values.

C.3 The dot product and covariance

Another mathematical property that may be useful is a dot product. Since AC systems deal with phasor mathematics and their geometric relationships, linking the covariance to a phasor operation such as the dot product may be useful. Consider the following proof linking a dot product to the covariance.

$$\begin{aligned}
X(t) &= X \cos(\omega t + \phi_X) \\
Y(t) &= Y \cos(\omega t + \phi_Y)
\end{aligned}$$

They can be represented as phasors as follows:

$$X = X \angle \phi_X$$

$$Y = Y \angle \phi_Y$$

The dot product between these two signals can be defined geometrically as:

$$X \cdot Y = XY \cos(\phi_X - \phi_Y)$$

However, this dot product is for vectors only and needs to be extended for the use in phasors. Considering the time domain signals X and Y their covariance can be defined as follows:

$$\text{cov}(X, Y) = \frac{1}{T} \int_0^T (X(t) - \bar{X})(Y(t) - \bar{Y}) dt$$

These time domain signals are already zero mean so the covariance reduces to:

$$\text{cov}(X, Y) = \frac{1}{T} \int_0^T (X \cos(\omega t + \phi_X))(Y \cos(\omega t + \phi_Y)) dt$$

$$\text{cov}(X, Y) = \frac{1}{2} XY (\phi_X - \phi_Y)$$

$$\text{cov}(X, Y) = \frac{1}{2} X \cdot Y$$

Therefore the covariance and the dot-product are equivalent with only a factor of half between them. This can also be simplified if the time scales are shifted to make one of the phasors have a zero angle as shown below:

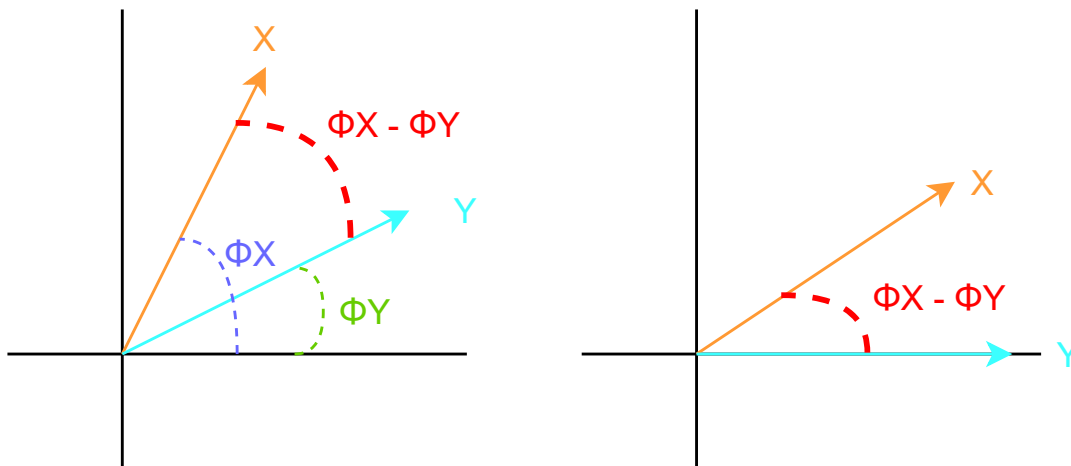


Figure 120: Shifted phasor diagram

Which gives a covariance of:

$$\text{cov}(X, Y) = \frac{1}{T} \int_0^T (X \cos(\omega t + (\phi X - \phi Y)))(Y \cos(\omega t)) dt$$

C.4 The relationship between the matrix method and the power triangle

It is possible to arrive at the standard power triangle used in AC systems by the matrix method. This method uses only covariance and has no “knowledge” of reactive, real or apparent power definitions from a circuit perspective. Yet the matrix method is able to describe the relationship between these three in the power triangle. It is not yet known if this is coincidental or not but it is an interesting case nonetheless. The following RL circuit example will show how the matrix method is able to produce the power triangle in this particular case.

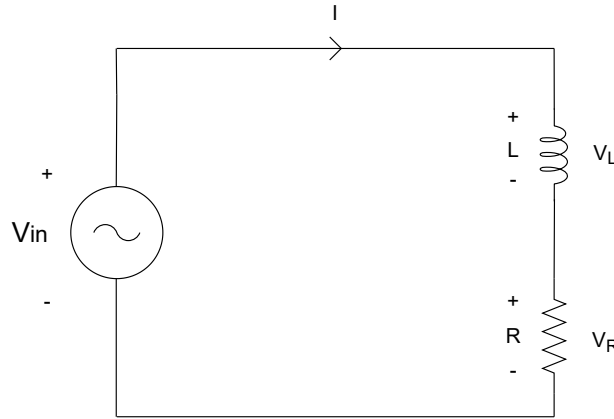


Figure 121: Diagram of a simple RL circuit fed by an AC source

The current I is common to all elements. Table 13 below shows the phasor and time domain definitions of the relevant current and voltage waveforms in the circuit.

Table 12: Table of phasor and time domain signals in RL circuit

Phasor	Time Domain
$V_{in} = V_{in} \angle \phi V_{in}$	$V_{in} \cos(\omega t + \phi V_{in})$
$V_L = V_{in} \angle \phi V_L$	$V_L \cos(\omega t + \phi V_L)$
$V_R = V_{in} \angle \phi V_R$	$V_R \cos(\omega t + \phi V_R)$
$I = I \angle \phi I$	$I \cos(\omega t + \phi I)$

The instantaneous power in each element can then be calculated by multiplying each elements current and voltages together:

Table 13: Table of instantaneous power signals in RL circuit

	Instantaneous Power
Source	$\frac{-V_{in}I}{2} \cos(\phi V_{in} - \phi I) + \frac{-V_{in}I}{2} \cos(2\omega t + \phi V_{in} + \phi I)$
Resistor	$\frac{V_R I}{2} \cos(\phi V_R - \phi I) + \frac{V_R I}{2} \cos(2\omega t + \phi V_R + \phi I)$
Inductor	$\frac{-V_L I}{2} \cos(\phi V_L - \phi I) + \frac{V_L I}{2} \cos(2\omega t + \phi V_L + \phi I)$

Using these instantaneous powers the covariance matrix can be calculated as:

$$\begin{matrix} S \\ R \\ L \end{matrix} \begin{bmatrix} \frac{S}{8} & -\frac{R}{8} & -\frac{L}{8} \\ \frac{(V_{in}I)^2}{8} & \frac{(V_R I)(V_{in}I) \cos(\phi V_{in} - \phi I)}{8} & -\frac{(V_L I)(V_{in}I) \sin(\phi V_{in} - \phi I)}{8} \\ -\frac{(V_R I)(V_{in}I) \cos(\phi V_{in} - \phi I)}{2} & \frac{(V_R I)^2}{8} & 0 \\ -\frac{(V_L I)(V_{in}I) \sin(\phi V_{in} - \phi I)}{2} & 0 & \frac{(V_L I)^2}{8} \end{bmatrix}$$

Now using the fact that power factor and reactive factor can be represented as:

$$\begin{aligned} pf &= \cos(\phi V_{in} - \phi I) \\ rf &= \sin(\phi V_{in} - \phi I) \end{aligned}$$

And that:

$$\begin{aligned} |S| &= \left(\frac{V_{in}I}{2}\right) \\ |Q| &= \left(\frac{V_L I}{2}\right) \\ |P| &= \left(\frac{V_R I}{2}\right) \\ P &= S pf \\ Q &= S rf \end{aligned}$$

The covariance matrix can be reduced to :

$$\begin{matrix} S \\ R \\ L \end{matrix} \begin{bmatrix} \frac{S}{2} & -\frac{R}{2} & -\frac{L}{2} \\ \frac{(S)^2}{2} & \frac{(P)^2}{2} & \frac{(Q)^2}{2} \\ -\frac{PSpf}{2} & 0 & 0 \\ -\frac{QStrf}{2} & 0 & 0 \end{bmatrix}$$

Now removing the factor of $\frac{1}{2}$:

$$\begin{matrix} S \\ R \\ L \end{matrix} \begin{bmatrix} S & -R & -L \\ (S)^2 & -(P)^2 & -(Q)^2 \\ -(P)^2 & (P)^2 & 0 \\ -(Q)^2 & 0 & (Q)^2 \end{bmatrix}$$

Using the zero sum property of the rows in the matrix it can be seen that the first row is $S^2 = P^2 + Q^2$. This shows that for this case the covariance matrix is a re-statement of the normal power triangle of the circuit. This case suggests that the covariance matrix is a projection where the power factor and reactive factor act as the projection angles. If the instantaneous source power is expanded completely this results in:

$$p(t) = \frac{-V_{in}I}{2} \cos(\phi V_{in} - \phi I) + \frac{-V_{in}I}{2} \cos(\phi V_{in} - \phi I) \cos(2\omega t) - \frac{-V_{in}I}{2} \sin(\phi V_{in} - \phi I) \sin(2\omega t)$$

The second two terms are the ones under consideration as these are the fluctuating terms that the covariance is able to capture. The fluctuations still carry the same average power term. Now lets expand this example to

an RLC circuit and see if the power triangle still falls out of the analysis. Consider the following RLC circuit example as an extension of this exercise:

This circuit is more complicated than the previous example but it has been chosen as it allows for a common current to flow through all the components and makes the analysis much simpler. Consider the circuit shown in *Figure 122* below:

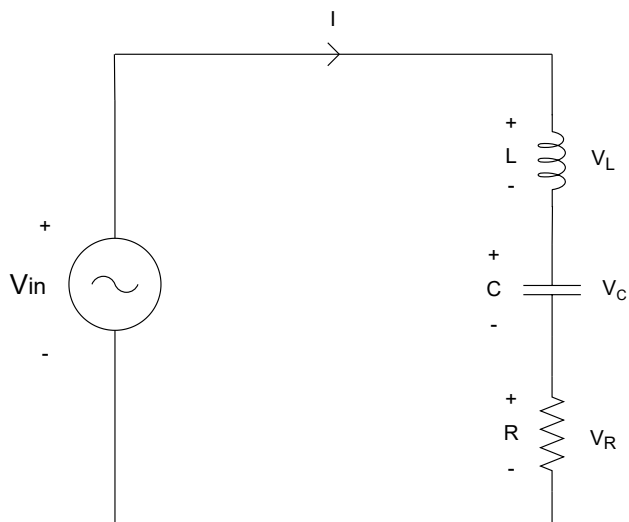


Figure 122: Diagram of a simple RLC circuit fed by an AC source

The voltages and currents can be defined in the same way as before:

Table 14: Table of phasor and time domain signals in RLC circuit

Phasor	Time Domain
$V_{in} = V_{in} \angle \phi V_{in}$	$V_{in} \cos(\omega t + \phi V_{in})$
$V_L = V_{in} \angle \phi V_L$	$V_L \cos(\omega t + \phi V_L)$
$V_R = V_{in} \angle \phi V_R$	$V_R \cos(\omega t + \phi V_R)$
$V_C = V_{in} \angle \phi V_C$	$V_C \cos(\omega t + \phi V_C)$
$I = I \angle \phi I$	$I \cos(\omega t + \phi I)$

The instantaneous power in each element can then be calculated by multiplying each elements current and voltages together:

Table 15: Table of instantaneous power signals in RLC circuit

	Instantaneous Power
Source	$\frac{-V_{in}I}{2} \cos(\phi V_{in} - \phi I) + \frac{-V_{in}I}{2} \cos(2\omega t + \phi V_{in} + \phi I)$
Resistor	$\frac{V_R I}{2} \cos(\phi V_R - \phi I) + \frac{V_R I}{2} \cos(2\omega t + \phi V_R + \phi I)$
Inductor	$\frac{-V_L I}{2} \cos(\phi V_L - \phi I) + \frac{V_L I}{2} \cos(2\omega t + \phi V_L + \phi I)$
Capacitor	$\frac{-V_C I}{2} \cos(\phi V_C - \phi I) + \frac{V_C I}{2} \cos(2\omega t + \phi V_C + \phi I)$

The variance of each component will be half the components power squared as before.

$$\begin{matrix} S \\ R \\ L \\ C \end{matrix} \left[\begin{array}{cccc}
\begin{matrix} S \\ \frac{(V_{in}I)^2}{8} \end{matrix} & \begin{matrix} R \\ -\frac{(V_R I)(V_{in}I) \cos(\phi V_{in} - \phi I)}{2} \end{matrix} & \begin{matrix} L \\ -\frac{(V_L I)(V_{in}I) \sin(\phi V_{in} - \phi I)}{2} \end{matrix} & \begin{matrix} C \\ \frac{(V_C I)(V_{in}I) \sin(\phi V_{in} - \phi I)}{2} \end{matrix} \\
-\frac{(V_R I)(V_{in}I) \cos(\phi V_{in} - \phi I)}{2} & \begin{matrix} R \\ \frac{(V_R I)^2}{8} \end{matrix} & 0 & 0 \\
-\frac{(V_L I)(V_{in}I) \sin(\phi V_{in} - \phi I)}{2} & 0 & \begin{matrix} L \\ \frac{(V_L I)^2}{8} \end{matrix} & -\frac{(V_L I)(V_C I)}{2} \\
\frac{(V_C I)(V_{in}I) \sin(\phi V_{in} - \phi I)}{2} & 0 & -\frac{(V_L I)(V_C I)}{2} & \begin{matrix} C \\ \frac{(V_C I)^2}{8} \end{matrix}
\end{array} \right]$$

Now to reduce this matrix the standard definitions of powers and factors can be replaced noting that the reactive power now has a Q_C and Q_L in place.

$$\begin{matrix} S \\ R \\ L \\ C \end{matrix} \left[\begin{array}{cccc}
\begin{matrix} S \\ \frac{(S)^2}{2} \end{matrix} & \begin{matrix} R \\ -\frac{P S p f}{2} \end{matrix} & \begin{matrix} L \\ -\frac{Q_L S r f}{2} \end{matrix} & \begin{matrix} C \\ \frac{Q_C S r f}{2} \end{matrix} \\
-\frac{P S p f}{2} & \begin{matrix} R \\ \frac{(P)^2}{2} \end{matrix} & 0 & 0 \\
-\frac{Q_L S r f}{2} & 0 & \begin{matrix} L \\ \frac{(Q_L)^2}{2} \end{matrix} & -\frac{Q_L Q_C}{2} \\
\frac{Q_C S r f}{2} & 0 & -\frac{Q_L Q_C}{2} & \begin{matrix} C \\ \frac{(Q_C)^2}{2} \end{matrix}
\end{array} \right]$$

Now removing the factor of $\frac{1}{2}$. Also note that $S r f$ is the total reactive power as seen by the source which would equate to $Q_L + Q_C$:

$$\begin{matrix} S \\ R \\ L \\ C \end{matrix} \left[\begin{array}{cccc}
\begin{matrix} S \\ S^2 \end{matrix} & \begin{matrix} R \\ -P^2 \end{matrix} & \begin{matrix} L \\ -Q_L(Q_L + Q_C) \end{matrix} & \begin{matrix} C \\ -Q_C(Q_L + Q_C) \end{matrix} \\
-P^2 & \begin{matrix} R \\ P^2 \end{matrix} & 0 & 0 \\
-Q_L(Q_L + Q_C) & 0 & \begin{matrix} L \\ Q_L^2 \end{matrix} & \begin{matrix} C \\ Q_L Q_C \end{matrix} \\
-Q_C(Q_L + Q_C) & 0 & Q_L Q_C & \begin{matrix} C \\ Q_C^2 \end{matrix}
\end{array} \right]$$

This is a bit of a different picture than before but adding the entries for the inductor and capacitor gives $(Q_L + Q_C)^2$ which then reduces to the normal power triangle again. These may be specialized cases and this is not yet confirmed to be a generalized result. During the development phase of the matrix method this link to the power triangle came out of an AC analysis and looked to be promising to investigate the reactive power flow in power electronics converters. The next section will analyze the matrix method when applied to a power factor correction circuit.

C.5 Power Factor Correction Circuit

Consider the following power factor correction circuit as seen in [Figure 123](#). This circuit is more complex than the previous RLC circuits as there is no longer a common current in all components. This means that it will be difficult to relate all the components to the power factor of the source. The current in the RL and C branch could have arbitrary phase angles relative to each other and can complicate the analysis. This means two power factors need to be identified as the power factor for the RL branch and the power factor of the whole circuit as seen by the source.

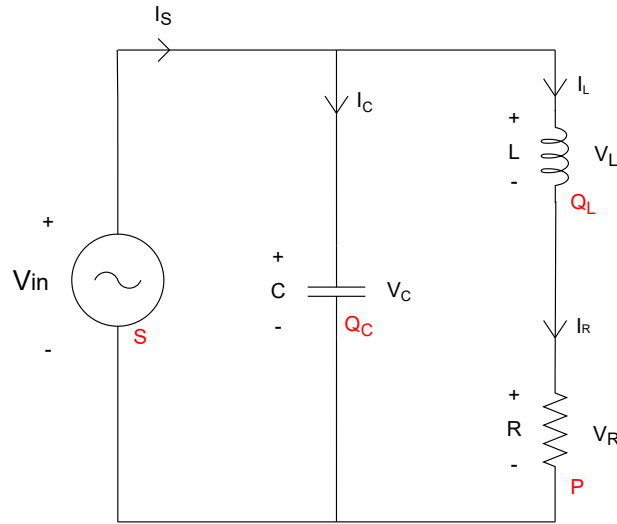


Figure 123: Diagram of a power factor correction circuit fed by an AC source

This makes the covariance matrix difficult to compute analytically even after simplification. The equations below show only the upper diagonal terms of the covariance matrix for this circuit:

$$\begin{aligned}
 cov(V_{in}, V_{in}) &= \frac{S^2}{2} \\
 cov(V_{in}, R) &= -SP((pf_{load}^2 - \frac{1}{2})pf + (pf_{load}rf_{load}rf)) \\
 cov(V_{in}, L) &= -SQ_L((pf_{load}^2 - \frac{1}{2})rf + (pf_{load}rf_{load}pf)) \\
 cov(V_{in}, C) &= -SQ_C\frac{rf}{2} \\
 cov(R, R) &= \frac{P^2}{2} \\
 cov(R, L) &= 0 \\
 cov(R, C) &= -Q_C P(pf_{load}rf_{load}) \\
 cov(L, L) &= \frac{Q_L^2}{2} \\
 cov(L, C) &= Q_C Q_L(pf_{load}^2 - \frac{1}{2}) \\
 cov(C, C) &= \frac{Q_C^2}{2}
 \end{aligned}$$

These complex terms highlight the fact that the power flow picture of power factor correction is not as simple as it is thought to be. Traditionally the RL load is considered to have some reactive power that is exchanged with the source. This reactive power is undesirable because it increases the effective currents and leads to increased loss. A capacitor is placed into the circuit near the load and it is sized so the power factor of the overall circuit reduces to 1. The capacitor and inductor are thought to exchange reactive power and the reactive power no longer needs to be sent all the way from the source. This might be true from a high level perspective but lets look at this more closely.

Figure 124 below shows the example circuit that is power factor corrected to unity from a power factor of 0.85. The circuit requires a 286.8 uF capacitor to correct the power factor.

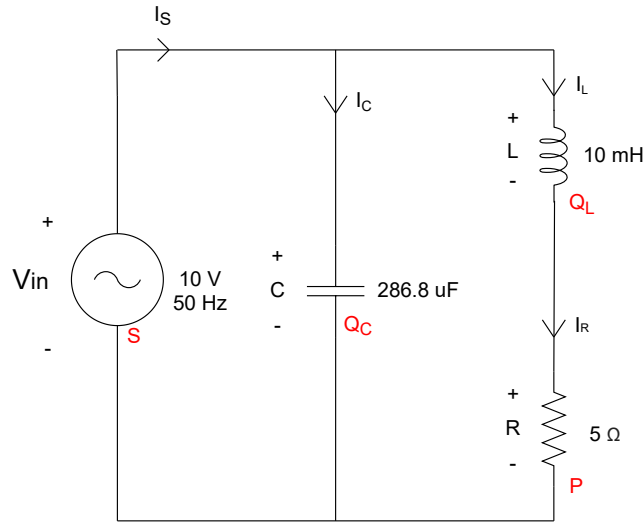


Figure 124: Diagram of a power factor correction circuit fed by an AC source

The instantaneous power supplied by the load and absorbed by the resistor in the uncorrected case in *Figure 125a* and uncorrected case in *Figure 125b*. It is clear that in the uncorrected case the power in the source is larger as it is also supplying the reactive power. In the corrected case the source sees unity power factor and supplies only the power required by the load. What is important in the corrected case is that the phase of the instantaneous powers are different. The power supplied by the source is not being delivered directly to the resistor. This is counter intuitive to the idea that the reactive powers are dealt with between the inductor and the capacitor and the source supplies directly to the resistor.

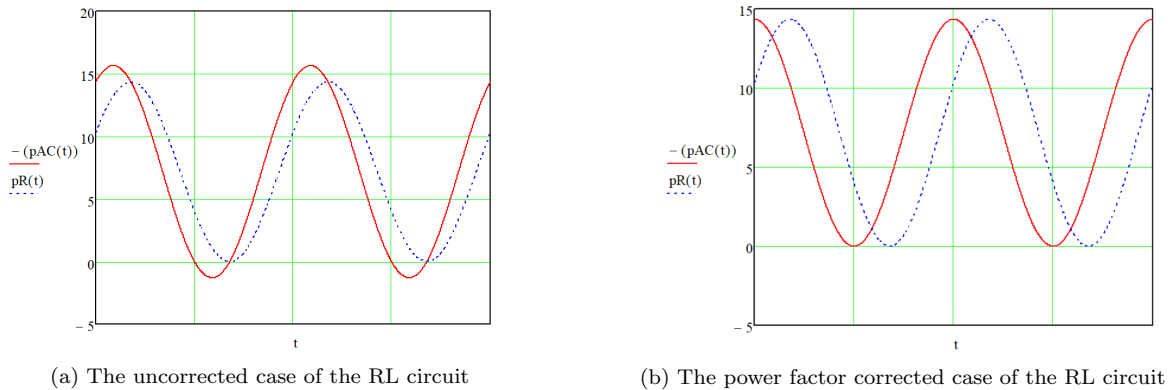


Figure 125: The uncorrected and power factor corrected case of an RL circuit

On an average basis the source is supplying only the average power required by the resistor but not on an instantaneous basis. The covariance matrix for this circuit in *Figure 124* is shown below:

$$\begin{matrix} V_{in} \\ R \\ L \\ C \end{matrix} \begin{bmatrix} V_{in} & R & L & C \\ 25.7 & -11.15 & -14.55 & 0 \\ -11.15 & 25.7 & 0 & -14.55 \\ -14.55 & 0 & 10.15 & 4.4 \\ 0 & -14.55 & 4.4 & 10.15 \end{bmatrix}$$

The diagonals of the covariance matrix appear to be half the powers squared of each component. This shows the activity of the components. The off-diagonal entries show the interactions between the components. *Figure 126* below shows an annotated diagram of the power interactions. These annotated diagrams are used in this chapter to graphically represent the covariance matrices. The standard will be the main diagonal entries of each element

shown in orange and the off diagonal interactions are shown by purple arrows between components with their respective magnitude.

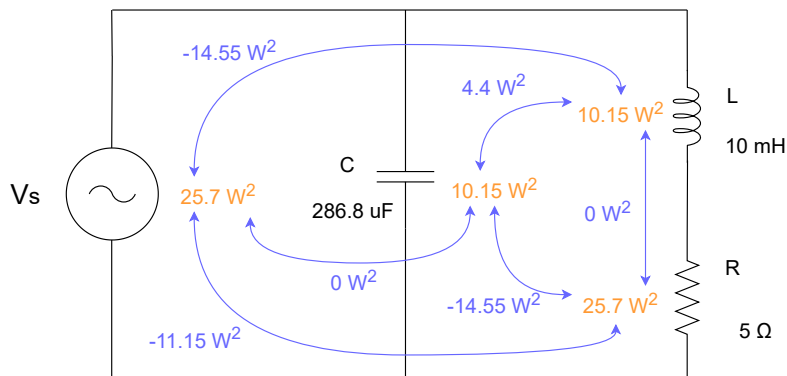


Figure 126: Diagram of a power factor correction circuit fed by an AC source with detailed power interactions

This diagram shows that the powers of the L and C are equal. This is expected due to the unity power factor. The power from the source and the resistor are also the same. It appears the source interacts with the inductor and resistor. Then the inductor and capacitor and then the capacitor and resistor. This is a convoluted path but as previously mentioned the power may not go directly to the resistor. The internal power processing of this circuit is more complex than originally thought. Care must be taken when thinking of the power as a flow quantity in the circuit. Using the properties of the covariance matrix the effective LC combination can be reduced as follows:

$$\begin{matrix} V_{in} \\ R \\ LC \end{matrix} \begin{bmatrix} V_{in} & R & LC \\ 25.7 & -11.15 & -14.55 \\ -11.15 & 25.7 & -14.55 \\ -14.55 & -14.55 & 29.1 \end{bmatrix}$$

The resulting simplified diagram is shown in Figure 127 below:

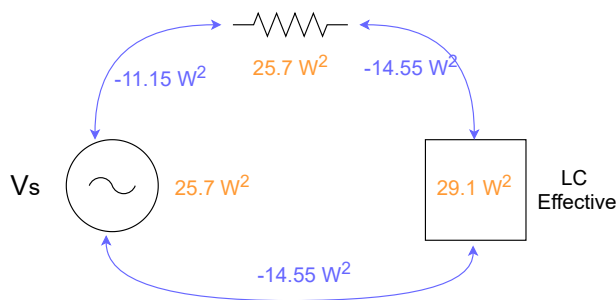


Figure 127: Diagram of effective power factor correction circuit from power interaction perspective

This shows the LC processing block plays a role in getting power to the resistor. The interactions on either side of the block are equal as this happens with unity power factor. This is attributed to having no excess reactive power in the circuit.

C.6 Power Factor Correction Special Case with 45° Angle In The Load

This is a special case circuit with a load power factor of 0.7 or a 45° angle in the load. The circuit is shown in Figure 128 below:

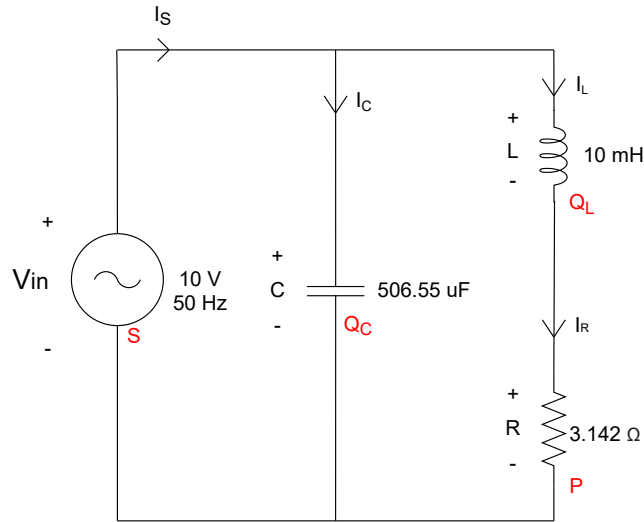


Figure 128: Diagram of special case power factor correction

The covariance matrix for this circuit can be calculated as follows:

$$\begin{matrix} V_{in} \\ R \\ L \\ C \end{matrix} \begin{bmatrix} V_{in} & R & L & C \\ 31.66 & 0 & -31.66 & 0 \\ 0 & 31.66 & 0 & -31.66 \\ -31.66 & 0 & 31.66 & 0 \\ 0 & -31.66 & 0 & 31.66 \end{bmatrix}$$

The annotated diagram is shown in *Figure 129* below:

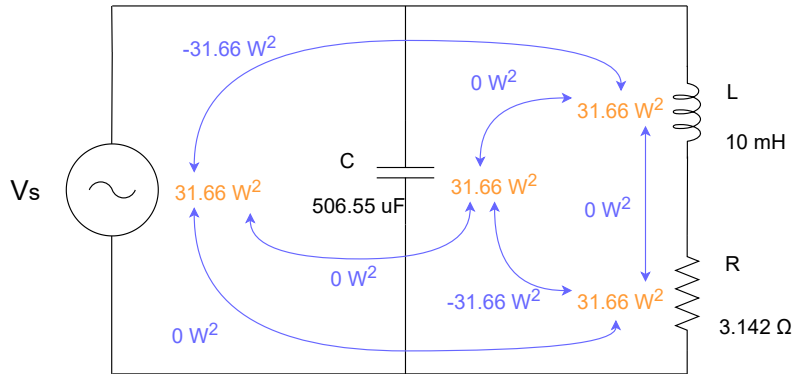


Figure 129: Diagram of special case power factor correction annotated with power interactions

This shows that the powers of the source and the inductor are exactly out of phase and shifted 90° from the resistor and capacitor which are also exactly out of phase with each other. This suggests that power flows through components might not be an entirely correct perception of power. It is known that the average power appears in the resistor as illustrated by the average term. The covariance matrix shows how the components are interacting with each other to process the power and as a result the delivery of the average power.

Using the properties of the covariance matrix the inductor and capacitor can be combined to an effective processing block as seen below:

$$\begin{matrix} V_{in} \\ R \\ LC \end{matrix} \begin{bmatrix} V_{in} & R & LC \\ 31.66 & 0 & -31.66 \\ 0 & 31.66 & -31.66 \\ -31.66 & -31.66 & 63.32 \end{bmatrix}$$

This is shown in *Figure 130* below:

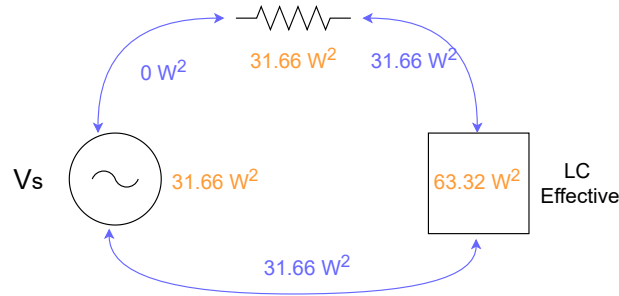


Figure 130: Diagram of special case power factor correction annotated reduced power interaction form

This shows the reactive components are heavily involved getting the power to the resistor.

As an alternative interpretation consider this:

In the simple case of the pure RL circuit below, the sum of the powers of the inductor and resistor equal the power in the source. The powers of the inductor and capacitor are 90° shifted and form an orthogonal base. Considering the projections of the source power onto the resistor and inductor as “dimensions” this produces the normal real and reactive powers. The projections are the covariance’s, or inner products.

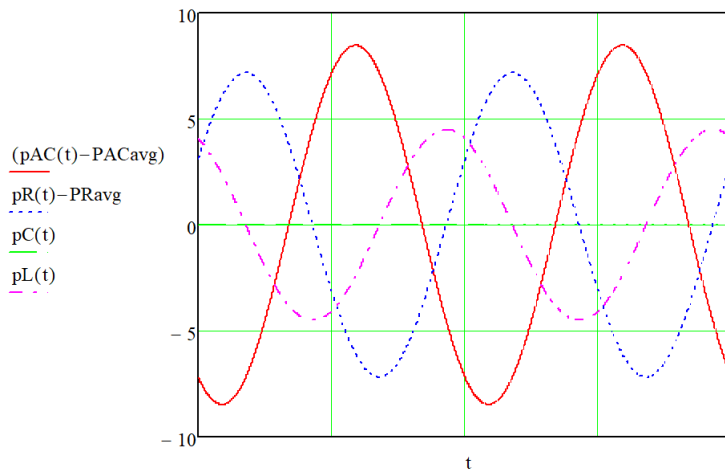


Figure 131: Uncorrected power factor of RL circuit

For the case of the power factor corrector below. The sum of the powers in the circuit add up to be the power in the source but now three components in the circuit and their powers are not all 90° shifted. However, considering the three circuit components to be three “dimensions” even if they do not form an orthogonal base, then taking the projection or inner product of each of these components onto the source power. This projection is again the covariance. Now it can be seen how each of the components contribute to the power of the source. This is now a multi dimensional power triangle. For a normal simple RL load the R and the L powers are at 90° so their interaction and projections are zero. But for the more complicated multidimensional case the individual power components are not at 90° so there is some in-between interaction.

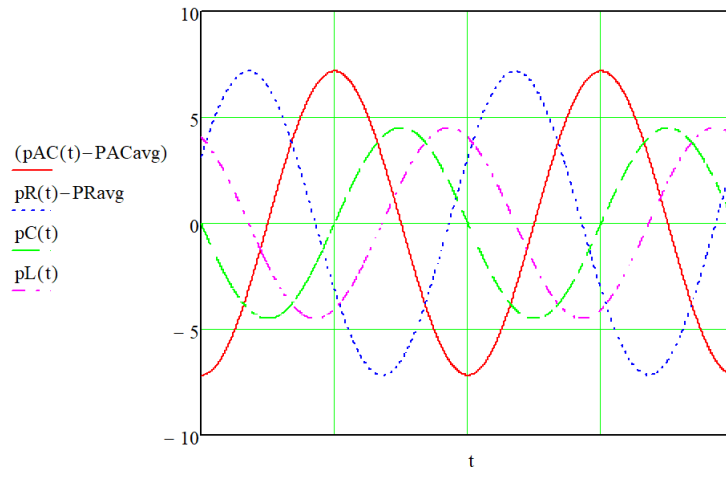


Figure 132: Power factor corrected RL circuit

D A brief overview of differential power methods

D.1 Introduction

This chapter outlines the work of Cobos et al and the theories surrounding differential power. This chapter is written as a short outline of their collective work and how it can be applied to power electronics. Since their papers are difficult to understand and practically apply when first encountered.

D.2 The fundamentals of differential power

The ideas of differential power processing have been around for quite some time. Originating with Wilson's paper on *Basic Considerations for DC to DC Conversion Networks* in 1966 which was subsequently proven by Wolaver in *Fundamental Study of DC to DC Conversion Systems* in 1969 [20, 21]. Simply put the idea is that a converter is configurable to process a certain amount of power. Each converter topology has a fundamental limit of processed power that is required to be processed and cannot be avoided. This power is known as "Differential Power". In practice the actual power processed by a topology is more than the fundamental limit. The goal of this method is to design topologies in such a way that their processed power approaches this fundamental limit.

Cobos et al. have recently rediscovered these principles and have put this idea to work in recent literature. Their extension on these methods breaks the power processed by a converter into three categories. Differential power as the fundamental lower limit that a topology must process in order to fulfill its conversion. Direct power as the portion of the power that may be transferred from source to load without contributing to the converter's losses. This power is not processed and is rather transferred directly from source to load. Direct power requires a direct line of current between source and load during a switching state. The direct line of current is merely a circuit connection between source and load that allows a loop current to join both circuit elements. Some topologies have a direct line of current such as the boost converter in the off state. Other topologies such as the buck-boost converter are not able to achieve direct power as there is no direct loop current between source and load in either switching state. This means the buck-boost converter must process all of its power.

Finally, Indirect power is the third category and is defined as the actual power that is processed by the converter in a system that is not operating at the fundamental limit of power processing. This means indirect power is greater than or equal to differential power when the topology is not in a completely ideal scenario.

Cobos et al. define the following relationships between these categories of power:

$$G = \max\left(\frac{I_{out}}{I_{in}}, \frac{V_{out}}{V_{in}}\right) \quad (8)$$

$$P_{differential} = P_{out} - P_{direct} \quad (9)$$

$$P_{differential} = \min(P_{indirect}) = \left(1 - \frac{1}{G}\right)P_{out} \quad (10)$$

$$P_{indirect} \geq P_{diff} \quad (11)$$

$$P_{dir} = i_{dir} \times \min(V_{in}, V_{out}) \quad (12)$$

Indirect power is essentially the power that is processed by inductors, capacitors and transformers since other switching elements in topologies only incur losses and do not process power. In order to calculate the indirect power a topology processes one can calculate the power processed by each of these elements in a switching state. This is because during steady state operation a converter should store and release the same amount of energy

in the reactive components.

$$P_{indirect} = P_{Transformer} + P_{Inductor} + P_{Capacitor} \quad (13)$$

This equation excludes the output filter capacitor since the output filter capacitor as it is considered to be part of the load. Since direct power can only be transferred when a direct path of current exists in a topology, this design method encourages taking advantage of direct paths of current to minimize the amount of power processed in a topology, leveraging off of direct power. The current I_{dir} in the above formula refers to the current that enters the node containing the output filter capacitor and load, it is not the current in the load.

Cobos et al. also define three different types of “cells” in their analysis of differential power. The isolated, step up and step down cells as depicted below:

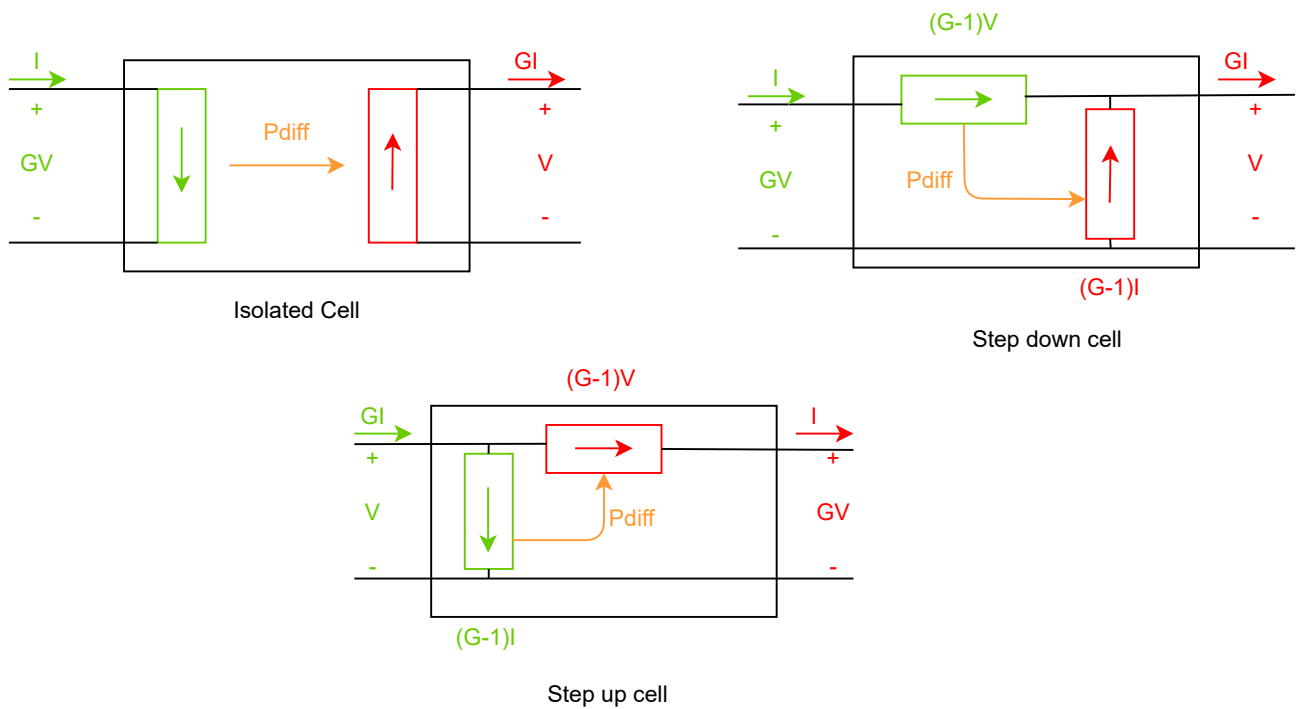


Figure 133: Three basic cell types defined for differential power processing

Notice how the isolated cell must transfer all of its power from source to load as differential power as it is not able to transfer any direct power. An example of this kind of cell is the buck-boost converter. Certain types of step up and step down cells are capable of transferring direct power during one of their switching states. Examples of these converters are the boost and the buck respectively. Take note of the definitions of I and V for the step up and step down cells. It is important to note if the cell type is referring to the input or output current/voltage in the equations below:

Equation 14 is the direct power for a step up cell:

$$P_{dir} = V_{in} \times I_{out} \quad (14)$$

Equation 15 is the direct power for a step down cell:

$$P_{dir} = V_{out} \times I_{in} \quad (15)$$

And differential power for both step up and step down cells is:

$$P_{diff} = P_{out} \times \left(1 - \frac{1}{G}\right) \quad (16)$$

Since the isolated cell cannot produce direct power $P_{dir} = 0$ and $P_{diff} = P_{out}$ as all power at the output has been processed.

D.3 Analysis of boost converter using differential power methods

This example will analyze a boost converter using differential power theories as an example on the application of the method to a power electronics converter. The table below describes the operating characteristics of the boost converter:

Table 16: Boost converter characteristics

Criteria	Value
V_{in}	50 V
V_{out}	300 V
P_{out}	250 W
I_{in}	≈ 5 A
I_{out}	≈ 833.33 m A
f_s	100 kHz

Figure 134 below shows the implementation of the boost converter:

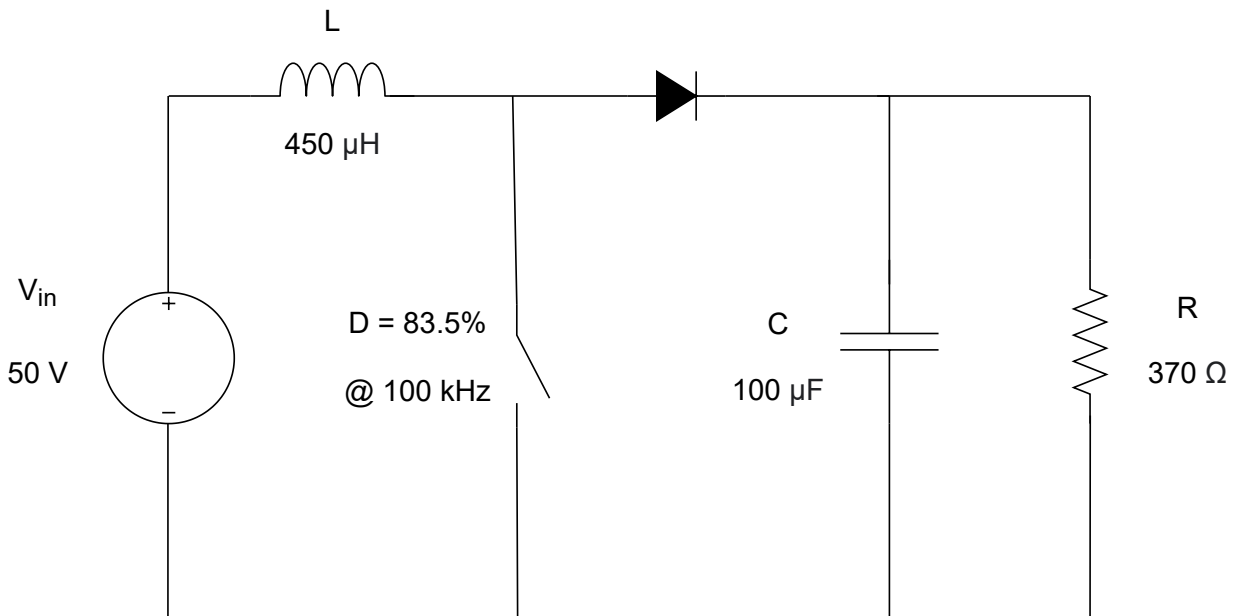


Figure 134: Diagram of boost converter

Since direct power is only transferable during the off state, due to the direct current path, consider the equivalent off state circuit:

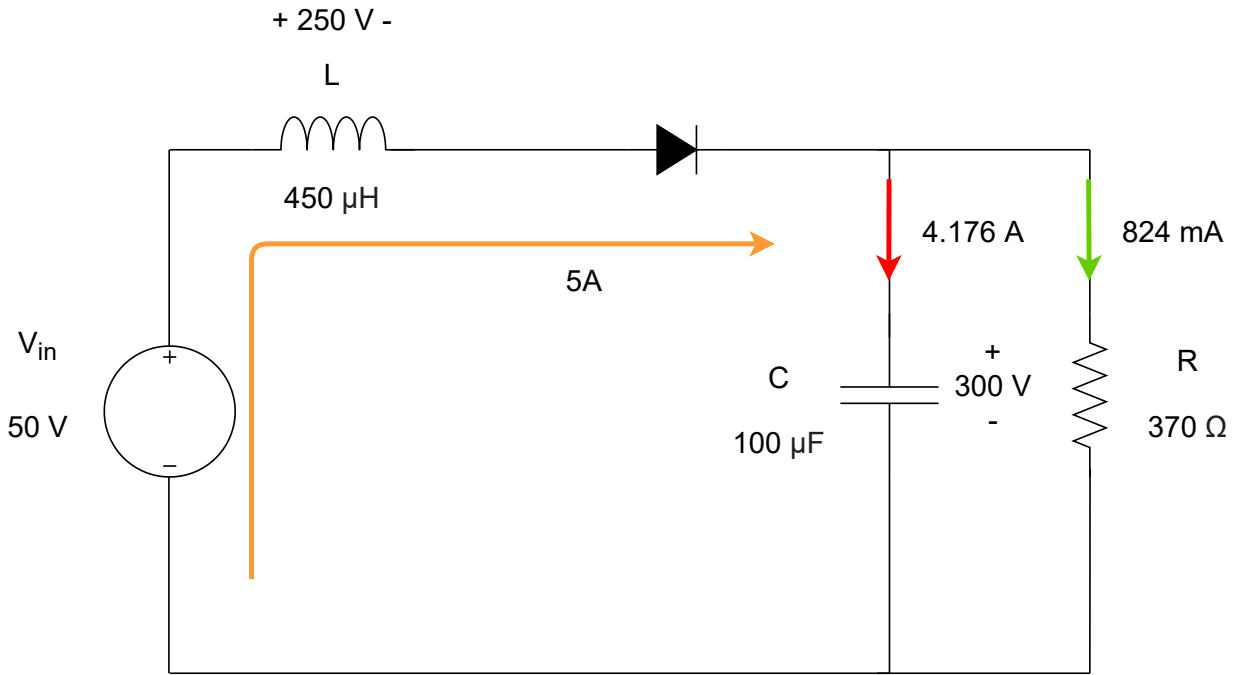


Figure 135: Boost converter off state

Using equations 8 to 12 the off state for the boost can be analyzed as follows:

The direct power caused by the direct current path denoted by the orange arrow is :

$$P_{dir} = I_{dir} \times V_{in}$$

$$P_{dir} = (5)(50) = 250W$$

The direct power given to the load resistor is:

$$P_{dir}R = (1 - D)P_{dir}$$

$$P_{dir}R = (1 - 0.835)250 = 41.25W$$

The total power evident at the output terminals is given by:

$$P_{tot} = I_{dir} \times V_o$$

$$P_{tot} = (5)(300) = 1500W$$

The indirect power in the boost is merely the power in the inductor since the output capacitor is not considered to be part of the indirect power calculation. This is also because the powers in each component are complementary in a switching cycle, so the power in each are the same. The average power in the inductor is:

$$P_{ind} = VI = (250)(5) = 1250W$$

Now the total power at the output is also the sum of the direct and indirect powers previously calculated

$$P_{tot} = P_{ind} + P_{dir}:$$

$$P_{tot} = 1250 + 250 = 1500W$$

To see how far from the fundamental limit of power processing this boost converter strays, the differential power can be calculated:

$$G = \max\left(\frac{I_{out}}{I_{in}}, \frac{V_{out}}{V_{in}}\right) = \max\left(\frac{824mA}{5A}, \frac{300V}{50V}\right) = 6$$

$$P_{differential} = \left(1 - \frac{1}{G}\right)P_{out} = \left(1 - \frac{1}{6}\right)(250) = 208.33W$$

This means that the boost converter by design has to process at least 208.33 W of power to achieve the conversion ratio, however in practice the converter is actually processing 1250 W of power to achieve the conversion ratio.

Cobos et al. use a nice graphical technique to describe this power relationship using what they call VA area diagrams. The caveat is that one needs to know the direct and indirect powers in order to construct the diagram. The analysis above outlines the mathematical method than can be extended to much more complex circuits than simple buck and boost converters. Since it is possible, although cumbersome, to mathematically determine the indirect power in multiple reactive components. To construct a VA area diagram one would have to do the mathematical analysis of a more complex system regardless to find the indirect power. The VA area technique is used as an illustration of the power processing in simpler step up and step down cells. This boost converter can be represented using the VA area technique as shown below:

The definitions for V and I follow the definitions from *Figure 133* for the step up cell:

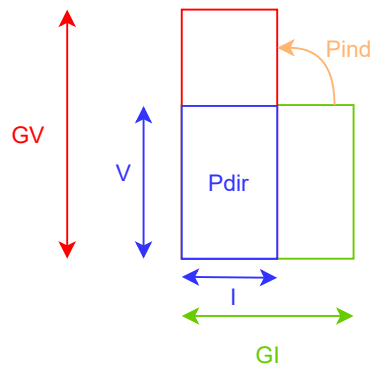


Figure 136: Generic VA area depiction of a step up cell

Below is the VA area diagram for the system in question:

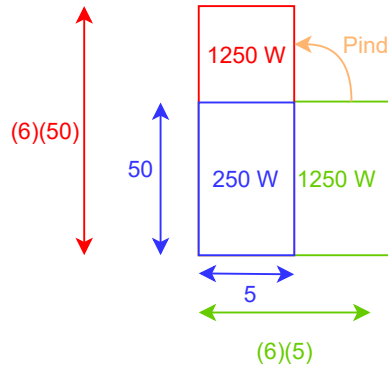


Figure 137: VA area depiction of the Boost converter system

This VA area analysis confirms the mathematical approach used earlier. This method does become difficult to apply to more complex converter topologies as a deeper understanding of the topologies operation is required to calculate the indirect power and it is not always as simple as it being one components average power. Consider the following more complex example of a quadratic boost converter.

D.4 Analysis of quadratic boost converter using differential power methods

This experiment will apply differential power methods to a complicated quadratic boost converter topology. This is more complex as there are now three reactive elements in the converter, excluding the output capacitor. The indirect power is no longer trivial to calculate and the direction of current paths needs to be considered to evaluate the indirect power in reactive components. The table below outlines the operating characteristics of the quadratic boost converter:

Table 17: Quadratic boost converter characteristics

Criteria	Value
V_{in}	50 V
V_{out}	300 V
P_{out}	250 W
I_{in}	$\approx 5A$
I_{out}	$\approx 833.33m A$
f_s	70 kHz

Figure 138 below shows the particular topology of quadratic boost that is being used in this assessment:

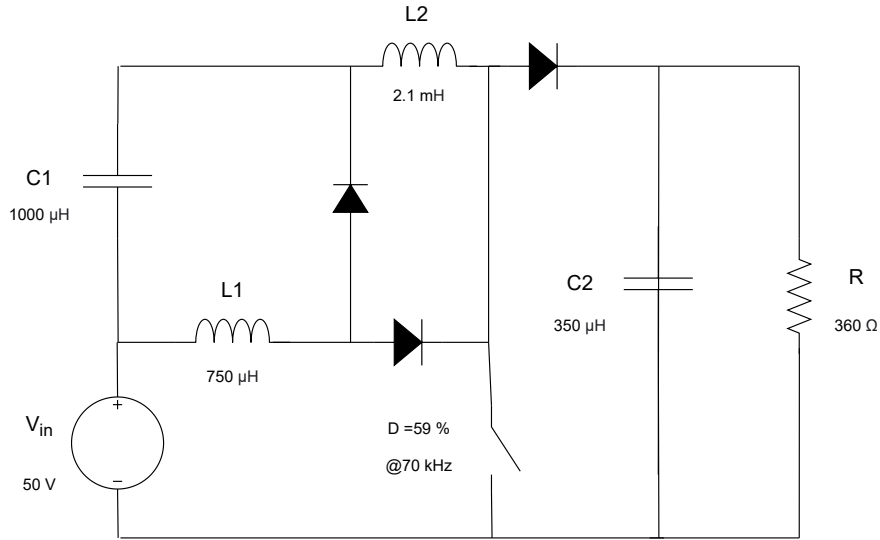


Figure 138: Diagram of quadratic boost converter

Since this quadratic boost also only transfers direct power during the off state, consider the equivalent off state circuit in *Figure 139*. The green arrow represents the path of direct current between source and load in this switching interval. The orange arrows represent the indirect power flow in the converter and the purple arrow represents direct power flow.

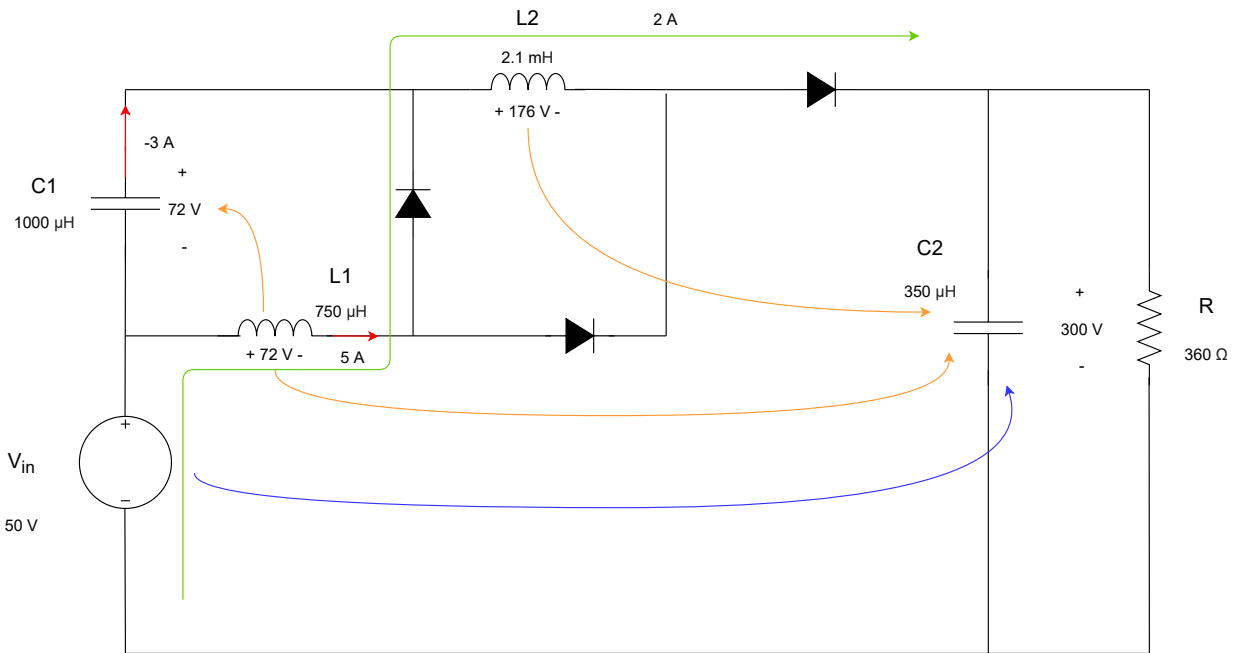


Figure 139: Diagram of quadratic boost converter equivalent off state

Using equations 8 to 12 the off state for the quadratic boost can be analyzed as follows:

The direct power (purple arrow) caused by the direct current path (green arrow) is :

$$P_{dir} = I_{dir} \times V_{in}$$

$$P_{dir} = (2)(50) = 100W$$

The direct power given to the load resistor is:

$$P_{dir}R = (1 - D)P_{dir}$$

$$P_{dir}R = (1 - 0.59)100 = 41W$$

The total power evident at the output terminals is given by:

$$P_{tot} = I_{dir} \times V_o$$

$$P_{tot} = (2)(300) = 600W$$

The indirect power in the quadratic boost is now the sum of the power in C1, L1 and L2 since the output capacitor is not considered to be part of the indirect power calculation. The average power in each of these components is:

$$P_{ind} = VI = (72)(-3) + (72)(5) + (176)(2) = 500W$$

Now the total power at the output is also the sum of the direct and indirect powers previously calculated

$$P_{tot} = P_{ind} + P_{dir}:$$

$$P_{tot} = 500 + 100 = 600W$$

To see how far from the fundamental limit of power processing this boost converter strays the differential power can be calculated:

$$P_{differential} = (1 - \frac{1}{G})P_{out} = (1 - \frac{1}{6})(250) = 208.33W$$

The differential power for this quadratic boost and the boost in the previous example is the same since the equation for differential power is only concerned with terminal characteristics. This means that any two converters with the same gain and output power will have the same fundamental lower limit of power processing. The implementation of the converter is the key aspect to process as little power as possible at a given gain and output power.

A VA area diagram for this example can also be seen below:

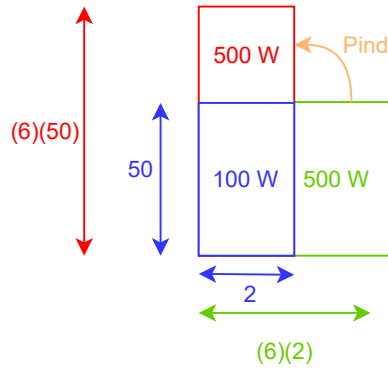


Figure 140: VA area depiction of the Quadratic Boost converter system

D.5 Differential power methods application to multi-port systems

As mentioned earlier the main focus of differential power methods is the terminal characteristics of a system rather than the internal processing of particular components. This method shines when applied to systems that require terminal evaluation. A prime example of this is with multi-port converter systems. The example to follow considers a multi-port system of converters using three converter cells to convert various voltage levels to a common bus voltage. The diagram below shows the proposed configuration:

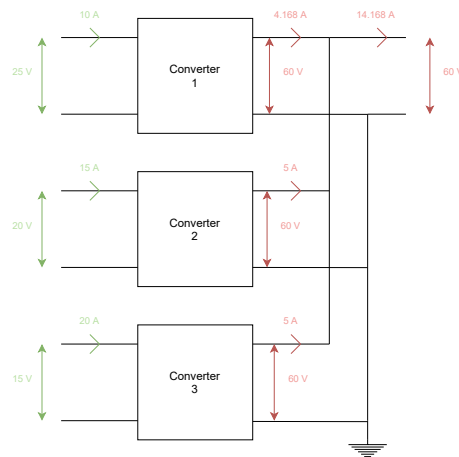


Figure 141: Proposed multi-port converter system

Using the VA area analysis technique to analyze the system is trivial. This involves creating a rectangle whose dimensions are the current and voltage of the input terminals. A second rectangle is created using the current and voltage of the output terminals. These two rectangles can then be overlapped. Where the two areas overlap is defined as direct power and the remaining non-overlapping area is then the differential power of the conversion system. The VA areas of each converter are shown below:

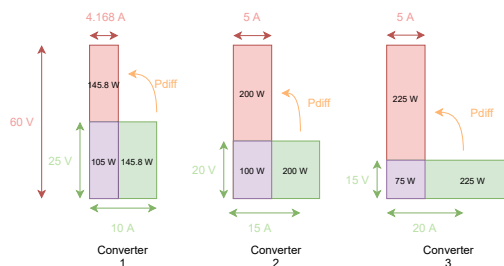


Figure 142: Proposed multi-port converter system VA areas

This shows that for the system as a whole the differential power is the sum of the individual components with a total of 573.5 W. The direct power available in the system is calculated the same way by summing the overlapping areas of each converter with a total of 297.2 W. However, this system can be evaluated and improved to optimize the amount of direct power. For the sake of brevity only one configuration will be considered to illustrate the merits of using differential power as a performance metric. Consider the following configuration that involves stacking the voltages of each individual converter to create the required bus voltage:

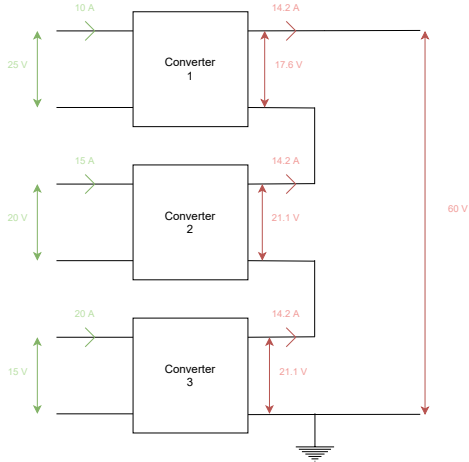


Figure 143: Alternative multi-port converter system

The VA areas of this solution is easily calculated as follows:

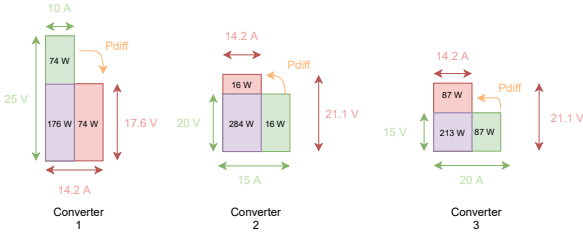


Figure 144: Alternative multi-port converter system VA area

The differential power of the system is still the sum of the individual components at 174 W. The direct power is calculated the same way and results in 673 W of direct power. This change in configuration of the same system with the same terminal characteristics results in a 226 % increase in direct power and a 330 % decrease in differential power. Of course the converter topologies chosen to implement these converters in the system may not perform at the fundamental limit of differential power. Each converter chosen will process power differently but this illustrates the merit in using differential power methods to design system using the terminal characteristics of the converters that comprise it. It allows the designer to set up the lowest possible baseline of power to be processed to begin with where the topology implementation will determine the real value of processed power.

D.6 Extending differential power methods

The previous sub-sections have outlined the basic principles of differential power methods. The analysis is easily carried out on system level as seen in the multi-port examples. Upon using it to select a topology it can become more difficult to apply to more complex converter topologies and scales in complexity proportional to the topology complexity. Although differential power can describe the power processing in a topology, it does not dive into the intricate balance of power transfer inside a topology. Understanding these internal power interactions that be able to give insight into which topology could be fundamentally better at power processing than another. For this reason these methods require extension to uncover the interior workings of power transfer

in a topology rather than sticking to the terminal perspective.

E More about differential power and the matrix method

E.1 Introduction

The matrix method perception of power in a converter has been inspired by differential power methods. It would be useful to be able to establish some common ground between the ideas of power that differential power presents and the matrix method. This chapter intends to investigate the link, if any, between differential power methods and the matrix method. Consistency with the accepted ideas of differential power is all the more useful to the matrix method approach. The examples covered in this chapter will analyze zero ripple approximations of converter topologies to see if a discernible link to differential power can be made from an analytical approach.

E.2 Linking the matrix method and differential power: Buck Converter

This experiment will characterize a buck converter as a zero ripple approximation to allow for a simple mathematical analysis of the power waveforms in the converter. The mathematical expressions for the power quantities in each component will be linked to concepts from differential power methods such as direct, indirect and differential power.

Using the zero ripple approximation [Figure 145](#) below shows the simplification of a Buck converter and its respective on and off state forms:

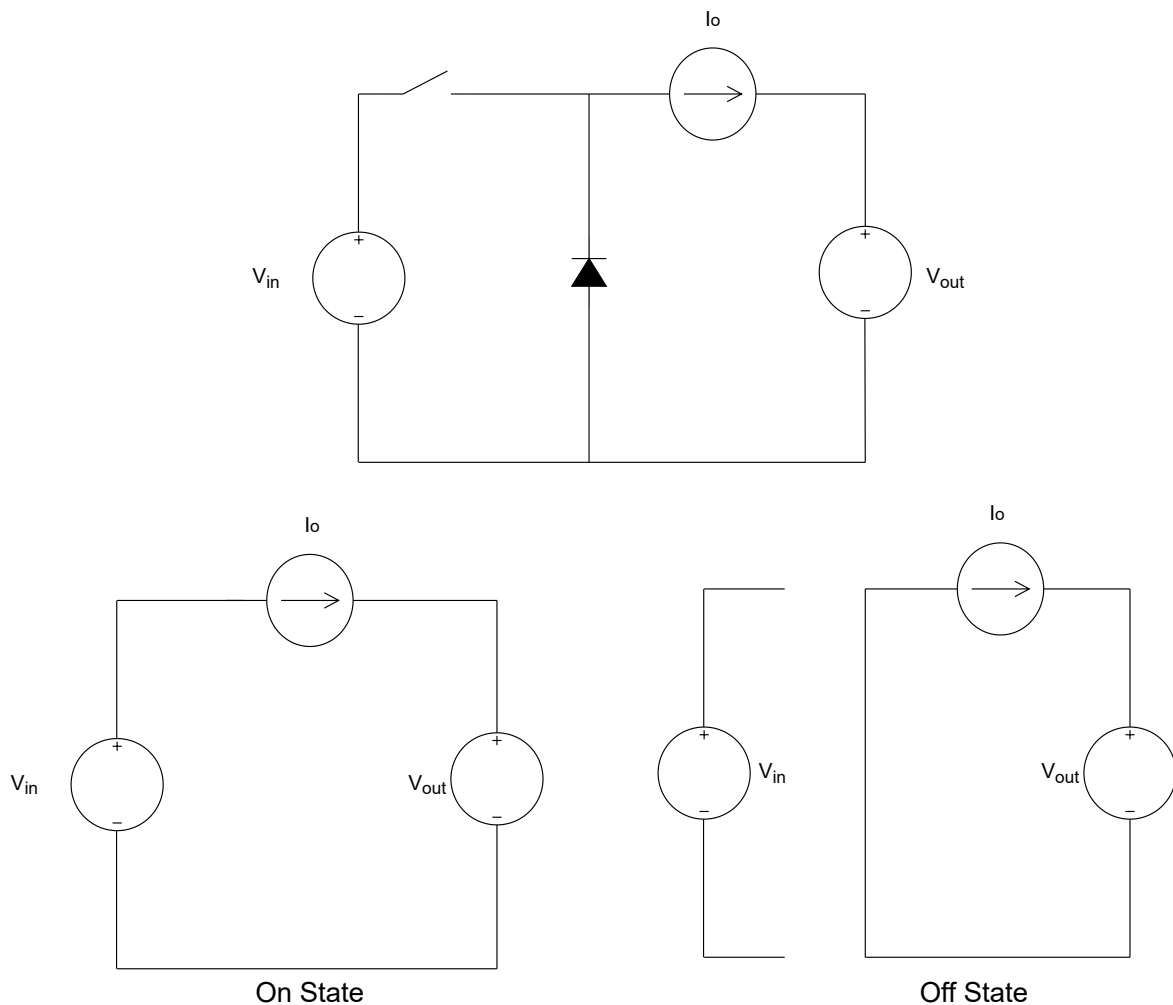


Figure 145: Diagram of the simplification of a Buck converter using the zero ripple approximation

The simplified power waveforms of each component are shown below in [Figure 146](#):

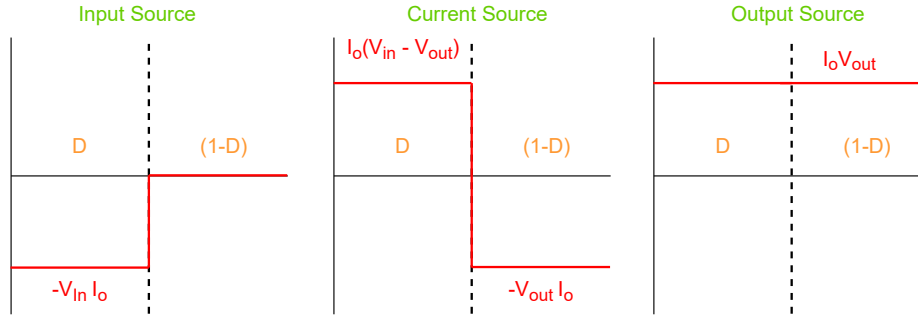


Figure 146: Associated power wave forms of simplified Buck converter

In the proceeding analysis the notation of 'S' denotes the input source, 'L' denotes the load source and the current source in the middle is to be denoted by 'X'. The on and off times relate to the duty cycle as per the normal expectation of a Buck converter. The input and output voltage of a Buck converter are related by the following equation:

$$V_{out} = DV_{in}$$

Now the power waveforms per state can be tabulated as follows:

Table 18: Table of on and off state powers

State	P_S	P_X	P_L
On State	$-V_{in}I_o$	$(V_{in} - V_{out})I_o$	$V_{out}I_o$
Off State	0	$-V_{out}I_o$	$V_{out}I_o$

The average power of a component can be calculated by taking a duty cycle weighted sum of the respective on and off state powers as Equation 17 follows:

$$P_{Aavg} = D(P_{Aon}) + (1 - D)(P_{Aoff}) \quad (17)$$

Using Equation 17 the average power in each component can be calculated as follows:

Table 19: Table of on and off state powers

	P_S	P_X	P_L
Average Power	$-DV_{in}I_o$	0	$DV_{in}I_o$

These on and off state powers can be manipulated to calculate the covariance matrix. Since the covariance is the product of two powers with their averages removed, the covariance matrix can also be calculated by creating a matrix of average powers and a matrix of the product of powers. The matrix of the product of powers will be called the double power matrix. The average power matrix can be deducted from the matrix of the product of powers to create the covariance matrix. This is the procedure to follow:

The average power product matrix can be calculated by calculating every combination of pairs of average powers shown in Table 19:

$$\begin{matrix} & S & X & L \\ S & \left[\begin{array}{ccc} (DV_{in}I_o)^2 & 0 & -(DV_{in}I_o)^2 \\ 0 & 0 & 0 \\ -(DV_{in}I_o)^2 & 0 & (DV_{in}I_o)^2 \end{array} \right] \\ X & & & \\ L & & & \end{matrix}$$

Notice that the rows and columns sum to zero as is expected. The average of the product of two components 'A' and 'B' can be calculated using Equation 18 below:

$$AB_{dob} = D(P_{Aon}P_{Bon}) + (1 - D)(P_{Aoff}P_{Boff}) \quad (18)$$

Using Equation 18 the average double power matrix can be obtained as follows:

$$\begin{matrix} & S & X & L \\ S & \left[\begin{array}{ccc} D(V_{in}I_o)^2 & -D(V_{in}I_o)^2(1 - D) & -(DV_{in}I_o)^2 \\ -D(V_{in}I_o)^2(1 - D) & D(V_{in}I_o)^2(1 - D) & 0 \\ -(DV_{in}I_o)^2 & 0 & (DV_{in}I_o)^2 \end{array} \right] \\ X & & & \\ L & & & \end{matrix}$$

Seeing as this matrix is merely the average powers of each component multiplied by another power throughout it follows logically that the rows and columns must sum to zero. Using this result the covariance matrix can be obtained by subtracting the average power matrix from the average double power matrix. This gives the following covariance matrix:

$$\begin{matrix} & S & X & L \\ S & \left[\begin{array}{ccc} D(1 - D)(V_{in}I_o)^2 & -D(1 - D)(V_{in}I_o)^2 & 0 \\ -D(1 - D)(V_{in}I_o)^2 & D(1 - D)(V_{in}I_o)^2 & 0 \\ 0 & 0 & 0 \end{array} \right] \\ X & & & \\ L & & & \end{matrix}$$

Consider the fact that Cobos et al. defines the basic step down cell as the Buck converter circuit with the following characteristics. Where P_{diff} is differential power, P_{dir} is direct power and G is the gain of the converter.

$$\begin{aligned} P_{diff} &= (G - 1)V_{out}I_{in} \\ P_{dir} &= V_{out}I_{in} \\ G &= \max\left(\frac{I_{out}}{I_{in}}, \frac{V_{out}}{V_{in}}\right) \end{aligned}$$

The covariance matrix for the buck converter can be manipulated to align with these definitions of power. Making the substitutions for $V_{in} = \frac{V_{out}}{D}$, $I_o = \frac{I_{in}}{D}$ and $D = \frac{1}{G}$ gives the following matrix

$$\begin{matrix} & S & X & L \\ S & \left[\begin{array}{ccc} G^2(I_{in}V_{out})^2(G - 1) & -G^2(I_{in}V_{out})^2(G - 1) & 0 \\ -G^2(I_{in}V_{out})^2(G - 1) & G^2(I_{in}V_{out})^2(G - 1) & 0 \\ 0 & 0 & 0 \end{array} \right] \\ X & & & \\ L & & & \end{matrix}$$

Substituting in for P_{diff} and P_{dir} the following covariance matrix is achieved:

$$\begin{matrix} & S & X & L \\ S & \left[\begin{array}{ccc} G^2P_{dir}P_{diff} & -G^2P_{dir}P_{diff} & 0 \\ -G^2P_{dir}P_{diff} & G^2P_{dir}P_{diff} & 0 \\ 0 & 0 & 0 \end{array} \right] \\ X & & & \\ L & & & \end{matrix}$$

In the simple cases where differential power has clearly defined equations for P_{diff} and P_{dir} such as in the buck converter it is easy to link these concepts to the matrix method. It is not yet clear if this can be generalized to other converter cells or if it is a special case for the easily defined buck and boost converters. This would require further investigation in future work. For the time being it would appear that the definitions of differential power can be found inside the entries of the co-variance matrix of a simple converter.

F Case study unabridged results and test files

F.1 The boost vs quadratic boost : stepped duty cycle

F.1.1 Unabridged results

$$\begin{matrix} V1 \\ L \\ C \\ R \end{matrix} \begin{bmatrix} V1 & L & C & R \\ 0.12 & 28.33 & -27.89 & -0.12 \\ 28.33 & 6732.88 & -6627.55 & -27.84 \\ -27.89 & -6627.55 & 6523.87 & 27.4 \\ -0.12 & -27.84 & 27.4 & 0.12 \end{bmatrix}$$

Figure 147: Boost converter @ 10% duty cycle.

$$\begin{matrix} V1 \\ L1 \\ L2 \\ C1 \\ C2 \\ R \end{matrix} \begin{bmatrix} V1 & L1 & L2 & C1 & C2 & R \\ 2641.06 & -2827.37 & -2749.94 & 100.1 & 2602.88 & 206.95 \\ -2827.37 & 3026.81 & 2943.93 & -107.16 & -2786.49 & -221.55 \\ -2749.94 & 2943.93 & 2863.32 & -104.23 & -2710.19 & -215.48 \\ 100.1 & -107.16 & -104.23 & 3.79 & 98.65 & 7.84 \\ 2602.88 & -2786.49 & -2710.19 & 98.65 & 2565.25 & 203.96 \\ 206.95 & -221.55 & -215.48 & 7.84 & 203.96 & 16.22 \end{bmatrix}$$

Figure 148: Quadratic boost converter @ 5.127% duty cycle.

$$\begin{matrix} V1 \\ L \\ C \\ R \end{matrix} \begin{bmatrix} V1 & L & C & R \\ 0.02 & 23.44 & -23.15 & -0.02 \\ 23.44 & 26419.54 & -26099.71 & -21.41 \\ -23.15 & -26099.71 & 25783.75 & 21.15 \\ -0.02 & -21.41 & 21.15 & 0.02 \end{bmatrix}$$

Figure 149: Boost converter @ 30% duty cycle.

$$\begin{matrix} V1 \\ L1 \\ L2 \\ C1 \\ C2 \\ R \end{matrix} \begin{bmatrix} V1 & L1 & L2 & C1 & C2 & R \\ 8000.42 & -9481.65 & -9408.74 & 1415.4 & 9234.19 & 148.31 \\ -9481.65 & 11237.13 & 11150.71 & -1677.45 & -10943.85 & -175.76 \\ -9408.74 & 11150.71 & 11064.96 & -1664.55 & -10859.69 & -174.41 \\ 1415.4 & -1677.45 & -1664.55 & 250.4 & 1633.67 & 26.24 \\ 9234.19 & -10943.85 & -10859.69 & 1633.67 & 10658.23 & 171.18 \\ 148.31 & -175.76 & -174.41 & 26.24 & 171.18 & 2.75 \end{bmatrix}$$

Figure 150: Quadratic boost converter @ 16.329% duty cycle.

$$\begin{matrix} V1 \\ L \\ C \\ R \end{matrix} \begin{bmatrix} V1 & L & C & R \\ 0.01 & 20.15 & -19.97 & -0.0 \\ 20.15 & 62525.85 & -61987.41 & -14.91 \\ -19.97 & -61987.41 & 61453.59 & 14.79 \\ -0.0 & -14.91 & 14.79 & 0.0 \end{bmatrix}$$

Figure 151: Boost converter @ 50% duty cycle.

$$\begin{matrix} V1 \\ L1 \\ L2 \\ C1 \\ C2 \\ R \end{matrix} \begin{bmatrix} V1 & L1 & L2 & C1 & C2 & R \\ 15431.75 & -22104.35 & -21931.64 & 6599.02 & 21634.0 & 223.49 \\ -22104.35 & 31662.13 & 31414.74 & -9452.39 & -30988.41 & -320.13 \\ -21931.64 & 31414.74 & 31169.28 & -9378.54 & -30746.29 & -317.63 \\ 6599.02 & -9452.39 & -9378.54 & 2821.91 & 9251.26 & 95.57 \\ 21634.0 & -30988.41 & -30746.29 & 9251.26 & 30329.03 & 313.32 \\ 223.49 & -320.13 & -317.63 & 95.57 & 313.32 & 3.24 \end{bmatrix}$$

Figure 152: Quadratic boost converter @ 29.289% duty cycle

$$\begin{matrix} V1 \\ L \\ C \\ R \end{matrix} \begin{bmatrix} V1 & L & C & R \\ 0.0 & 15.19 & -15.11 & -0.0 \\ 15.19 & 149031.16 & -148259.64 & -8.15 \\ -15.11 & -148259.64 & 147492.11 & 8.1 \\ -0.0 & -8.15 & 8.1 & 0.0 \end{bmatrix}$$

Figure 153: Boost converter @ 70% duty cycle

$$\begin{matrix} V1 \\ L1 \\ L2 \\ C1 \\ C2 \\ R \end{matrix} \begin{bmatrix} V1 & L1 & L2 & C1 & C2 & R \\ 15209.15 & -27398.66 & -27302.6 & 12161.21 & 27127.32 & 150.99 \\ -27398.66 & 49357.58 & 49184.53 & -21907.93 & -48868.78 & -272.0 \\ -27302.6 & 49184.53 & 49012.1 & -21831.12 & -48697.44 & -271.05 \\ 12161.21 & -21907.93 & -21831.12 & 9724.09 & 21690.97 & 120.73 \\ 27127.32 & -48868.78 & -48697.44 & 21690.97 & 48384.81 & 269.31 \\ 150.99 & -272.0 & -271.05 & 120.73 & 269.31 & 1.5 \end{bmatrix}$$

Figure 154: Quadratic boost converter @ 45.227% duty cycle.

	$V1$	L	C	R		$V1$	$L1$	$L2$	$C1$	$C2$	R
$V1$	0.0	10.4	-10.38	0.0	$V1$	20362.8	-66648.02	-64559.33	46170.99	64550.24	194.6
L	10.4	619491.62	-618384.62	1.68	$L1$	-66648.02	218140.81	211304.46	-151118.93	-211274.72	-636.94
C	-10.38	-618384.62	617279.59	-1.67	$L2$	-64559.33	211304.46	204682.36	-146382.99	-204653.55	-616.98
R	0.0	1.68	-1.67	0.0	$C1$	46170.99	-151118.93	-146382.99	104688.94	146362.38	441.25
					$C2$	64550.24	-211274.72	-204653.55	146362.38	204624.74	616.89
					R	194.6	-636.94	-616.98	441.25	616.89	1.86

Figure 155: Boost converter @ 90% duty cycle

Figure 156: Quadratic boost converter @ 65.377% duty cycle

F.1.2 LTSpice Netlists

10% boost.

```

V1 Source 0 50
L1 Source InductorNode 36.99u Rpar=0 Cpar=0
C1 ResistorNode 0 8.096u
R1 ResistorNode 0 12.34
V2 Signal 0 PULSE(0 20 0 0.01u 0.01u 1us 10us)
D1 InductorNode ResistorNode D
S1 InductorNode 0 Signal 0 SW
.model D D
.lib <YOUR_SPICE_INSTALLATION_DIRECTORY>LTspiceXVII\lib\cmp\standard.dio
.tran 0 452ms 450ms 10ns startup
.options plotwinsize=0
.options numdgt=10
.model SW SW(Ron=1m Roff=1Meg Vt = 0.5 Vh = 0)
.backanno
.end

```

30% boost.

```

V1 Source 0 50
L1 Source InductorNode 142.78u Rpar=0 Cpar=0
C1 ResistorNode 0 14.702u
R1 ResistorNode 0 20.4
V2 Signal 0 PULSE(0 20 0 0.01u 0.01u 3us 10us)
D1 InductorNode ResistorNode D
S1 InductorNode 0 Signal 0 SW
.model D D
.lib <YOUR_SPICE_INSTALLATION_DIRECTORY>LTspiceXVII\lib\cmp\standard.dio
.tran 0 452ms 450ms 10ns startup
.options plotwinsize=0
.options numdgt=10
.model SW SW(Ron=1m Roff=1Meg Vt = 0.5 Vh = 0)
.backanno
.end

```

50% boost.

```

V1 Source 0 50
L1 Source InductorNode 333.33u Rpar=0 Cpar=0
C1 ResistorNode 0 12.5u
R1 ResistorNode 0 40
V2 Signal 0 PULSE(0 20 0 0.01u 0.01u 5us 10us)

```

```

D2 InductorNode ResistorNode D
S1 InductorNode 0 Signal 0 SW
.model D D
.lib <YOUR_SPICE_INSTALLATION_DIRECTORY>LTspiceXVII\lib\cmp\standard.dio
.tran 0 452ms 450ms 10ns startup
.options plotwinsize=0
.options numdgt=10
.model SW SW(Ron=1m Roff=1Meg Vt = 0.5 Vh = 0)
.backanno
.end

```

70% boost.

```

V1 Source 0 50
L1 Source InductorNode 777.72u Rpar=0 Cpar=0
C1 ResistorNode 0 6.3005u
R1 ResistorNode 0 111.1
V2 Signal 0 PULSE(0 20 0 0.01u 0.01u 7us 10us)
D1 InductorNode ResistorNode D
S1 InductorNode 0 Signal 0 SW
.model D D
.lib <YOUR_SPICE_INSTALLATION_DIRECTORY>LTspiceXVII\lib\cmp\standard.dio
.tran 0 452ms 450ms 10ns startup
.options plotwinsize=0
.options numdgt=10
.model SW SW(Ron=1m Roff=1Meg Vt = 0.5 Vh = 0)
.backanno
.end

```

90% boost.

```

V1 Source 0 50
L1 Source InductorNode 3m Rpar=0 Cpar=0
C1 ResistorNode 0 900n
R1 ResistorNode 0 1000
V2 Signal 0 PULSE(0 20 0 0.01u 0.01u 9us 10us)
D2 InductorNode ResistorNode D
S1 InductorNode 0 Signal 0 SW
.model D D
.lib <YOUR_SPICE_INSTALLATION_DIRECTORY>LTspiceXVII\lib\cmp\standard.dio
.tran 0 452ms 450ms 10ns startup
.options plotwinsize=0
.options numdgt=10
.model SW SW(Ron=1m Roff=1Meg Vt = 0.5 Vh = 0)
.backanno
.end

```

10% Quadratic boost.

```

L1 N004 N005 20u
L2 N001 N002 25u
R1 N003 0 12.34
V1 N004 0 50
V2 Signal 0 PULSE(0 5 0 0.01u 0.01u 0.51269us 10us)
S1 N002 0 Signal 0 SW
C1 N001 N004 100u
C2 N003 0 650n
D4 N002 N003 D
D1 N005 N002 D
D2 N005 N001 D

```

```

.model D D
.lib <YOUR_SPICE_INSTALLATION_DIRECTORY>LTspiceXVII\lib\cmp\standard.dio
.model SW SW(Ron=1m Roff=1Meg Vt = 0.5 Vh = 0)
.tran 0 452ms 450ms 10ns startup
.options plotwinsize=0
.options numdgt=10
.backanno
.end

```

30% Quadratic boost.

```

L1 N004 N005 60u
L2 N001 N002 80u
R1 N003 0 12.34
V1 N004 0 50
V2 Signal 0 PULSE(0 5 0 0.01u 0.01u 1.63289us 10us)
S1 N002 0 Signal 0 SW
C1 N001 N004 100u
C2 N003 0 1.5u
D1 N002 N003 D
D2 N005 N002 D
D3 N005 N001 D
.model D D
.lib <YOUR_SPICE_INSTALLATION_DIRECTORY>LTspiceXVII\lib\cmp\standard.dio
.model SW SW(Ron=1m Roff=1Meg Vt = 0.5 Vh = 0)
.tran 0 452ms 450ms 10ns startup
.options plotwinsize=0
.options numdgt=10
.backanno
.end

```

50% Quadratic boost.

```

L1 N004 N005 180u
L2 N001 N002 300u Ipk=5 Rser=64m
R1 N003 0 40
V1 N004 0 50
V2 Signal 0 PULSE(0 5 0 0.01u 0.01u 3.1us 10us)
C2 N003 0 0.82u
C1 N001 N004 100u
D1 N002 N003 D
D2 N005 N002 D
D3 N005 N001 D
S1 N002 0 Signal 0 SW
.model D D
.lib <YOUR_SPICE_INSTALLATION_DIRECTORY>LTspiceXVII\lib\cmp\standard.dio
.options plotwinsize=0
.options numdgt=10
.model SW SW(Ron=1m Roff=1Meg Vt = 0.5 Vh = 0)
.tran 0 452ms 450ms 10ns startup
.backanno
.end

```

70% Quadratic boost.

```

L1 N004 N005 600u
L2 N001 N002 1m
R1 N003 0 111.1
V1 N004 0 50
V2 Signal 0 PULSE(0 5 0 0.01u 0.01u 4.52266us 10us)

```

```

S1 N002 0 Signal 0 SW
C1 N001 N004 100u
C2 N003 0 0.4u
D1 N002 N003 D
D2 N005 N002 D
D3 N005 N001 D
.model D D
.lib <YOUR_SPICE_INSTALLATION_DIRECTORY>LTspiceXVII\lib\cmp\standard.dio
.model SW SW(Ron=1m Roff=1Meg Vt = 0.5 Vh = 0)
.tran 0 452ms 450ms 10ns startup
.options plotwinsize=0
.options numdgt=10
.backanno
.end

```

90% Quadratic boost.

```

L1 N004 N005 2m
L2 N001 N002 6m Rser=1.8
R1 N003 0 1000
V1 N004 0 50
V2 Signal 0 PULSE(0 20 0 0.01u 0.01u 6.98us 10us)
C1 N001 N004 1000u V=160 Rser=160m
C2 N003 0 80n Rser=52m
D1 N002 N003 D
D2 N005 N002 D
D3 N005 N001 D
S1 N002 0 Signal 0 SW
.model D D
.lib <YOUR_SPICE_INSTALLATION_DIRECTORY>LTspiceXVII\lib\cmp\standard.dio
.tran 0 452ms 450ms 10ns startup
.options plotwinsize=0
.options numdgt=10
.model SW SW(Ron=1m Roff=1Meg Vt = 0.5 Vh = 0)
.backanno
.end

```

F.2 Step up converters

F.2.1 Unabridged results

$$\begin{array}{c} V1 \\ L \\ C \\ R \end{array} \begin{bmatrix} V1 & L & C & R \\ 0.0 & 13.95 & -13.89 & -0.0 \\ 13.95 & 193224.23 & -192389.45 & -6.27 \\ -13.89 & -192389.45 & 191558.28 & 6.24 \\ -0.0 & -6.27 & 6.24 & 0.0 \end{bmatrix}$$

Figure 157: Boost converter 4X step up

$$\begin{array}{c} V1 \\ L \\ C \\ R \end{array} \begin{bmatrix} V1 & L & C & R \\ 15943.43 & -80513.53 & 64251.87 & 35.7 \\ -80513.53 & 406589.41 & -324468.8 & -180.27 \\ 64251.87 & -324468.8 & 258934.45 & 143.86 \\ 35.7 & -180.27 & 143.86 & 0.08 \end{bmatrix}$$

Figure 158: Buck-boost converter 4X step up

$$\begin{array}{c} V1 \\ L1 \\ L2 \\ C1 \\ C2 \\ R \end{array} \begin{bmatrix} V1 & L1 & L2 & C1 & C2 & R \\ 17427.51 & -34425.06 & -33995.64 & 16799.67 & 33907.36 & 255.71 \\ -34425.06 & 68000.82 & 67152.58 & -33184.87 & -66978.2 & -505.12 \\ -33995.64 & 67152.58 & 66314.91 & -32770.93 & -66142.71 & -498.82 \\ 16799.67 & -33184.87 & -32770.93 & 16194.45 & 32685.83 & 246.5 \\ 33907.36 & -66978.2 & -66142.71 & 32685.83 & 65970.95 & 497.52 \\ 255.71 & -505.12 & -498.82 & 246.5 & 497.52 & 3.75 \end{bmatrix}$$

Figure 159: Quadratic boost converter A 4X step up

$$\begin{array}{c} V1 \\ L1 \\ L2 \\ C1 \\ C2 \\ C3 \\ R \end{array} \begin{bmatrix} V1 & L1 & L2 & C1 & C2 & C3 & R \\ 5775.62 & -23260.4 & -5791.21 & 9010.6 & 22546.29 & -9016.22 & 531.2 \\ -23260.4 & 93677.64 & 23323.2 & -36288.79 & -90801.65 & 36311.39 & -2139.33 \\ -5791.21 & 23323.2 & 5806.85 & -9034.93 & -22607.16 & 9040.56 & -532.64 \\ 9010.6 & -36288.79 & -9034.93 & 14057.53 & 35174.69 & -14066.29 & 828.73 \\ 22546.29 & -90801.65 & -22607.16 & 35174.69 & 88013.95 & -35196.6 & 2073.65 \\ -9016.22 & 36311.39 & 9040.56 & -14066.29 & -35196.6 & 14075.05 & -829.25 \\ 531.2 & -2139.33 & -532.64 & 828.73 & 2073.65 & -829.25 & 48.86 \end{bmatrix}$$

Figure 160: Quadratic boost converter B 4X step up

$$\begin{array}{c} V1 \\ L \\ C \\ R \end{array} \begin{bmatrix} V1 & L & C & R \\ 0.0 & 12.58 & -12.56 & 0.0 \\ 12.58 & 588900.59 & -587851.59 & 3.13 \\ -12.56 & -587851.59 & 586804.45 & -3.13 \\ 0.0 & 3.13 & -3.13 & 0.0 \end{bmatrix}$$

Figure 161: Boost converter 10X step up. Sum of main diagonal

$$\begin{array}{c} V1 \\ L \\ C \\ R \end{array} \begin{bmatrix} V1 & L & C & R \\ 6166.28 & -67755.25 & 61464.05 & 10.46 \\ -67755.25 & 744496.55 & -675368.59 & -114.91 \\ 61464.05 & -675368.59 & 612659.29 & 104.24 \\ 10.46 & -114.91 & 104.24 & 0.02 \end{bmatrix}$$

Figure 162: Buck-boost converter 10X step up

	V1	L1	L2	C1	C2	R
V1	12803.36	-40305.5	-40413.7	27598.84	40105.06	201.18
L1	-40305.5	126883.37	127223.97	-86882.26	-126252.36	-633.34
L2	-40413.7	127223.97	127565.49	-87115.49	-126591.27	-635.04
C1	27598.84	-86882.26	-87115.49	59491.86	86450.19	433.67
C2	40105.06	-126252.36	-126591.27	86450.19	125624.49	630.19
R	201.18	-633.34	-635.04	433.67	630.19	3.16

Figure 163: Quadratic boost converter A 10X
step up

	V1	L1	L2	C1	C2	C3	R
V1	2843.34	-28707.25	-2833.77	13510.83	28276.51	-13493.16	301.2
L1	-28707.25	289837.14	28610.64	-136409.44	-285488.18	136231.06	-3040.97
L2	-2833.77	28610.64	2824.24	-13465.36	-28181.34	13447.75	-300.18
C1	13510.83	-136409.44	-13465.36	64199.97	134362.64	-64116.01	1431.21
C2	28276.51	-285488.18	-28181.34	134362.64	281204.48	-134186.93	2995.34
C3	-13493.16	136231.06	13447.75	-64116.01	-134186.93	64032.17	-1429.34
R	301.2	-3040.97	-300.18	1431.21	2995.34	-1429.34	31.91

Figure 164: Quadratic boost converter B 10X
step up

F.2.2 LTSpice Netlists

4X boost.

```

V1 Source 0 50
L1 Source InductorNode 1m Rpar=0 Cpar=0
C1 ResistorNode 0 4.6875u
R1 ResistorNode 0 160
V2 Signal 0 PULSE(0 20 0 0.01u 0.01u 7.5us 10us)
D1 InductorNode ResistorNode D
S1 InductorNode 0 Signal 0 SW
.model D D
.lib <YOUR_SPICE_INSTALLATION_DIRECTORY>LTspiceXVII\lib\cmp\standard.dio
.tran 0 452ms 450ms startup
* .options plotwinsize=0
* .options numdgt=10
.model SW SW(Ron=1m Roff=1Meg Vt = 0.5 Vh = 0)
.backanno
.end

```

4X buck-boost.

```

L1 N002 0 900u
R1 N003 0 160
V1 N001 0 50
C1 N003 0 500n
D1 N003 N002 D
S1 N002 N001 Signal 0 SW
V3 Signal 0 PULSE(0 20 0 0.01u 0.01u 8us 10us)
.model D D
.lib <YOUR_SPICE_INSTALLATION_DIRECTORY>LTspiceXVII\lib\cmp\standard.dio
.tran 0 452ms 450ms 10ns startup
.options plotwinsize=0
.options numdgt=10

```

```
.model SW SW(Ron=1m Roff=1Meg Vt = 0.5 Vh = 0)
.backanno
.end
```

4X Quadratic boost converter A

```
L1 N004 N005 700u
L2 N001 N002 1.1m
R1 N003 0 150
V1 N004 0 50
V2 Signal 0 PULSE(0 20 0 0.01u 0.01u 5us 10us)
C1 N001 N004 1000u V=160 Rser=160m
C2 N003 0 250n
D1 N002 N003 D
D2 N005 N002 D
D3 N005 N001 D
S1 N002 0 Signal 0 SW
.model D D
.lib <YOUR_SPICE_INSTALLATION_DIRECTORY>LTspiceXVII\lib\cmp\standard.dio
.tran 0 452ms 450ms 10ns startup
.options plotwinsize=0
.options numdgt=10
.model SW SW(Ron=1m Roff=1Meg Vt = 0.5 Vh = 0)
.backanno
.end
```

4X Quadratic boost converter B

```
L1 N004 N005 1200u
L2 N001 N002 1.6m
R1 N003 0 160
V1 N004 0 50
V2 Signal 0 PULSE(0 20 0 0.01u 0.01u 6us 10us)
C1 N001 N004 10u V=160
C2 N003 0 400n
D1 N002 N003 D
D3 N005 N001 D
S1 N005 0 Signal 0 SW
C3 N005 N002 20u
.model D D
.lib <YOUR_SPICE_INSTALLATION_DIRECTORY>LTspiceXVII\lib\cmp\standard.dio
.tran 0 700ms 698ms 10ns startup
.options plotwinsize=0
.options numdgt=10
.model SW SW(Ron=1m Roff=1Meg Vt = 0.5 Vh = 0)
.backanno
.end
```

10X boost.

```
V1 Source 0 50
L1 Source InductorNode 3m Rpar=0 Cpar=0
C1 ResistorNode 0 900n
R1 ResistorNode 0 1025
V2 Signal 0 PULSE(0 20 0 0.01u 0.01u 9us 10us)
D1 InductorNode ResistorNode D
S1 InductorNode 0 Signal 0 SW
.model D D
.lib <YOUR_SPICE_INSTALLATION_DIRECTORY>LTspiceXVII\lib\cmp\standard.dio
.tran 0 452ms 450ms 10ns startup
```

```

.options plotwinsize=0
.options numdgt=10
.model SW SW(Ron=1m Roff=1Meg Vt = 0.5 Vh = 0)
.backanno
.end

```

10X buck-boost.

```

L1 N002 0 1.5m
R1 N003 0 1000
V1 N001 0 50
C1 N003 0 90n
D1 N003 N002 D
S1 N002 N001 Signal 0 SW
V2 Signal 0 PULSE(0 20 0 0.01u 0.01u 9.07us 10us)
.model D D
.lib <YOUR_SPICE_INSTALLATION_DIRECTORY>LTspiceXVII\lib\cmp\standard.dio
.tran 0 452ms 450ms 10ns startup
.options plotwinsize=0
.options numdgt=10
.model SW SW(Ron=1m Roff=1Meg Vt = 0.5 Vh = 0)
.backanno
.end

```

10X Quadratic boost converter A

```

L1 N004 N005 1m
L2 N001 N002 4m
R1 N003 0 1110
V1 N004 0 50
V2 Signal 0 PULSE(0 20 0 0.01u 0.01u 6.98us 10us)
C1 N001 N004 1000u
C2 N003 0 80n
D1 N002 N003 Did1
D2 N005 N002 Did1
D3 N005 N001 Did1
S1 N002 0 Signal 0 SW
.model D D
.lib <YOUR_SPICE_INSTALLATION_DIRECTORY>LTspiceXVII\lib\cmp\standard.dio
.tran 0 452ms 451ms startup
* .options plotwinsize=0
* .options numdgt=10
.model SW SW(Ron=1m Roff=1Meg Vt = 0.5 Vh = 0)
.model Did1 D(Ron=0.0001 Roff=100G Vfwd=0)
.backanno
.end

```

10X Quadratic boost converter B

```

L1 N004 N005 2m
L2 N001 N002 2.5m
R1 N003 0 1000
V1 N004 0 50
V2 Signal 0 PULSE(0 20 0 0.01u 0.01u 8.18us 10us)
C1 N001 N004 10u V=160
C2 N003 0 80n
D1 N002 N003 D
D2 N005 N001 D
S1 N005 0 Signal 0 SW
C3 N005 N002 20u

```

```
.model D D
.lib <YOUR_SPICE_INSTALLATION_DIRECTORY>LTspiceXVII\lib\cmp\standard.dio
.tran 0 700ms 698ms 10ns startup
.options plotwinsize=0
.options numdgt=10
.model SW SW(Ron=1m Roff=1Meg Vt = 0.5 Vh = 0)
.backanno
.end
```

F.3 Step down converters

F.3.1 Unabridged results

$$\begin{array}{c}
 V1 \\
 L \\
 C \\
 R
 \end{array}
 \begin{bmatrix}
 V1 & L & C & R \\
 187579.54 & -190761.25 & -2686.9 & 5502.71 \\
 -190761.25 & 193996.93 & 2732.47 & -5596.05 \\
 -2686.9 & 2732.47 & 38.49 & -78.82 \\
 5502.71 & -5596.05 & -78.82 & 161.42
 \end{bmatrix}$$

Figure 165: Buck converter 4X
step down

$$\begin{array}{c}
 V1 \\
 L1 \\
 L2 \\
 C1 \\
 C2 \\
 R
 \end{array}
 \begin{bmatrix}
 V1 & L1 & L2 & C1 & C2 & R \\
 7.25 & 335.9 & 1336.08 & -1336.7 & -328.39 & -11.61 \\
 335.9 & 15556.7 & 61879.29 & -61907.69 & -15209.11 & -537.79 \\
 1336.08 & 61879.29 & 246134.8 & -246247.8 & -60496.68 & -2139.14 \\
 -1336.7 & -61907.69 & -246247.8 & 246360.84 & 60524.46 & 2140.12 \\
 -328.39 & -15209.11 & -60496.68 & 60524.46 & 14869.29 & 525.77 \\
 -11.61 & -537.79 & -2139.14 & 2140.12 & 525.77 & 18.59
 \end{bmatrix}$$

Figure 166: SEPIC 4X step down.

$$\begin{array}{c}
 V1 \\
 L1 \\
 L2 \\
 C1 \\
 C2 \\
 R
 \end{array}
 \begin{bmatrix}
 V1 & L1 & L2 & C1 & C2 & R \\
 2.54 & 197.9 & 803.31 & -992.41 & 9.6 & -19.45 \\
 197.9 & 15403.85 & 62525.22 & -77244.14 & 747.33 & -1514.2 \\
 803.31 & 62525.22 & 253793.89 & -313538.94 & 3033.47 & -6146.25 \\
 -992.41 & -77244.14 & -313538.94 & 387348.43 & -3747.58 & 7593.13 \\
 9.6 & 747.33 & 3033.47 & -3747.58 & 36.26 & -73.46 \\
 -19.45 & -1514.2 & -6146.25 & 7593.13 & -73.46 & 148.85
 \end{bmatrix}$$

Figure 167: Cuk converter 4X
step down

$$\begin{array}{c}
 V1 \\
 L1 \\
 L2 \\
 C1 \\
 C2 \\
 R
 \end{array}
 \begin{bmatrix}
 V1 & L1 & L2 & C1 & C2 & R \\
 377771.68 & -175341.47 & -178148.51 & -51171.89 & 24320.62 & 2522.22 \\
 -175341.47 & 81384.16 & 82687.04 & 23751.26 & -11288.33 & -1170.68 \\
 -178148.51 & 82687.04 & 84010.78 & 24131.5 & -11469.05 & -1189.42 \\
 -51171.89 & 23751.26 & 24131.5 & 6931.6 & -3294.4 & -341.65 \\
 24320.62 & -11288.33 & -11469.05 & -3294.4 & 1565.74 & 162.38 \\
 2522.22 & -1170.68 & -1189.42 & -341.65 & 162.38 & 16.84
 \end{bmatrix}$$

Figure 168: Quadratic buck converter 4X
step down

$$\begin{array}{c}
 V1 \\
 L \\
 C \\
 R
 \end{array}
 \begin{bmatrix}
 V1 & L & C & R \\
 561637.86 & -566212.47 & -3165.58 & 6704.57 \\
 -566212.47 & 570824.33 & 3191.37 & -6759.18 \\
 -3165.58 & 3191.37 & 17.84 & -37.79 \\
 6704.57 & -6759.18 & -37.79 & 80.04
 \end{bmatrix}$$

Figure 169: Buck converter 10X
step down

$$\begin{array}{c}
 V1 \\
 L1 \\
 L2 \\
 C1 \\
 C2 \\
 R
 \end{array}
 \begin{bmatrix}
 V1 & L1 & L2 & C1 & C2 & R \\
 29.54 & 419.88 & 4243.96 & -4250.96 & -410.8 & -27.3 \\
 419.88 & 5967.86 & 60320.41 & -60419.85 & -5838.76 & -387.96 \\
 4243.96 & 60320.41 & 609691.24 & -610696.32 & -59015.57 & -3921.35 \\
 -4250.96 & -60419.85 & -610696.32 & 611703.06 & 59112.85 & 3927.82 \\
 -410.8 & -5838.76 & -59015.57 & 59112.85 & 5712.46 & 379.57 \\
 -27.3 & -387.96 & -3921.35 & 3927.82 & 379.57 & 25.22
 \end{bmatrix}$$

Figure 170: SEPIC 10X step down.

$$\begin{array}{c}
 V1 \\
 L1 \\
 L2 \\
 C1 \\
 C2 \\
 R
 \end{array}
 \begin{bmatrix}
 V1 & L1 & L2 & C1 & C2 & R \\
 15.92 & 303.3 & 3127.48 & -3425.72 & 15.09 & -32.38 \\
 303.3 & 5778.75 & 59587.75 & -65270.11 & 287.47 & -616.96 \\
 3127.48 & 59587.75 & 614440.56 & -673034.3 & 2964.24 & -6361.75 \\
 -3425.72 & -65270.11 & -673034.3 & 737215.61 & -3246.92 & 6968.42 \\
 15.09 & 287.47 & 2964.24 & -3246.92 & 14.3 & -30.69 \\
 -32.38 & -616.96 & -6361.75 & 6968.42 & -30.69 & 65.87
 \end{bmatrix}$$

Figure 171: Cuk converter 10X
step down

$$\begin{array}{c}
 V1 \\
 L1 \\
 L2 \\
 C1 \\
 C2 \\
 R
 \end{array}
 \begin{bmatrix}
 V1 & L1 & L2 & C1 & C2 & R \\
 1122263.9 & -544727.57 & -552615.35 & -58004.52 & 28788.92 & 4268.09 \\
 -544727.57 & 264401.38 & 268229.97 & 28154.39 & -13973.64 & -2071.66 \\
 -552615.35 & 268229.97 & 272114.0 & 28562.07 & -14175.99 & -2101.66 \\
 -58004.52 & 28154.39 & 28562.07 & 2997.98 & -1487.96 & -220.6 \\
 28788.92 & -13973.64 & -14175.99 & -1487.96 & 738.51 & 109.49 \\
 4268.09 & -2071.66 & -2101.66 & -220.6 & 109.49 & 16.23
 \end{bmatrix}$$

Figure 172: Quadratic buck converter 10X
step down.

F.3.2 LTSpice Netlists

4X buck

```

L1 N002 N003 1.56m
R1 N003 0 62.5
V1 N001 0 500
C1 N003 0 60n
D1 0 N002 D
S1 N002 N001 Signal 0 SW
V2 Signal 0 PULSE(0 20 0 0.01u 0.01u 2.5us 10us)
.model D D

```

```

.lib <YOUR_SPICE_INSTALLATION_DIRECTORY>LTspiceXVII\lib\cmp\standard.dio
.tran 0 452ms 450ms 10ns startup
.options plotwinsize=0
.options numdgt=10
.model SW SW(Ron=1m Roff=1Meg Vt = 0.5 Vh = 0)
.backanno
.end

```

4X SEPIC

```

L1 N001 N002 1.6m
R1 N004 0 64
V1 N001 0 500
C1 N004 0 330n
D1 N003 N004 D
S1 0 N002 Signal 0 SW
V2 Signal 0 PULSE(0 20 0 0.01u 0.01u 2.03us 10us)
C3 N003 N002 330n
L2 N003 0 2m
.model D D
.lib <YOUR_SPICE_INSTALLATION_DIRECTORY>LTspiceXVII\lib\cmp\standard.dio
.tran 0 452ms 450ms 10ns startup
.options plotwinsize=0
.options numdgt=10
.model SW SW(Ron=1m Roff=1Meg Vt = 10 Vh = -2.5)
.backanno
.end

```

4X CUK

```

L1 N001 N002 1.8m
R1 N004 0 62.5
V1 N001 0 500
C1 N004 0 50n
D1 N003 0 D
S1 0 N002 Signal 0 SW
V2 Signal 0 PULSE(0 20 0 0.01u 0.01u 2us 10us)
C2 N003 N002 300n
L2 N003 N004 1.8m
.model D D
.lib <YOUR_SPICE_INSTALLATION_DIRECTORY>LTspiceXVII\lib\cmp\standard.dio
.tran 0 452ms 450ms 10ns startup
.options plotwinsize=0
.options numdgt=10
.model SW SW(Ron=1m Roff=1Meg Vt = 10 Vh = -2.5)
.backanno
.end

```

4X Quadratic buck

```

R1 N004 0 62.5
V1 N001 0 500
C1 N004 0 0.2u
S1 N002 N001 Signal 0 SW
V2 Signal 0 PULSE(0 20 0us 0.01u 0.01u 1.333us 10us)
L1 N003 N004 800u
C2 N004 N005 0.2u
L2 N002 N005 800u
D1 N005 N003 Didl
D2 0 N002 Didl

```

```

D3 N002 N003 Did1
.model D D
.lib <YOUR_SPICE_INSTALLATION_DIRECTORY>LTspiceXVII\lib\cmp\standard.dio
.tran 0 720ms 700ms 10ns startup
.model SW SW(Ron=1m Roff=1Meg Vt = 5 Vh = -2.5)
.model Did1 D(Ron=0.0001 Roff=100G Vfwd=0)
.options plotwinsize=0
.options numdgt=10
.backanno
.end

```

10X buck

```

L1 N002 N003 300u
R1 N003 0 10
V1 N001 0 500
C1 N003 0 375n
D1 0 N002 D
S1 N002 N001 Signal 0 SW
V2 Signal 0 PULSE(0 20 0 0.01u 0.01u 1us 10us)
.model D D
.lib <YOUR_SPICE_INSTALLATION_DIRECTORY>LTspiceXVII\lib\cmp\standard.dio
.tran 0 452ms 450ms 10ns startup
.options plotwinsize=0
.options numdgt=10
.model SW SW(Ron=1m Roff=1Meg Vt = 0.5 Vh = 0)
.backanno
.end

```

10X SEPIC

```

L1 N001 N002 320u
R1 N004 0 10.5
V1 N001 0 500
C1 N004 0 1u
D1 N003 N004 D
S1 0 N002 Signal 0 SW
V2 Signal 0 PULSE(0 20 0 0.01u 0.01u 0.94us 10us)
C3 N003 N002 1u
L2 N003 0 1m
.model D D
.lib <YOUR_SPICE_INSTALLATION_DIRECTORY>LTspiceXVII\lib\cmp\standard.dio
.tran 0 452ms 450ms 10ns startup
.options plotwinsize=0
.options numdgt=10
.model SW SW(Ron=1m Roff=1Meg Vt = 10 Vh = -2.5)
.backanno
.end

```

10X CUK

```

L1 N001 N002 300u
R1 N004 0 10
V1 N001 0 500
C1 N004 0 400n
D1 N003 0 D
S1 0 N002 Signal 0 SW
V2 Signal 0 PULSE(0 20 0 0.01u 0.01u 0.91us 10us)
C2 N003 N002 1100n
L2 N003 N004 300u

```

```
.model D D
.lib <YOUR_SPICE_INSTALLATION_DIRECTORY>LTspiceXVII\lib\cmp\standard.dio
.tran 0 452ms 450ms 10ns startup
.options plotwinsize=0
.options numdgt=10
.model SW SW(Ron=1m Roff=1Meg Vt = 10 Vh = -2.5)
.backanno
.end
```

10X Quadratic Buck

```
R1 N004 0 10
V1 N001 0 500
C1 N004 0 0.6u
S1 N002 N001 Signal 0 SW
V2 Signal 0 PULSE(0 20 0us 0.01u 0.01u 0.5us 10us)
L1 N003 N004 150u
C2 N004 N005 0.6u
L2 N002 N005 150u
D1 N005 N003 Did1
D2 0 N002 Did1
D3 N002 N003 Did1
.model D D
.lib <YOUR_SPICE_INSTALLATION_DIRECTORY>LTspiceXVII\lib\cmp\standard.dio
.tran 0 720ms 700ms 10ns startup
.model SW SW(Ron=1m Roff=1Meg Vt = 5 Vh = -2.5)
.model Did1 D(Ron=0.0001 Roff=100G Vfwd=0)
.options plotwinsize=0
.options numdgt=10
.backanno
.end
```

F.4 Matrix method and ripple

F.4.1 Unabridged results

$$\begin{array}{c}
 V1 \\
 L \\
 C \\
 R
 \end{array}
 \begin{bmatrix}
 V1 & L & C & R \\
 0 & 0 & 0 & 0 \\
 0 & 30103 & -29972 & 0 \\
 0 & -29972 & 29843 & 0 \\
 0 & 0 & 0 & 0
 \end{bmatrix}
 \qquad
 \begin{array}{c}
 V1 \\
 L1 \\
 C1 \\
 R
 \end{array}
 \begin{bmatrix}
 V1 & L1 & C1 & R \\
 29 & -1 & -29 & 0 \\
 -1 & 31113 & -30978 & 0 \\
 -29 & -30978 & 30873 & 0 \\
 0 & 0 & 0 & 0
 \end{bmatrix}$$

Figure 173: Boost converter zero ripple 4X step up Figure 174: Boost converter defined ripple 4X step up.

$$\begin{array}{c}
 V1 \\
 L \\
 C \\
 R
 \end{array}
 \begin{bmatrix}
 V1 & L & C & R \\
 2952 & 3 & -2943 & 1 \\
 3 & 39335 & -39167 & -1 \\
 -2943 & -39167 & 26493.5 & 0 \\
 1 & -1 & 0 & 0
 \end{bmatrix}$$

Figure 175: Boost converter on border of DCM 4X step up

F.4.2 LTSpice Netlists

Zero ripple boost

```

V1 Source 0 50
R1 ResistorNode 0 160
V2 Signal 0 PULSE(0 20 0 0.01u 0.01u 7.5us 10us)
D1 InductorNode ResistorNode D
S1 InductorNode 0 Signal 0 SW
I1 Source InductorNode 1.25
V3 ResistorNode 0 200
.model D D
.lib <YOUR_SPICE_INSTALLATION_DIRECTORY>LTspiceXVII\lib\cmp\standard.dio
.tran 0 50ms 40ms 10ns startup
.options plotwinsize=0
.options numdgt=10
.model SW SW(Ron=1m Roff=1Meg Vt = 0.5 Vh = 0)
.backanno
.end

```

Normal ripple boost

```

V1 Source 0 50
L1 Source InductorNode 1m Rpar=0 Cpar=0
C1 ResistorNode 0 4.6875u
R1 ResistorNode 0 160
V2 Signal 0 PULSE(0 20 0 0.01u 0.01u 7.5us 10us)
D1 InductorNode ResistorNode D
S1 InductorNode 0 Signal 0 SW
.model D D
.lib <YOUR_SPICE_INSTALLATION_DIRECTORY>LTspiceXVII\lib\cmp\standard.dio
.tran 0 452ms 450ms 10ns startup
.options plotwinsize=0
.options numdgt=10

```

```
.model SW SW(Ron=1m Roff=1Meg Vt = 0.5 Vh = 0)
.backanno
.end
```

DCM border ripple boost

```
V1 Source 0 50
L1 Source InductorNode 40u Rpar=0 Cpar=0
C1 ResistorNode 0 250n
R1 ResistorNode 0 150
V2 Signal 0 PULSE(0 20 0 0.01u 0.01u 7.5us 10us)
D1 InductorNode ResistorNode D
S1 InductorNode 0 Signal 0 SW
.model D D
.lib <YOUR_SPICE_INSTALLATION_DIRECTORY>LTspiceXVII\lib\cmp\standard.dio
.tran 0 452ms 450ms 10ns startup
.options plotwinsize=0
.options numdgt=10
.model SW SW(Ron=1m Roff=1Meg Vt = 0.5 Vh = 0)
.backanno
.end
```

F.5 Cascaded boost

F.5.1 Unabridged results

$$\begin{matrix} & V1 & L & C & R \\ V1 & \left[\begin{array}{cccc} 0.0 & 13.95 & -13.89 & -0.0 \\ 13.95 & 193224.23 & -192389.45 & -6.27 \\ -13.89 & -192389.45 & 191558.28 & 6.24 \\ -0.0 & -6.27 & 6.24 & 0.0 \end{array} \right] \end{matrix}$$

Figure 176: Boost converter 4X step up

$$\begin{matrix} & V1 & L1 & L2 & C1 & C2 & R \\ V1 & \left[\begin{array}{cccccc} 0.11 & 83.35 & 83.78 & -82.43 & -83.37 & -0.34 \\ 83.35 & 66069.23 & 66409.95 & -65342.6 & -66080.4 & -273.05 \\ 83.78 & 66409.95 & 66752.43 & -65679.57 & -66421.18 & -274.46 \\ -82.43 & -65342.6 & -65679.57 & 64623.96 & 65353.65 & 270.05 \\ -83.37 & -66080.4 & -66421.18 & 65353.65 & 66091.58 & 273.1 \\ -0.34 & -273.05 & -274.46 & 270.05 & 273.1 & 1.13 \end{array} \right] \end{matrix}$$

Figure 177: Cascaded boost converter 4X step up

$$\begin{matrix} & V1 & L & C & R \\ V1 & \left[\begin{array}{cccc} 0.0 & 13.95 & -13.89 & -0.0 \\ 13.95 & 193224.23 & -192389.45 & -6.27 \\ -13.89 & -192389.45 & 191558.28 & 6.24 \\ -0.0 & -6.27 & 6.24 & 0.0 \end{array} \right] & & & \\ L & & & & \\ C & & & & \\ R & & & & \end{matrix} \quad \begin{matrix} & V1 & L1,L2 & C1,C2 & R \\ V1 & \left[\begin{array}{cccc} 0.11 & 167.13 & -165.8 & -0.34 \\ 167.13 & 265641.56 & -263523.75 & -547.51 \\ -165.8 & -263523.75 & 261422.84 & 543.15 \\ -0.34 & -547.51 & 543.15 & 1.13 \end{array} \right] \end{matrix}$$

Figure 178: Boost converter 4X step up

Figure 179: Cascaded boost converter 4X step up

F.5.2 LTSpice Netlists

Cascaded boost 4X step up

```

V3 Source 0 50
L2 Source N001 700u
C2 N002 0 650n
V4 Signal1 0 PULSE(0 5 0 0.01u 0.01u 5us 10us)
D2 N001 N002 D
S1 N001 0 Signal1 0 SW
L1 N002 N003 1.33m
C1 N004 0 300n
R1 N004 0 155
V2 Signal2 0 PULSE(0 5 0 0.01u 0.01u 5us 10us)
D1 N003 N004 D
S2 N003 0 Signal2 0 SW
.model D D
.lib <YOUR_SPICE_INSTALLATION_DIRECTORY>LTspiceXVII\lib\cmp\standard.dio
.tran 0 752ms 750ms 10ns startup
.model SW SW(Ron=1m Roff=1Meg Vt = 0.5 Vh = 0)
.options plotwinsize=0
.options numdgt=10
.backanno

```

.end

F.6 Interleaved boost converter

F.6.1 Unabridged results

$$\begin{array}{c}
 V1 \\
 L1 \\
 L2 \\
 C \\
 R
 \end{array}
 \begin{bmatrix}
 V1 & L1 & L2 & C & R \\
 16 & 16 & 16 & -109 & 61 \\
 16 & 47903 & -15850 & -31783 & -146 \\
 16 & -15850 & 47903 & -31783 & -146 \\
 -109 & -31783 & -31783 & 63399 & 0 \\
 61 & -146 & -146 & 0 & 230
 \end{bmatrix}$$

Figure 180: Interleaved boost converter 4X step up.

$$\begin{array}{c}
 V1 \\
 L1 \\
 L2 \\
 C \\
 R
 \end{array}
 \begin{bmatrix}
 V1 & L1 & L2 & C & R \\
 4 & 2 & 2 & -13 & 6 \\
 2 & 147761 & -16090 & -131418 & -7 \\
 2 & -16090 & 147811 & -131468 & -7 \\
 -13 & -131418 & -131468 & 262404 & 1 \\
 6 & -7 & -7 & 1 & 8
 \end{bmatrix}$$

Figure 181: Interleaved boost converter 10X step up.

For comparison here are the boost converters matrices again:

$$\begin{array}{c}
 V1 \\
 L \\
 C \\
 R
 \end{array}
 \begin{bmatrix}
 V1 & L & C & R \\
 0.0 & 13.95 & -13.89 & -0.0 \\
 13.95 & 193224.23 & -192389.45 & -6.27 \\
 -13.89 & -192389.45 & 191558.28 & 6.24 \\
 -0.0 & -6.27 & 6.24 & 0.0
 \end{bmatrix}$$

Figure 182: Boost converter 4X step up

$$\begin{array}{c}
 V1 \\
 L \\
 C \\
 R
 \end{array}
 \begin{bmatrix}
 V1 & L & C & R \\
 0.0 & 12.58 & -12.56 & 0.0 \\
 12.58 & 588900.59 & -587851.59 & 3.13 \\
 -12.56 & -587851.59 & 586804.45 & -3.13 \\
 0.0 & 3.13 & -3.13 & 0.0
 \end{bmatrix}$$

Figure 183: Boost converter 10X step up

F.6.2 LTSpice Netlists

Interleaved boost 4X step up

```

V1 Source 0 50
L1 Source InductorNode 900u Rpar=0 Cpar=0
C1 ResistorNode 0 150n
R1 ResistorNode 0 160
V2 Signal 0 PULSE(0 20 0 0.01u 0.01u 7.5us 10us)
D1 InductorNode ResistorNode D
S1 N001 0 Signal 0 SW
S2 InductorNode 0 Signal1 0 SW
D2 N001 ResistorNode D
L2 Source N001 900u Rpar=0 Cpar=0
V3 Signal1 0 PULSE(0 20 5u 0.01u 0.01u 7.5us 10us)
.model D D
.lib <YOUR_SPICE_INSTALLATION_DIRECTORY>LTspiceXVII\lib\cmp\standard.dio
.tran 0 452ms 450ms 10ns startup
.options plotwinsize=0
.options numdgt=10

```

```
.model SW SW(Ron=1m Roff=1Meg Vt = 0.5 Vh = 0)
.backanno
.end
```

Interleaved boost 10X step up

```
V1 Source 0 50
L1 Source InductorNode 3m Rpar=0 Cpar=0
C1 ResistorNode 0 200n
R1 ResistorNode 0 1025
V2 Signal 0 PULSE(0 20 0 0.01u 0.01u 9us 10us)
D1 InductorNode ResistorNode D
S1 N001 0 Signal 0 SW
S2 InductorNode 0 Signal1 0 SW
D2 N001 ResistorNode D
L2 Source N001 3m Rpar=0 Cpar=0
V3 Signal1 0 PULSE(0 20 5u 0.01u 0.01u 9us 10us)
.model D D
.lib <YOUR_SPICE_INSTALLATION_DIRECTORY>LTspiceXVII\lib\cmp\standard.dio
.tran 0 452ms 450ms 10ns startup
.options plotwinsize=0
.options numdgt=10
.model SW SW(Ron=1m Roff=1Meg Vt = 0.5 Vh = 0)
.backanno
.end
```

F.7 Linearity of the matrix method

F.7.1 Unabridged results

$$\begin{array}{c} V1 \\ L \\ C \\ R \end{array} \begin{bmatrix} V1 & L & C & R \\ 0.01 & 10.07 & -10.01 & -0.01 \\ 10.07 & 20010.93 & -19876.81 & -29.62 \\ -10.01 & -19876.81 & 19743.59 & 29.42 \\ -0.01 & -29.62 & 29.42 & 0.04 \end{bmatrix} \quad \begin{array}{c} V1 \\ L \\ C \\ R \end{array} \begin{bmatrix} V1 & L & C & R \\ 0.06 & 119.99 & -119.16 & -0.18 \\ 119.99 & 244433.41 & -242753.23 & -368.16 \\ -119.16 & -242753.23 & 241084.6 & 365.63 \\ -0.18 & -368.16 & 365.63 & 0.55 \end{bmatrix}$$

Figure 184: Boost converter 3X @ 100W step up.

Figure 185: Boost converter 3X @350 W step up

F.7.2 LTSpice Netlists

Boost converter 3X @ 100W

```

V1 Source 0 50
L1 Source InductorNode 1.6667m Rpar=0 Cpar=0
C1 ResistorNode 0 296.3n
R1 ResistorNode 0 225
V2 Signal 0 PULSE(0 20 0 0.01u 0.01u 6.66us 10us)
D1 InductorNode ResistorNode D
S1 InductorNode 0 Signal 0 SW
.model D D
.lib <YOUR_SPICE_INSTALLATION_DIRECTORY>LTspiceXVII\lib\cmp\standard.dio
.tran 0 452ms 450ms 10ns startup
.options plotwinsize=0
.options numdgt=10
.model SW SW(Ron=1m Roff=1Meg Vt = 0.5 Vh = 0)
.backanno
.end

```

Boost converter 3X @ 350W

```

V1 Source 0 50
L1 Source InductorNode 476.19u Rpar=0 Cpar=0
C1 ResistorNode 0 1.037u
R1 ResistorNode 0 64.2857
V2 Signal 0 PULSE(0 20 0 0.01u 0.01u 6.66us 10us)
D1 InductorNode ResistorNode D
S1 InductorNode 0 Signal 0 SW
.model D D
.lib <YOUR_SPICE_INSTALLATION_DIRECTORY>LTspiceXVII\lib\cmp\standard.dio
.tran 0 452ms 450ms 10ns startup
.options plotwinsize=0
.options numdgt=10
.model SW SW(Ron=1m Roff=1Meg Vt = 0.5 Vh = 0)
.backanno
.end

```
